CHEMICAL VAPOR DEPOSITED REUSABLE FLUORESCENT THIN FILM SENSOR NANOPROBES FOR THE DETECTION OF HEAVY METAL IONS

A Thesis Submitted to
the Graduate School of Engineering and Sciences of
İzmir Institute of Technology
in Partial Fulfillment of the Requirements for the Degree of

DOCTOR OF PHILOSOPHY

in Chemical Engineering

by
Merve KARABIYIK

December 2023
İZMİR

We approve the thesis of **Merve KARABIYIK**

Examining Committee Members:

Prof. Dr. Özgenç EBİL
Chemical Engineering, Izmir Institute of Technology

Assoc. Prof. Dr. Ayben TOP
Chemical Engineering, Izmir Institute of Technology

Prof. Dr. Yaşar AKDOĞAN
Materials Science and Engineering, Izmir Institute of Technology

Prof. Dr. Nalan KABAY
Chemical Engineering, Ege University

Prof. Dr. Levent BALLİCE
Chemical Engineering, Ege University

5 December 2023

Prof. Dr. Özgenç EBİL
Supervisor, Chemical Engineering,
Izmir Institute of Technology

Prof. Dr. Aysun SOFUOĞLU
Head of the Department of Chemical Engineering

Prof. Dr. Mehtap EANES
Dean of the Graduate School of Engineering and Science

ACKNOWLEDGEMENTS

I am heartily thankful to people who helped me in my PhD thesis.

First of all, I would like to express my sincere gratitude to my supervisor, Prof. Dr. Özgenç EBİL who expanded my horizons with his knowledge, guidance, encouragement, perceptiveness, sincerity, valuable advice and approaches made me believe in myself and supported me in completing my PhD thesis.

I wish to thank to thesis committee members Prof. Dr. Yaşar AKDOĞAN, Assoc. Prof. Dr. Ayben TOP for their valuable opinions and contributions. Throughout my study, I have benefited greatly from their valuable information, guidance and constructive suggestions. Also, thank you for agreeing to be on my defense jury. I would like to thank Dr. Erdal UZANLAR for his valuable opinions and contributions to a part of my work.

I would like to thank Chemist Belgin TUNÇEL KIRKAR for her help in Fluorescence Spectroscopy analysis. I wish to thank staff at İzmir Institute of Technology Integrated Research Centers (IYTE-TAM) for their help in analyses.

I would also like to thank all my friends the Department of Chemical Engineering. One of my most special thanks to my friend and lab-mate Dr. Gizem CİHANOĞLU. I would like to thank for her support, sincerity, contributions, and opinions during my experiments. Her love and sincerity have always been with me.

This long marathon would not have been easy without the support of my family. First of all, I would like to express my gratitude to the two most special people in my life, my mother and father, for the love, dedication, understanding and support that they have shown me throughout my life. Also, a special thanks to my husband, Fatih KARABIYIK. I would like to thank very much for his endless dedication, help, understanding and support throughout doctoral study. They always encouraged me in my graduate endeavor.

ABSTRACT

CHEMICAL VAPOR DEPOSITED REUSABLE FLUORESCENT THIN FILM SENSOR NANOPROBES FOR THE DETECTION OF HEAVY METAL IONS

Heavy metal pollution has made a serious threat to the environment and human health day by day due to developing science, technology and industrial activities, therefore, the importance of selective detection of heavy metals has increased. Heavy metals gradually accumulate in the human body, especially via water sources. Among heavy metals, cadmium is one of the most carcinogenic ones and has harmful effects even in trace amounts. Despite it, detection studies of cadmium ion are very few. This thesis study focuses on the development of Initiated Chemical Vapor Deposition (iCVD) synthesized polymer thin film based quantum dot-nitroxide radical fluorescence sensor nanoprobe, which has a multi-use property and high durability, unlike sensor probes developed for single use in liquid media, and selective detection of Cd^{2+} ions in real water sources. By examining the effects of pH, concentration, solvent type and reaction time, the most suitable conditions to improve the interaction between Cd^{2+} ion and the newly developed sensor nanoprobe were investigated. The results proved that it is possible to detect the target ion easily even in complex environments where other heavy metal ions are present. Cd^{2+} ion detection limit with this proposed nanoprobe was found as 0.195 μM and high recovery percentage (>90%) obtained in standard addition method. In the multi-use study, it was confirmed that nanoprobe could be used repeatedly for the selective and sensitive detection of Cd^{2+} ion without being influenced by the content of daily water samples. This thesis is a great guide for new fluorescent sensor applications.

Keywords: Initiated Chemical Vapor Deposition (iCVD) method, fluorescence sensor nanoprobe, heavy metal ion detection, selective Cd^{2+} ion detection.

ÖZET

AĞIR METAL İYONLARININ TESPİTİ İÇİN TEKRAR KULLANILABİLİR KİMYASAL BUHAR BİRİKTİRME İLE ELDE EDİLMİŞ FLORESAN İNCE FİLM SENSÖR NANOPROBLARI

Ağır metal kirliliği, gelişen bilim, teknoloji ve endüstriyel faaliyetlere bağlı olarak her geçen gün çevre ve insan sağlığı açısından ciddi bir tehdit haline gelmiş, dolayısıyla ağır metallerin seçici tespitlerinin önemi artmıştır. Ağır metaller, özellikle su kaynakları yoluyla insan vücudunda giderek birikmektedir. Ağır metaller arasında en kanserojen olanlardan biri olan kadmiyum, eser miktarlarda bile zararlı etkilere sahiptir. Buna rağmen kadmiyum iyonunun tespitine yönelik çalışmalar oldukça azdır. Bu tez çalışması, sıvı ortamda tek kullanım için geliştirilen sensör problarından farklı olarak çoklu kullanım özelliğine ve yüksek dayanıklılığa sahip Başlatılmış Kimyasal Buhar Biriktirme (iCVD) ile sentezlenmiş polimer ince film tabanlı kuantum nokta-nitroksit radikal floresan sensör nanoprobunun geliştirilmesine ve Cd^{+2} iyonunun gerçek su kaynaklarında seçici tespitine odaklanmaktadır. pH, konsantrasyon, çözücü türü ve reaksiyon süresinin etkileri incelenerek Cd^{+2} iyonu ile yeni geliştirilen sensör nanoprobu arasındaki etkileşimi arttırmak için en uygun koşullar araştırılmıştır. Sonuçlar, diğer ağır metal iyonlarının mevcut olduğu karmaşık ortamlarda bile hedef iyonun kolayca tespit edilmesinin mümkün olduğunu kanıtlamıştır. Önerilen bu nanoprob ile Cd^{+2} iyonu tespit limiti 0,195 µM olarak bulunmuş ve standart ekleme yönteminde yüksek geri kazanım yüzdesi (>%90) elde edilmiştir. Çoklu kullanım çalışmasında nanoprobun günlük su örneklerinin içeriğinden etkilenmeden Cd^{+2} iyonunun seçici ve hassas tespiti için tekrar tekrar kullanılabileceği doğrulanmıştır. Bu tez, yeni floresan sensör uygulamaları için büyük bir yol gösterici niteliğindedir.

Anahtar Kelimeler: Başlatılmış Kimyasal Buhar Biriktirme (iCVD) yöntemi, floresan sensör nanoprobu, ağır metal iyon tespiti, seçici Cd^{+2} iyonu tespiti.

TABLE OF CONTENTS

LIST OF FIGURES

Figure **Page**

LIST OF TABLES

CHAPTER 1

INTRODUCTION

During the last hundred years, various industrial activities and modern industrialization have significantly increased environmental problems, and the most important of them is heavy metal pollution. Heavy metals have serious effects on the environment as well as harmful effects on human health and over time, the exposure of living beings to these metals has increased because these inorganic pollutants are discharged into waters, soils and atmosphere due to the rapid growth of agriculture and metal industries, improper waste disposal, fertilizers and pesticides (Balali-Mood et al. 2021; Es-said et al. 2021; Wang et al. 2022). Pollution of the environment, especially water and air, with toxic metals is a major worldwide problem because millions of people around the world are affected by it. In addition, contamination of food and water sources with heavy metals is another major concern for human and animal health. For this reason, the concentrations of heavy metals in air, food and water resources are evaluated and reasonable levels are calculated for the environment and living life (Afkhami et al. 2015; Chen et al. 2020; Balali-Mood et al. 2021). It is inevitable that humans will be exposed to metals because metals, like other environmental pollutants, can be found naturally in the environment also. Today, the word 'heavy metal' is used to describe metallic chemical elements that are toxic to the environment and humans. They have high weight or density. According to their density, heavy metals can be listed that are greater than 5 g/cm^3 and are more commonly found in daily lives as follows; chromium, cobalt, copper, manganese, iron, nickel, zinc, arsenic, silver, cadmium, gold, mercury and lead (Briffa, Sinagra, and Blundell 2020).

Heavy metals are not biodegradable, they accumulate in our bodies when ingested or inhaled therefore they classified as hazardous. This bioaccumulation causes biological and physiological complications. Some heavy metals are essential for life and are called essential elements required for various biochemical and physiological functions like copper. However, they can be toxic when present in large amounts (Gong et al. 2016; Elmizadeh et al. 2019; Briffa, Sinagra, and Blundell 2020; García-Miranda Ferrari et al.

2020). Heavy metals, in addition to causing serious problems, are classified and divided into different groups according to whether they are carcinogenic or not. The International Agency for Research on Cancer (IARC) divided them into four groups as given in Table 1.1 (Briffa, Sinagra, and Blundell 2020; Kim et al. 2020).

Table 1.1. Classification of heavy metal carcinogenicity.

Group	Carcinogenicity level in humans	Evidence	Heavy metal classification
Group 1	Carcinogenic	*	• Aluminum compounds • Arsenic compounds • Cadmium and cadmium compounds • Chromium VI compounds • Nickel compounds
Group 2A	Probably carcinogenic	**	Lead compounds
Group 2B	Possibly carcinogenic	***	• Vanadium pentoxide • Molybdenum trioxide • Methylmercury • Nickel metallic and alloys • Lead • Cobalt
Group 3	Carcinogenicity not classifiable	****	• Chromium III compounds • Chromium metallic compounds • Copper • Mercury and mercury compounds • Selenium and selenium compounds
Group 4	Probably not carcinogenic	*****	• Manganese • Silver • Zinc

* Enough evidence in humans, ** Limited evidence in humans, sufficient evidence in animals, *** Limited evidence in humans, insufficient evidence in animals, **** Insufficient evidence in humans, insufficient evidence in animals, ***** Evidence suggests no carcinogenic properties in humans or animals.

In addition to carcinogenic effects given above, according to the World Health Organization (WHO), cadmium, lead, mercury, and arsenic are classified as extremely toxic and mutagenic agents (Gong et al. 2016; Li and Li 2021). Therefore, it is of great

importance to develop an effective and sensitive method for the detection of trace amounts of toxic heavy metals in real-world samples. Some analytical techniques have been used for the detection of heavy metal ions such as atomic absorption spectroscopy (AAS), inductively coupled plasma optical emission spectrometry (ICP-OES), stripping voltammetry, electrochemical method, X-ray fluorescence spectrometry (XRF), inductively coupled plasma mass spectrometry (ICP-MS) and ion selective electrodes (ISEs). However, developing a new method for the detection of metal ions has particularly important since most of them are costly, have complex sample pretreatment, require large sample volumes, time-consuming procedures and poor selectivity (Afkhami et al. 2015; Gong et al. 2016; Elmizadeh et al. 2019; Chen et al. 2020; García-Miranda Ferrari et al. 2020; Wang et al. 2022). Among usual methods, especially fluorescence methods have attracted great attention for the detection of heavy metal ions due to their advantages such as high sensitivity, selectivity, simplicity, being economical and not using any expensive equipment or complex processes and detection procedures. In addition, detecting heavy metal ions by fluorescence method is of great importance in terms of eliminating the above mentioned shortcomings of other detection methods (Gong et al. 2016; Elmizadeh et al. 2019; Chen et al. 2020; Wang et al. 2022).

1.1. Fluorescent Sensors

For design and fabrication of fluorescent sensors, selection of an appropriate probe is vital to performances of sensor arrays. Detection units must have a high response rate and repeatability. Particularly in fluorescent sensor methods, organic dyes and their derivatives, semiconductor quantum dots (QDs), silica nanoparticles (NPs), metal-organic frameworks (MOFs) and zero-dimensional carbon dots (CDs) have been separately designed or combined as metal ion detection platforms (Amjadi, Shokri, and Hallaj 2016; Gong et al. 2016; Li and Li 2021; Yan et al. 2022). In comparison with other fluorophores, semiconductor QDs are great alternative for heavy metal ions fluorescent sensors. Disadvantages seen in other fluorophores, such as small stokes shifts, excitation or emission wavelengths that are easily affected by environmental changes, and the self-quenching effect that limits their applications, have increased interest in semiconductor

quantum dots (QDs). Hence, they have been used in many studies for heavy metal ion detection due to their extraordinary optical properties such as high photoluminescence frequency, large Stokes shift, broad absorption spectra, narrow emission spectra, resistance to photo bleaching, long fluorescence lifetime and tunable size (Gong et al. 2016; Elmizadeh et al. 2019; Chen et al. 2020; Li and Li 2021; Wang et al. 2022).

1.1.1. Quantum Dot Fundamentals

Semiconductor nanoparticles have unique optical, electronic and photo physical properties, and with these properties, they have attracted attention in applications such as biological labeling, imaging, solar cells, composites and target material detection (Chern et al. 2019; Faten 2020). Quantum dots (QDs) are semiconductor nanocrystals that exhibit fluorescent properties, and this property occurs due to quantum confinement. Quantum confinement occurs when a material is miniaturized to lower or similar size to the characteristic length of its property under interest. For QDs, this characteristic length is the exciton Bohr radius, which is the distance between the electron-hole pair, and QDs on the same size scale or smaller than the characteristic exciton Bohr radius of their material exhibit quantum confinement (Chern et al. 2019; Yan et al. 2022). Recombination of the electron-hole pair causes QD fluorescence. Fluorescence is initiated by photoexcitation of an electron from the valence band of the QD to the conduction band. Then the electron relaxes to the lowest energy level in the conduction band. The energy difference between the conduction and valence band is preserved in the form of emitted photons, so the size of this gap determines the energy and wavelength of light emitted from the QD. The QD band gap is directly related to its diameter, so simply by controlling the size of the QDs, a variety of particles with different colors can be produced that emit at specific wavelengths (Chern et al. 2019; Faten 2020; Yan et al. 2022).

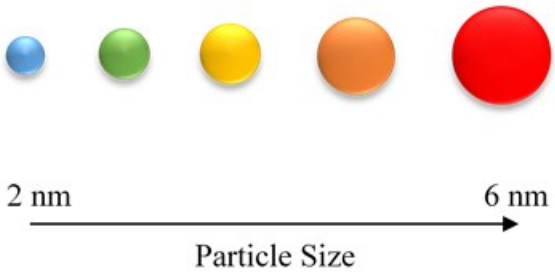

Figure 1.1. The size of QD nanoparticles determines the color emitted.

QD-containing fluorescent probes have been minimally investigated in the fluorescence detection of heavy metal ions. In literature, CdX (X = Te, Se, S) QDs, ZnS QDs, Au QDs etc. were used as fluorescent QDs probes (Banerjee, Kar, and Santra 2008; Xu, Miao, et al. 2011; Cai et al. 2014; Ding et al. 2014; Zhao et al. 2014; Gong et al. 2016; Niu et al. 2016; Chen et al. 2020; Yin, Yang, and Liu 2020; Preeyanka and Sarkar 2021). In general, two methods have been used to detect heavy metal ions by QD fluorescent probes as Turn-off and Turn-on (Banerjee, Kar, and Santra 2008; Xu, Miao, et al. 2011; Cai et al. 2014; Ding et al. 2014; Zhao et al. 2014; Gong et al. 2016; Niu et al. 2016; Yin, Yang, and Liu 2020; Preeyanka and Sarkar 2021). Comparing these methods, Turn-on mechanism was used less, however, in the studies carried out so far, a significant number of defects were caused by the Turn-off mode. Since, many different factors other than the target material can cause the "off" state of photoluminescence (PL), in other words, PL quenching mode, in the detection of this material. Thus, the Turn-on mode seems more preferable because the PL "off-on" conversion in the "on" mode can reduce the probability of false positives (Xu, Miao, et al. 2011).

In some literature studies, when only QDs were used as fluorescent probes, it was observed that there were disadvantages such as non-specific binding with heavy metal ions, and the detection mechanism was based on PL quenching which is the less preferred one as mentioned above (Banerjee, Kar, and Santra 2008; Chen et al. 2019). In these studies, QD fluorescent probes either do not respond to certain ions such as lithium, sodium, zinc and cadmium or undergo luminescence quenching in the presence of various transition and heavy metal ions like copper, iron, nickel and mercury (Banerjee, Kar, and Santra 2008). This showed that the selective detection of heavy metal ions cannot be successfully achieved with QD fluorescent probes alone. Therefore, the use of nanoprobes consisting of a ligand attached to QDs is of great importance, as the ligands are compatible

with QDs and are successful in target metal detection (Banerjee, Kar, and Santra 2008). Different from previous approaches to detect metal ions by fluorescence quenching mechanism, detection with probes based on QD-ligand and fluorescence enhancement has recently started to be developed (Banerjee, Kar, and Santra 2008; Zhang and Chen 2014; Gong et al. 2016; Elmizadeh et al. 2019; Khan, Mitra, and Sahoo 2020). QD-ligand probes are rare in literature, hence the development of these fluorescent sensor probe types for heavy metal ion detection have become attracted.

1.1.2. Ligand Based QD Fluorescent Sensors

Fluorescence quenching of QDs in a controlled manner by ligand in QD-ligand probe structure has led to the development of special fluorescent nanoprobes for different sensor applications and in the detection of target material, PL enhancement with this probe has been achieved (Chen et al. 2008; Tansakul et al. 2010). The better the fluorescence quenching, the better the detection of the target substance will be, so ligand selection is of great importance in detection process. In the literature studies reviewed, it was seen that the ligands that most effectively quenched the fluorescence of fluorophores were nitroxide radicals (Chen et al. 2008; Tansakul et al. 2010; Xu, Miao, et al. 2011; Adegoke et al. 2012).

Nitroxide radicals can be defined as stable radicals with a displaced unpaired electron in their N-O bond. Due to their structure, nitroxide radicals can come over a reversible electrochemical redox reaction. When oxidized, nitroxide radicals lose an electron and transform into oxoammonium cations stable at ambient conditions. But if they gain an electron, the reduction reaction converts the neutral radicals into aminoxyl anions. The aminoxyl anion (NO^{-}) tends to combine with a proton which present in water or an organic solvent containing some water to form hydroxylamine (Karoui et al. 2010; Tansakul et al. 2010; Haugland, Lovett, and Anderson 2018; Liu, Zhao, et al. 2019; Zhou et al. 2020; Xie et al. 2021).

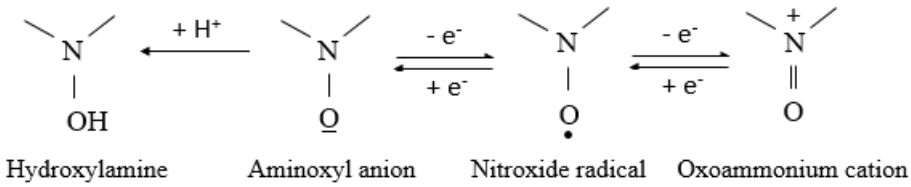

Figure 1.2. Reversible electrochemical redox reactions of a nitroxide radical.

The chemical structures of nitroxide radicals affect their redox potential and the reversibility of the reaction. Literature studies have demonstrated that especially functionalized 2,2,6,6 tetramethylpiperidine-N-oxyl (TEMPO) radicals interact more with the surface of QDs, creating strong binding (Maurel et al. 2006; Scaiano et al. 2006; Tansakul et al. 2010; Lin et al. 2012). In quenching efficiency studies, 4-Amino TEMPO (4AT), one of the functionalized TEMPO radicals, was found to be three times more effective as a quencher compared to other TEMPO radicals that are amino pyrrolidine, carboxylic acid and bisamino (Tansakul et al. 2010). In addition, it was found as a very suitable structure with regards to a ligand for sensor operations in the detection of target materials (Chen et al. 2008; Tansakul et al. 2010; Adegoke et al. 2012).

Although different target molecules and ions detection studies have been carried out in the literature with the QD-4AT nanoprobe structure, there is no study on heavy metal ion detection with this nanoprobe. For this reason, the first step of the study's uniqueness is shown at this point.

1.1.3. Progress, Shortcomings and Opportunities in Fluorescence Sensor Probes Developed for Heavy Metal Ion Detection

In literature, although the QD-ligand structure has not been studied much for heavy metal ion detection as a fluorescent sensor probe, there are a few studies in this sense, and these provide ideas for ion detection, use in real sources, difficulties experienced and how to overcome these difficulties in new studies.

The studies were carried out to detect target heavy metal ions with QD based probes created with different ligand structures, and in general, the common point of all

studies was to detect these metal ions at acceptable concentration limits which will not be harmful to the environment and human health in different sources. It was achieved with detection limit examinations. In addition, the recovery rate percentages were investigated and how successful the probes were in detecting ions in real sources was also examined. These literature studies have contributed to providing important ideas in the development of new fluorescent probes.

In some of these studies, copper ion (Cu^{2+}), which is one of the transition metal elements and is of vital importance for human health and many living tissues but it can become toxic and harmful if the appropriate concentration is not achieved, was detected. While some of them aimed to selectively detect Cu^{2+} with developed fluorescent probe (Ding et al. 2014; Zhao et al. 2014), another one worked on multi-ion detection by detecting silver and mercury ions in addition to copper (Gong et al. 2016). Selective sensing platforms were improved for detection of target ions as fluorescence probes such as l-Glutathione capped (GSH) ZnSe QDs, silicon QDs (SiQDs) and CdTe QDs in the presence of L-cysteine. When the study results were compared, the detection limits were found to be low as 0.013 (Ding et al. 2014), 0.51 (Zhao et al. 2014) and 0.088 ng/mL (Gong et al. 2016). In one of them, the practicality of the fluorescent probe were tested by using simulated samples only (Ding et al. 2014), while in the others, studies were carried out on the environment and other water resources (Zhao et al. 2014; Gong et al. 2016). In addition, recovery percentages varied between 95-108%, and these results showed that reliable probes have been developed for target Cu^{2+}ion detection.

Silver ion (Ag^{+}), which is an industrial heavy metal, tends to cause many diseases, and some CdTe QD based probes have been developed to detect this ion in literature such as Mercaptosuccinic acid (MSA) modified (Cai et al. 2014), dual modified (Chen et al. 2020), L-cysteine modified (Gong et al. 2016) and synthetic heterocycle ligand capped CdTe QDs (Elmizadeh et al. 2019). In addition to the detection limits being at nano-molar (nM) levels, the recovery rate percentage in one of the studies was found to be 89-92% (Cai et al. 2014), which was tested in fixer samples, and it was seen to have lower sensitivity than others testing in lake, soda, flume water etc. (Gong et al. 2016; Elmizadeh et al. 2019; Chen et al. 2020).

One of the most toxic heavy metals is mercury (Hg^{2+}) and it has strong toxicity and bioaccumulation properties, so it can cause serious problems for human health. Therefore, some detection studies have been carried out using QD-based fluorescence sensors for Hg^{2+} ion. While nitrogen doped graphene (N-GQDs) and carbon QDs (N-

CQDs) were preferred as probes in some studies (Zhang and Chen 2014; Shi et al. 2015), in another one, detection study was carried out for this ion with L-cysteine modified CdTe QDs (Gong et al. 2016). Detection limit values of 8.6 nM, 0.23 μM and 0.52 nM were found for N-GQDs, N-CQDs and L-cysteine modified CdTe QD probes, respectively. These results showed that CdTe based QDs has better selectivity towards Hg^{2+} ions among the other probes. Even though the detection studies were done with nitrogen doped QDs in different real water sources like tap and lake water, only the recovery rate examination was carried out in the study using CdTe QD fluorescent probe.

In these ion detection studies, in order to optimize the sensing platforms, some parameter effects were investigated like pH, reaction time and temperature, ion concentration, buffer types and QD volumes in the probe solution (Cai et al. 2014; Ding et al. 2014; Zhang and Chen 2014; Zhao et al. 2014; Shi et al. 2015; Gong et al. 2016; Elmizadeh et al. 2019; Chen et al. 2020). Also, most of them carried out target ion detection with fluorescence quenching mechanism, that is, turn-off, and this increased the questionability of the sensitivity of the sensor probes developed in the studies in ion detection because turn-off mechanism causes some previously mentioned detection deficiencies.

Cadmium ion (Cd^{2+}) is one of the heavy metals that is widely used, has high toxic properties and often causes human poisoning even at trace levels. While there are different probe structures developed in addition to QD-based probes in literature for detection of other heavy metal ions as given Table 1.2, the number of developed sensor structures and techniques for Cd^{2+} ion detection are very few and expensive (Remelli et al. 2016). Therefore, it is very important to develop simple but effective detection technique for Cd^{2+} ions.

Table 1.2. Fluorescence probes developed in literature.

Fluorescent Probe	Mechanism	Analyte	Detection Limit (LOD)	References
Carbon nanoparticles	Turn-off	Hg^{2+}	0.23nM	(Lu et al. 2012)
ONPCRs[a]	Turn-off	Ag^{+}, Hg^{2+}	0.68 nM 1.73 nM	(Wang and Ding 2014)
Carbon dots	Turn-on	Cu^{2+}	23nM	(Zong et al. 2014)
SH-Au NPs	Turn-on	Cr^{6+}	2.9nM	(Li, Wei, et al. 2017)

(cont. on next page)

Table 1.2 (cont.)

N-CNPs	Turn-off	Cr^{6+}	0.13μM	(Li, Hong, et al. 2017)
Ag NPs	Turn-on	Cr^{6+}	1nM	(Ravindran et al. 2012)
g-C_3N_4[b]	Turn off	Cr^{6+}	0.15μM	(Rong et al. 2015)
CDs@g-C_3N_4	Turn-on	Cr^{6+} Cu^{2+} Pb^{2+}	0.54 nM 0.18nM 0.2nM	(Radhakrishnan, Sivanesan, and Panneerselvam 2020)
g-C_3N_4/LDH	Turn-off	Cu^{2+}	20nM	(Huang et al. 2014)
g-C_3N_4	Turn-off	Cu^{2+}	0.5nM	(Tian et al. 2013)
g-C_3N_4	Turn-off	Cu^{2+}	1.2nM	(Cheng et al. 2014)
MoS_2 Nanosheet	Turn-on	Pb^{2+}	0.22μM	(Wang et al. 2016)
GO/ss-DNA	Turn-off	Pb^{2+}	50nM	(Wen et al. 2011)
R-GO/CdS/ aptamer	Turn-on	Pb^{2+}	0.05nM	(Zang et al. 2014)
Cou-T and Rh-T[c]	Turn-on	Fe^{2+}	0.75μM	(Maiti et al. 2015)

[a] : Fluorescent oxygen-doped, nitrogen-rich, photoluminescent polymer carbon nanoribbons
[b] : Graphitic carbon nitride nanosheets
[c] : Coumarin and rhodamine-linked nitroxide probes

The environmental problem caused by Cd^{2+} arises as a result of human activities, such as its use as pigments, alloys in the automotive industry, a stabilizer for plastics, batteries and in nuclear reactors (Bassam et al. 2021). The fact that these activities cause high levels of Cd^{2+} formation in water, air and soil is the main reason for significant exposure to Cd^{2+}. Many studies have illustrated the negative effects of long-term use of water contaminated with this element on human health (Balali-Mood et al. 2021; Bassam et al. 2021). As previously stated in Table 1.1, Cd^{2+} has been classified as carcinogenic to humans (Group 1) by the International Agency for Research on Cancer (IARC). The World Health Organization (WHO) fixed the concentration of Cd^{2+} in drinking water at 3 μg/L due to toxicity and adverse effects on human health (WHO 2011). All fluorescent sensor probes examined were produced in liquid media and are suitable for one-time use only. In addition to being a huge burden in terms of cost, this is also one of the biggest problems that consumes time. Moreover, although cadmium is one of the ions with the most serious toxic properties among the heavy metal ions, studies on the detection of this ion are very few in the literature and the existing ones have some deficiencies. Therefore, in order to prevent problems, early detection especially in different water sources where

cadmium may accumulate, will be an important contribution to take precautions and to protect the environment and human health.

Considering the fluorescent probes developed for Cd^{2+} ion in the literature, complex structures have been improved to increase selectivity so far. Living cell imaging of Cd^{2+} ion was performed by using supramolecular ligand (pyridine-2,6-diylbis (methyleneimino- 2,1-phenylene)bis(phenyl methanone) and 0.01μM detection limit was found (Chithiraikumar, Balakrishnan, and Neelakantan 2017). By developing glutathione-capped Zn−Ag− In−S (GSH@ZAIS) QDs, evidence of Cd^{2+} ion detection was made by examining fluorescence enhancement but detection limit calculation was not made (Preeyanka and Sarkar 2021). In another study, QD surface was modified with the metal ion selective ligand and dopant based core–shell CdS:Mn/ZnS QDs was developed. Luminescence intensity increased with detection of Cd^{2+} ion with this nanoprobe but again detection limit was not investigated in this study (Banerjee, Kar, and Santra 2008). In another one, Cd^{2+} ion detection was performed with a very complex chemosensor structure in liquid medium and the detection limit was found around 1μM (Bronson et al. 2005). To detect Cd^{2+} ion in aqueous media, initially, CdTe QDs was effectively quenched by sulfur anions (S^{2-}) and then detection process was applied. Detection limit was found as 0.5 μM (Xu, Miao, et al. 2011). In addition to the minority of studies on Cd^{2+} ion detection in the literature, the use of highly complex structures and carrying out very few detection limit studies have clearly shown the deficiencies in the fluorescent nanoprobes developed for Cd^{2+} ion.

1.2. Motivation

The effects of heavy metal ions on both the environment and human health are quite serious, and for this reason, detection studies of these ions have been carried out, especially in water resources, and different fluorescent sensor probes have been developed for this purpose. However, the biggest inadequacy seen in all the studies examined is that the developed probes were produced in liquid media, which brings a burden in terms of time and cost since they are disposable. In addition, although cadmium ion is the most serious carcinogenic ion among heavy metal ions, the fact that the number

of probes developed in the literature for the detection of this ion is low and that they have quite complex structures reveals the disadvantages of the studies carried out. The main motivation of this thesis study is based on the development of a polymer-QD-ligand based fluorescent sensor nanoprobe that can detect heavy metal ions in different water sources, which has never been developed before, and can be used multiple times rather than disposable. While polymer thin films provide the opportunity of a surface to which the QD-ligand structure can be attached, this thin polymer film structure, which can have high chemical and mechanical resistance, extends the life of the sensor and provides an important solution to the cost and time problems encountered in the literature. The production of polymer films was carried out using an initiated chemical vapor deposition (iCVD) system, and the surface modifications of the produced films were adapted to the QD-ligand structure desired to be attached to the surface.

1.3. Thesis Overview

The main objective of this PhD thesis was to develop a new multi-use polymer-QD-ligand fluorescence sensor nanoprobe for detection of heavy metal ions in real water sources.

The details of each chapter were described below:

i. In Chapter 2, general information about iCVD method used in the production of polymer thin films developed for fluorescent probes in this study is presented. Research on the iCVD system, which has wide application areas, is also included in detail.
ii. In Chapter 3, studies on the development of polymer bonded CdTe QD-4Amino TEMPO (4AT) nitroxide radical fluorescence nanoprobe for sensor studies are included. The main purpose of this study is to investigate how the polymer surface to which the QD-4AT probe can be attached can be produced in the iCVD system and with which functional group, method and reaction conditions the polymer surface functionalization can be performed most effectively. In addition, the mechanism and reaction conditions used in the production of the QD-4AT probe were examined in detail and the most suitable method was investigated.

iii. In Chapter 4, the details of the production of cross-linked copolymer films in the iCVD system, which can be used in sensor structures, are resistant to different types of chemical and mechanical factors, and do not affect the optical properties of coated surfaces, and the determination of the robust cross-linked polymer film by applying the necessary chemical and mechanical resistance tests are discussed.
iv. In Chapter 5, the binding of the QD-4AT nanoprobe to produced high mechanical strength cross-linked copolymer film, the heavy metal ion detection with this polymer-based nanoprobe to investigate which heavy metal is more selective towards it, the detection study in real water sources and the multi-use study are investigated in detail.

1.4. Contributions to the Literature

The contributions of this PhD thesis to the literature are listed below:

i. Chapter 3: In literature, there are different sensor structures developed for the detection of many ions and molecules in real sources (Chen et al. 2006; Chen et al. 2008; Tansakul et al. 2010; Adegoke et al. 2012; Lemon et al. 2015). Although fluorescent sensors developed with QD-ligand structure provide successful results in detecting target ions or molecules, they have been studied in very few numbers. However, these developed structures have a structure that is easily affected by some chemical or mechanical factors, which causes structural deterioration of the sensors. For this reason, it has become necessary to develop structures that are resistant to environmental conditions, as opposed to being disposable and perishable. In Chapter 3, for the first time in literature, polymer bonded CdTe QD-nitroxide radical complex was improved as fluorescence nanoprobe and polymer films were fabricated via iCVD system. The fluorescence quenching efficiency of the nitroxide radical was investigated for QD-nitroxide radical on-off complex structure in target molecule or ion detection, and time-dependent fluorescence quenching analysis illustrated that more than 50% decrease in fluorescence intensity occurred within the first 15 minutes. Fluorescence spectroscopy, microscopy and EPR analysis results revealed the possibility of multiple and easy

use of polymer bonded QD-nitroxide radical complex as sensor structures in various applications.

ii. Chapter 4: Optical materials like glass, mirror, filter, etc. are widely used in a wide range of applications such as various electro-optical devices, electronics, medical equipment, and the aviation industry. Due to widespread use, these materials can work in adverse conditions and be exposed to various solvents, dust, moisture and rapid temperature changes. Such conditions can reduce the performance and lifespan of these materials. Repairing damaged optical surfaces is often expensive, if not impossible, and therefore protecting the materials is very important. This is achieved by protective coating of the surfaces. The coating material must not interfere with the optical performance of the system, and the coating must provide acceptable chemical and/or physical protection. In this sense, polymer films attract a lot of attention because they can provide physical and chemical protection to optical surfaces. In Chapter 4, for the first time in literature, cross-linked copolymer thin films were deposited on optical surfaces in iCVD system by using glycidyl methacrylate (GMA) as epoxy monomer and ethylene glycol dimethacrylate (EGDMA) and 2,4,6,8-tetramethyl-2,4,6,8 tetravinylcyclotetrasiloxane (V4D4) as cross-linkers. To investigate the protection performance of the polymeric films, some chemical and mechanical durability tests were applied as durability in various solvents, adhesion to substrate and thermal resistance. Especially, p(GMA-co-V4D4) copolymers demonstrated high protection against water (<1% thickness loss), salt solution (<1.5% thickness loss), organic solvents (<5% thickness loss) and provided high optical transparency (~90% in visible spectrum). This proves that it is a good alternative as ideal coating materials for protection purposes in different applications.

CHAPTER 2

INITIATED CHEMICAL VAPOR DEPOSITION (iCVD) METHOD

In this section, general information is presented about the iCVD technique, in which polymer films were produced to which the QD-nitroxide radical complex nanoprobes were attached. In addition to studies on iCVD method, which have a wide application area, coatings that are particularly protective and have high mechanical strength are examined in detail.

2.1. Initiated Chemical Vapor Deposition

Polymer films and coatings can be produced using various methods. For instance, polymer solutions or emulsions can be prepared and they are coated on surfaces by spinning or dipping based on the evaporation of the solvents. Sometimes a curing or annealing step may be required after evaporation of the solvent to improve the coating quality (Träger 2012). Some adverse effects may occur in coatings produced by polymerization reactions using solvents in liquid phase. For example, in addition to damaging the substrate materials, they can also cause harmful effects because they cannot be completely removed from the coatings at the end of the operations (Bose et al. 2011). Therefore, systems operated under vacuum conditions are generally preferred overcome these effects and they are divided into two categories: physical vapor deposition (PVD) and chemical vapor deposition (CVD). PVD processes provide the deposition of thin films via condensation of the desired material from the vapor phase. Although CVD processes are similar to PVD processes, the most important difference is that a chemical reaction occurs in CVD processes (Träger 2012; Piegari and Flory 2013). The gaseous

reactants, that is, precursors are carried into the reaction chamber under vacuum conditions then with polymerization reaction deposition occurs on substrate and thin film coating is produced. There are many types of CVD processes, and the differences between them often arise from the activation techniques of the reaction such as plasma-assisted, hot wire, photo-initiated etc. (Träger 2012). CVD is also widely used in thin and hard film coatings to protect the coated product against external factors.

The initiated chemical vapor deposition (iCVD) method is one of the CVD processes and in recent years, it has been used as the most important coating process of polymeric thin films by means of its features, such as low production cost, low temperature conditions, three-dimensional geometry coating performance, fully meeting the required conditions etc. (Parker, Baechle, and Demaree 2011).

2.1.1. The Reaction Mechanism of iCVD Technique

In iCVD technique, initiator and monomer are introduced into the system by providing vacuum in the reaction chamber. The substrate to be coated is placed on the cooled bottom of the reaction chamber (<40^{o}C) and a filament array is placed 2 or 3 cm above this surface (Coclite et al. 2009). The monomer and initiator are transported to the reaction chamber in the vapor phase and, if necessary, the monomer or initiator is heated to provide the required vapor pressure. To obtain radicals through thermal decomposition of the initiator, the filament is heated between 200 and 400^{o}C (Lau and Gleason 2006a). One of the most advantageous aspects of the iCVD system, compared to other CVD techniques, is the use of both low filament temperatures and the coating on the substrate surface at room temperature, as given above. While the initiator decomposes in these temperature ranges, no disruption occurs in the monomers and they settle directly on the substrate surface without any change in their functionality (Coclite, Shi, and Gleason 2013). The temperature of this substrate is kept below 40^{o}C to ensure adsorption of monomers to the surface, as mentioned above. Free radicals are created in the gas phase by thermal decomposition of the initiator by filaments. These radicals then come to the substrate surface and initiate the polymerization reaction by attacking the monomer units

and causing the formation of active monomers known as monomer radicals (Lau and Gleason 2006b, 2008).

Free radical polymerization occurs as a reaction in iCVD system. Briefly, in this reaction, free radicals attack inactive monomer molecules and make them active, that is, they form monomer radicals and active monomers carry unpaired electrons. Then, a monomer radical attacks another inactive monomer, forming a chain. An unpaired electron is delivered to the growing chain end, thus free radical polymerization occurs by adding radicals to the growing chain at each step (Allcock, Lampe, and Mark 2003). Free radical polymerization consist of three main stages as initiation, propagation and termination. In the initiation step of iCVD polymerization, reactive molecules with active sites called radicals are formed, thus both free radical formation from the initiator and monomer activation occur at this stage (Lau and Gleason 2006b). The transfer of the unpaired electron to the end of the growing chain occurs in the propagation step, when the active monomer attacks the monomers that do not have an active side, and the transfer of this electron continues throughout the growth process of the chain (Allcock, Lampe, and Mark 2003). This step is performed on the substrate surface in the iCVD system (Lau and Gleason 2006b). In the termination step, which is the last step where the final product polymer is obtained, polymerization stops and the active site of the growing chain is eliminated (Lau and Gleason 2006b).

The mechanism of the iCVD technique can be stated in four general steps as shown in Figure 2.1 below (Lau and Gleason 2007c):

- Transport of monomer and initiator in the vapor phase to the reaction chamber.
- Decomposition of the initiator into radicals in the vapor phase by passing through the heating filaments (200-400^{o}C).
- Adsorption of monomer molecules and free radicals onto the cooled substrate surface.
- The free radical polymerization reaction takes place on the substrate surface to produce a polymer thin film.

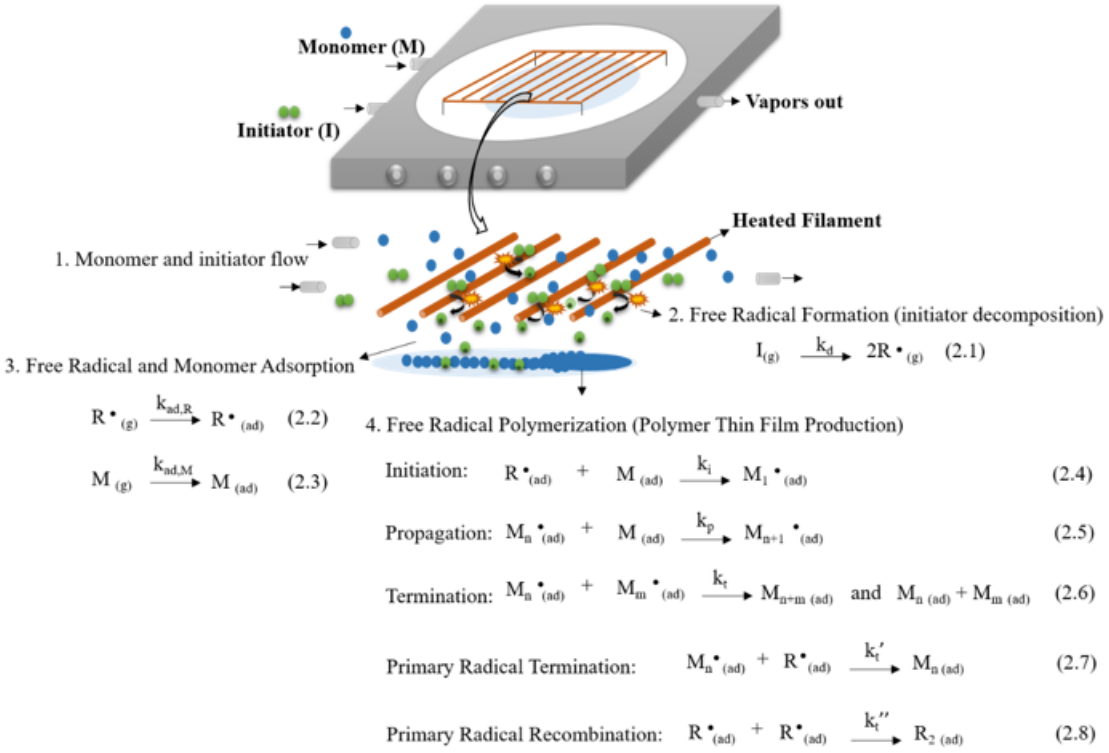

Figure 2.1. General mechanism of iCVD system, I: initiator, M: monomer, R: radical.

2.2. iCVD Polymer Thin Films

In literature, there are wide range of studies about fabrication of polymeric films which have several different functionalities such as hydrophobicity, antimicrobial or dielectric property and resistivity (Lau and Gleason 2007c; Martin et al. 2007; Trujillo, Wu, and Gleason 2010; Alf, Hatton, and Gleason 2011; Bose et al. 2011; Coclite, Shi, and Gleason 2013) for using in barrier coatings, drug delivery, dielectric coatings, biosensors, tissue engineering etc. (Gleason 2015). A brief literature review about the iCVD polymeric materials used in this thesis study is given in following sections.

2.2.1. Protective Coatings

The need to protect structures and systems used in many different fields, such as aviation, military or civil electro-optical device industry, etc., depending on the environment they are exposed to, has increased considerably in recent years. Nowadays, many studies are carried out on the production of protective coating in order to both reduce costs and increase the lifespan. In particular, various polymer coatings have become very attractive in terms of providing physical and chemical protection (Singh et al. 1996; Resnick and Buck 1997; Scheirs 1997; Chambers et al. 2006; Boentoro and Szyszka 2013; Zhao et al. 2021). Compared to many other polymer types, especially poly(glycidyl methacrylate) (pGMA) is one of the most preferred polymers in several fields because it can be converted into different types of functionalities through epoxy ring opening reactions with various chemical groups by means of the epoxy group (-C_2H_3O) in its structure (Kim et al. 1996; Lee et al. 1996; Li et al. 2005; Labbé et al. 2011; Sarıipek and Karaman 2014; Gleason 2015; Muzammil, Khan, and Stuparu 2017; Irzhak, Uflyand, and Dzhardimalieva 2022). Amine, sulfhydryl or hydroxyl functional groups can be covalently attached to pGMA films through the ring opening reactions and this causes some modifications of polymeric surfaces, contributing to the imparting of a variety of different functional properties to the produced polymer (Allmér, Hult, and Rånby 1989; Mori, Uyama, and Ikada 1994; Zhang et al. 1995; Tarducci et al. 2000; Allcock, Lampe, and Mark 2003; Lau and Gleason 2006c; Baxamusa, Im, and Gleason 2009; Alf et al. 2010; Xu and Gleason 2010a; Kimmins, Wyman, and Cameron 2014; Sarıipek and Karaman 2014). In addition, the epoxy group in the structure of GMA monomer ensures that the polymer films produced have very high mechanical properties (Martin et al. 2007). In particular, cross-linked pGMA has illustrated high resistance to both physically and chemically harsh environments, making it favorable for protective coating applications (Mao and Gleason 2004; Chan and Gleason 2006; Mao and Gleason 2006; Özpirin and Ebil 2018). In addition to hardening of coatings (Weinberger 2000) cross-linking improves many functional properties such as mechanical strength, chemical resistance and thermal stability (Guo et al. 2015).

In Arndt et al. (1999) study, in order to investigate the composition of cross-linking polymer network with FT-IR analysis poly(vinyl alcohol)-poly(acrylic acid)

(PVA/PAA) networks have been synthesized by cross-linking PVA and PAA. The effect of cross-linking parameters like cross-linking density, heat treatment process time and temperature and pH effect were examined to adjust mechanical properties and sensitivity of the hydrogels which were aimed to be used in the actuator sensor systems for process control application (Arndt et al. 1999). Hilt et al. (2003) prepared a crosslinked poly(methacrylic acid) (PMAA) network containing high amounts of poly(ethylene glycol) dimethacrylate (PEGDMA) and patterned onto a microcantilever to develop ultrasensitive microsensor. The sensitivity and uniqueness of the microsensor platform were investigated by examining the environmental pH effect and also the amount of the cross-linking, the length of the cross-linker and monomer types were the main parameters to examine the swelling properties of the polymer. Highly sensitive microsensor was created for the detection of any analyte (Hilt et al. 2003). Mao et al. (2006) synthesized copolymer films of glycidyl methacrylate (GMA) with 2,2,3,3,4,4,5,5,6,6,7,7-dodecafluoroheptyl acrylate (DFHA) and with (perfluoroalkyl)ethyl methacrylate (PFEMA) in iCVD system. Vacuum annealing of the as-deposited copolymer films enabled cross linking via epoxy groups of the GMA units. The hardness and the modulus of the annealed copolymers films investigated and observed that increasing of GMA fraction improved these mechanical properties. According to results, the mechanical properties, low surface energy and optical clarity demonstrated by the developed cross-linked copolymer films have verified that they are desirable for many applications (Mao and Gleason 2006). Riche et al. (2011) modified the inner side of poly(dimethylsiloxane) (PDMS) microfluidic devices with a cross-linked fluoropolymer barrier coating which consists of 1H,1H,2H,2H-perfluorodecyl acrylate (PFDA) cross-linked with ethylene glycol diacrylate (EGDA) via iCVD system in order to provide resistivity to absorption and swelling. The results demonstrated that the cross-linked barrier film ensured the devices to be used as continuous flow reactors for reaction synthesis (Riche et al. 2011). In Birck et al. (2016) study, poly(vinyl alcohol) (PVOH) films were crosslinked with citric acid (CTR) and hydroxypropyl-b-cyclodextrin (HPbCD) for creation of antimicrobial films. Antimicrobial tests were made against *Staphylococcus aureus, Escherichia coli* and *Candida* and the results illustrated that antibacterial and antifungal activity were enhanced with high crosslinking times (Birck et al. 2016). Petruczok et al. (2013) reported cross-linked poly(divinylbenzene) (pDVB) and poly(4-vinylpyridine-co-divinylbenzene) thin film production by iCVD method. The composition of the cross-linked polymer film was analyzed with FT-IR spectroscopy to investigate the parameter

effects on cross-linking. The results showed that the modulus of the copolymer could be tuned by varying the DVB monomer feed rate and deposition conditions of iCVD system and specific cross-linked thin films could be produced for various applications (Petruczok, Yang, and Gleason 2013). Poly(tetravinyltetramethylcyclotetrasiloxane) (poly(V4D4)) is considered one of the best candidates for protective coating applications. A robust superhydrophobic polymer films were fabricated by Yoo and co-workers (2013) via iCVD system. Poly(1,3,5,7-tetravinyl-1,3,5,7- tetramethylcyclotetra siloxane) (poly(V4D4)) and poly(1H,1H,2H,2H-perfluorodecylacrylate) (poly(PFDA)) layers constituted stacked polymer films. It was illustrated that p(V4D4) layer in p(V4D4-L-PFDA) robust film enhanced the stability to many mechanical and chemical stresses such as thermal, organic solvent, UV etc. (Yoo et al. 2013).

All these studies demonstrated that in order to crosslink the polymer network, copolymer films can be produced by using different cross-linkers, apart from the annealing process. Ethylene glycol dimethacrylate (EGDMA) and 2,4,6,8-tetramethyl-2,4,6,8-tetravinylcyclotetrasiloxane (V4D4) are used as cross-linkers in the formation of polymer films with high durable properties (Yang et al. 2011; Bose, Heming, and Lau 2012; Yang and Gleason 2012; Seok et al. 2018; Lee et al. 2019). Especially, since there has been no study in the literature on the creation of robust polymer film structures with pGMA in the iCVD system using these cross-linkers, the strong cross-linked copolymer p(GMA-co-EGDMA) and p(GMA-co-V4D4) films produced in this thesis show the uniqueness of the study.

CHAPTER 3

POLYMER-BONDED CDTE QUANTUM DOT-NITROXIDE RADICAL NANOPROBES FOR FLUORESCENT SENSORS

3.1. Introduction

Semiconductor nanoparticles, or quantum dots (QDs), are of particular interest in biological and chemical sensor applications due to their wide absorption and narrow emission spectra, high quantum efficiency, photo-bleaching resistance, and high photochemical stability compared to other fluorophores (Zhao, Bagwe, and Tan 2004; Medintz et al. 2005; Wu and Xia 2005; Yu and Lowe 2009; Serra 2011; Prabhakaran et al. 2012; Liu, Teng, et al. 2019), and they are also increasingly sought after in labeling, imaging and detection applications (Snee et al. 2006; Selvan et al. 2007; Liu et al. 2008; Sevim Ünlütürk, Akdoğan, and Özçelik 2021). In recent years, fluorescent sensor studies in which QD nanoparticles were used for different substance detection have attracted much attention (Laferrière et al. 2006; Scaiano et al. 2006; Chen et al. 2008; Tansakul et al. 2010; Xu, Chen, et al. 2011; Adegoke et al. 2012). Various techniques such as atomic absorption spectrometry (AAS), atomic emission spectrometry (AES) and inductively coupled plasma mass spectrometry (ICP-MS) have been used to detect target materials in the chemical or biological fields (Suvarapu and Baek 2015). Although these conventional techniques have high sensitivity and accuracy, they require complex operators which limit their applications especially in terms of bulky instrumentation, extensive sample preprocessing and in situ analysis (Suvarapu and Baek 2015). Electrochemical methods,

This chapter has been published as:
Karabiyik, Merve, and Özgenç Ebil. 2022. "Polymer-bonded CdTe quantum dot-nitroxide radical nanoprobes for fluorescent sensors." *Journal of Materials Science* 57 (34):16258-16279. https://doi.org/10.1007/s10853-022-07640-8.

surface plasmon resonance (SPR) detections, quartz crystal microbalance (QCM), chemiluminescence (CL) and fluorescence methods are among the newly developed sensing platforms (Wing Fen and Mahmood Mat Yunus 2013; Yang Shen 2019; Khanmohammadi et al. 2020). When compared with them, fluorescence methods have the advantages of high sensitivity, high accuracy, and relative simplicity (Li and Wang 2008; Koneswaran and Narayanaswamy 2009). The controlled QD fluorescence quenching (decreasing the fluorescence intensity) phenomenon, which has led to the development of special fluorescent nanoprobes, has been particularly exploited in fluorescent sensor applications (Dang and Guo 2006; Chen et al. 2008; Tansakul et al. 2010; Lin et al. 2012; De Acha et al. 2019). In literature studies, the most effective quenchers of fluorescence of organic fluorophore were found to be nitroxide radicals which are also called as profluorescent nitroxides (Chen et al. 2008; Tansakul et al. 2010; Xu, Chen, et al. 2011; Adegoke et al. 2012). Fluorophores join a fluorescent moiety labeled with a paramagnetic nitroxide, and in these spin-labeled profluorophores, the paramagnetic nitroxide radical acts as an effective quencher of the fluorophore. As a result, fluorophore-nitroxide complex can be an on–off switch when the paramagnetic nitroxide is transformed to a diamagnetic species such as hydroxylamine or alkoxyamine (Green et al. 1990; Bian et al. 2005; Dang and Guo 2006; Chen et al. 2008; Tansakul et al. 2010). There are many studies in the literature based on profluorescent nitroxides, especially nitroxide radical 2,2,6,6-tetramethylpiperidineN-oxide (TEMPO) for evaluation of quenching effect on the emission of different QDs (Laferrière et al. 2006; Maurel et al. 2006; Scaiano et al. 2006; Tansakul et al. 2010; Xu, Chen, et al. 2011; Adegoke et al. 2012; Lin et al. 2012). It was shown that stronger binding can be achieved to the QD surface with functionalized TEMPO radical compared to non-functionalized form of TEMPO (Maurel et al. 2006; Scaiano et al. 2006; Tansakul et al. 2010). Tansakul et al. (2010) studied four different ligand-bearing TEMPO molecules for quenching of QDs and compared the radicals with respect to effectiveness in fluorescence quenching. Quenching efficiency measurements based on the concentration of nitroxide required to achieve a 50% reduction in the emission intensity revealed that 4-Amino TEMPO (4AT) is three times more effective as a quencher than carboxylic acid nitroxide, which is an order of magnitude more effective than amino pyrrolidine nitroxide and bisamino nitroxide, respectively (4AT > carboxylic acid nitroxide > amino pyrrolidine nitroxide > bisamino nitroxide) (Tansakul et al. 2010).

The main purpose of this study is to develop a polymer-bonded QD-4aminoTEMPO nanoprobe as a sensor structure based on the fluorescence quenching. In the literature, similar nanoprobe structures have been demonstrated only in liquid media rendering them single-use, disposable and non-reusable sensors. The synthesis of a polymer-bonded nanoprobe structure, its suitability for use in sensor applications and its fluorescence performance have not been shown in the literature before. It was shown that 4AT, which is also used as quencher in this study, is the most effective quencher in the fluorescence quenching of the QDs (Tansakul et al. 2010). Figure 3.1 shows non-functionalized TEMPO radical and 4 different ligand bearing TEMPO radicals.

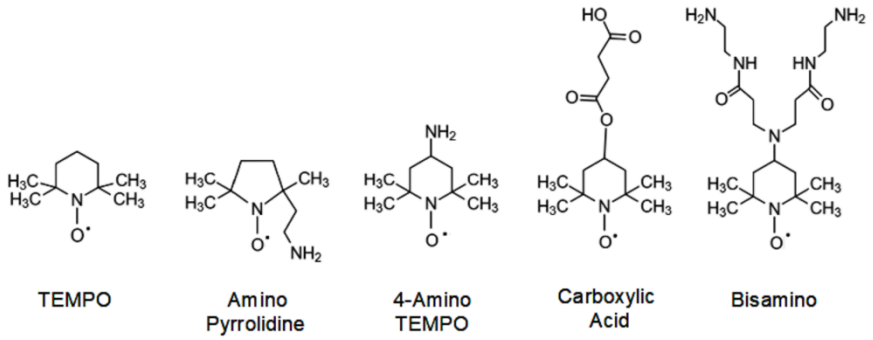

Figure 3.1. Non-functionalized TEMPO radical and commonly used ligand-bearing nitroxide radicals.

CdSe and CdTe QDs are the most preferred quantum dots in visible light applications, immunolabeling, in vivo imaging, sensor applications, etc. CdSe and CdTe QDs with carboxylic acid capping ligands can be easily attached to amine-functionalized surfaces (Medintz et al. 2005; Xu and Gleason 2010a; Prabhakaran et al. 2012; McElroy et al. 2014; Zhou et al. 2016). Combining the unique optical properties of QDs with flexibility of polymers offers great potential especially for sensing applications. In particular, the integration of sensor structures containing QDs into mechanically and chemical durable polymer films would be useful to make them reusable as previously demonstrated the sensor structures are generally disposable and easily degradable in liquid media (Özpirin and Ebil 2018). A variety of methods have been used in the literature for polymer surface modification and functionalization such as physicochemical

methods including thin film coating, bulk phase desorption, etc., and mechanical methods including micromanipulation and roughening. In addition, biological methods, physical adsorption, and chemical conjugation have also been successfully applied for surface modification of polymers (Hoffman 1996; Asatekin et al. 2010; Nemani et al. 2018; Varghese and Mittal 2018; Pinson and Thiry 2020). Thin-film coating methods attract attention as a versatile and powerful tool for the modification of surfaces due to the ability of immobilization of different surface functionalities on polymer and better binding of the film to the substrate compared to other methods (Jaganathan et al. 2015). Thin-film coating methods are generally classified under wet and dry processes. Wet processes have some drawbacks associated with solvent substrate interaction, uniformity, temperature control, impurities, etc. (Li et al. 2005; Sarıipek and Karaman 2014).

In recent years, a novel technology, initiated chemical vapor deposition (iCVD), has become very popular technique for the deposition of variety of polymer films due to its low thermal budget and higher deposition rates (Sarıipek and Karaman 2014). In iCVD method, the unsaturated bonds of the monomer units adsorbed on the substrate surface are activated by free radicals produced during the thermal decomposition of an initiator molecule (typically at low filament temperatures of 200–400^{o}C) to form monomer radicals on the substrate surface where they polymerize (substrate temperatures of 0–40^{o}C) (Gleason 2015). In iCVD process, the free radical polymerization takes place in solid phase without any solvent. Substrates with complex geometries can be coated conformal using iCVD with high uniformity and without any solvent related issues that are seen in wet processes (Coclite et al. 2009; Sarıipek and Karaman 2014; Gleason 2015). In addition, low-temperature iCVD process enables coatings on temperature sensitive materials such as paper, polymers, membranes, etc., without damaging functional groups of the monomers with precise thickness and morphology control (Coclite et al. 2009; Aresta et al. 2012; Sarıipek and Karaman 2014; Gleason 2015). It has been demonstrated that the functional groups of the monomers are successfully transferred to the polymeric films formed by preserving their properties (Coclite et al. 2009; Aresta et al. 2012; Sarıipek and Karaman 2014; Gleason 2015). Different types of surfaces including fabric, plastic, silicon, inorganic semiconductor materials, glass, microporous membranes, carbon nanotubes, etc., have been found to be successfully coated via iCVD (Lau et al. 2003; Lau and Gleason 2006b, a; Lau and Gleason 2007b). When compared to other CVD methods such as plasma enhanced chemical vapor deposition (PECVD) and hot wire chemical vapor deposition (HWCVD), iCVD has been the most preferred CVD method

for the fabrication of thin polymeric films due to fast deposition rates, low process temperature and acceptable vacuum levels, ability to coat complex 3D geometries conformal, and precise film thickness and microstructure control (Lau and Gleason 2007a).

Among many other polymeric materials, poly(glycidyl methacrylate) (pGMA), is one of the most suited iCVD polymer due to its epoxy group that can be converted into different kinds of functionalities via ring-opening reactions with several nucleophiles (Kim et al. 1996; Lee et al. 1996; Li et al. 2005; Labbé et al. 2011; Sarıipek and Karaman 2014; Gleason 2015; Muzammil, Khan, and Stuparu 2017; Irzhak, Uflyand, and Dzhardimalieva 2022). Especially, cross-linked (either via ring-opening or copolymerization) pGMA is both mechanically and chemically highly durable in harsh environments making it suitable for protective coating applications. In addition, a variety of chemical groups such as primary amine, sulfhydryl, or hydroxyl groups can be covalently bonded to pGMA (with nucleophilic attack) through the ring opening reaction leading to further functionalization and modifications of polymeric or inorganic surfaces. The rate of ring-opening reaction varies with the type of nucleophile used (Allmér, Hult, and Rånby 1989; Mori, Uyama, and Ikada 1994; Zhang et al. 1995; Tarducci et al. 2000; Allcock, Lampe, and Mark 2003; Lau and Gleason 2006c; Baxamusa, Im, and Gleason 2009; Alf et al. 2010; Xu and Gleason 2010a; Kimmins, Wyman, and Cameron 2014; Sarıipek and Karaman 2014). In particular, amine functional surfaces have attracted special attention for sensor applications since they react with several groups such as epoxy, aldehyde, carbonyl, carboxylic acid, and sulfonyl chloride (Alf et al. 2010; Xu and Gleason 2010a). It has been shown that using tertiary amines in epoxy ring opening reactions are preferred since they are considered as highly reactive catalysts for nucleophilic ring-opening reactions under appropriate conditions (Wu and Xia 2005; Barbey and Klok 2010; Sarıipek and Karaman 2014). Copolymers containing dimethyl amino ethyl methacrylate (DMAEMA), diethyl amino ethyl methacrylate (DEAEMA), diisopropyl amino ethyl methacrylate (DiPAEMA) and morpholinoethyl methacrylate (MEMA) have been found to be highly effective in these reactions (Yu and Lowe 2009). In the literature, epoxy ring opening reaction by DEAEMA that contains tertiary amine group was proven to be very efficient (Barbey and Klok 2010; Sarıipek and Karaman 2014). In addition, several studies were performed by investigating of the role of amine and hydroxyl containing compounds (water, alcohols, phenols, acids) which considerably promote the interaction of epoxy compounds with amines and other nucleophilic reagents

(Laferrière et al. 2006). In the presence of hydroxyl containing compounds, the epoxy ring carbon atom becomes more sensitive to nucleophilic attack. Ethanol was used in reaction medium to catalyze the epoxy ring opening reaction successfully (Allmér, Hult, and Rånby 1989). However, it is still difficult to conclude whether copolymers containing tertiary amines or homopolymers to catalyze the epoxy ring opening reaction in an alcohol solution is more effective.

In this study, two different methods were used for epoxy ring-opening reaction, one involving DEAEMA with tertiary amine group to catalyze the ring opening reaction of pGMA, and the other in which ethanol was used to catalyze the ring opening reaction of pGMA homopolymer. The aim of the study is to develop robust, polymer-bonded QD nanoprobes as an alternative to the single use and easily degradable sensor structures.

Here, in the first part of the study we report iCVD synthesis and functionalization of pGMA and p(GMA-co-DEAEMA) copolymer thin films via epoxy ring opening reactions to enable the binding of CdTe QDs on the functionalized polymeric surfaces. The effect of different amine functional groups, aromatic primary amine (aniline), aliphatic primary amine (propylamine) and aliphatic tertiary amine (Et_3N) on epoxy ring opening reaction and QD attachment were also evaluated.

In the second part of the study, the synthesis and attachment of QD-4AT nanoprobes to functionalized pGMA thin films (selected as the better method for epoxy ring opening) and the feasibility of using QD-4AT nanoprobes as fluorescent sensor structures for sensor applications were reported. The covalent attachment of nanoprobes to polymer surface opens up the possibility of using the sensor multiple times as opposed to solution-based single use fluorescent sensors reported in the literature.

3.2. Materials and Methods

The study consists of two parts in terms of development of polymeric sensor nanoprobe complex. In the first part, functionalization of iCVD deposited polymers with different amine functional groups by epoxy ring opening reactions to bind CdTe QDs on the functionalized polymers was carried out. The effect of different amine groups on functionalization was evaluated. In the second part of the study, the interaction between

QDs and 4-Amino TEMPO (4AT) was examined by electron paramagnetic resonance spectroscopy (EPR). The effect of reaction time on binding performance and the type of bonding between QDs and 4AT molecules were investigated. In addition, the fluorescence quenching mechanism was investigated by fluorescence analysis and the suitability of QD-4AT complex for fluorescent sensor applications was evaluated by integrating QD-4AT complex to the polymer surface.

3.2.1. Homo- and Copolymer Deposition in iCVD System

A custom-built iCVD system was used to fabricate homo- and copolymer films. The vacuum chamber had a backside cooled via an external circulator enabling a substrate temperature between -20 and 50^{o}C with 0.1^{o}C accuracy. Thermal energy for decomposition of the initiator was supplied by a heated filament array (Nichrome, 80% Ni/20% Cr) placed 3 cm above the cooled substrate. GMA (Sigma-Aldrich, 97%) as epoxy monomer and DEAEMA (Sigma-Aldrich, 99%) as amine group monomer were used without further purification. GMA and DEAEMA monomers were heated to 65^{o}C and 80^{o}C, respectively, in stainless steel containers. Tert-butyl peroxide (TBPO, Sigma-Aldrich, 98%) was used as initiator at room temperature. All depositions were performed on crystalline silicon (c-Si) substrates.

3.2.2. Epoxy Ring Opening Reactions

3.2.2.1. Procedure 1: p(GMA-co-DEAEMA) Amine Functionalization

Copolymer p(GMA-co-DEAEMA) thin films were fabricated using DEAEMA and GMA monomers via iCVD. As a low-temperature process, iCVD process allows retention of functional groups during polymerization as shown in Figure 3.2. Resulting

copolymer film contains both the epoxy and the amine group, and surface functionalization can be carried out on copolymer films. Three different amine functional groups were used to compare their reactivity in the epoxy ring opening reaction. 1M aqueous solutions of aromatic primary amine (Aniline, Sigma-Aldrich, 99.5%), aliphatic primary amine (propylamine, Sigma-Aldrich, 98%) and aliphatic tertiary amine (Et_3N, Sigma-Aldrich, 99%) were prepared. iCVD fabricated copolymer films were immersed into mechanically stirred amine solutions at room temperature for two hours. Copolymer films were then rinsed with deionized water and dried at 60°C for 1 h under vacuum.

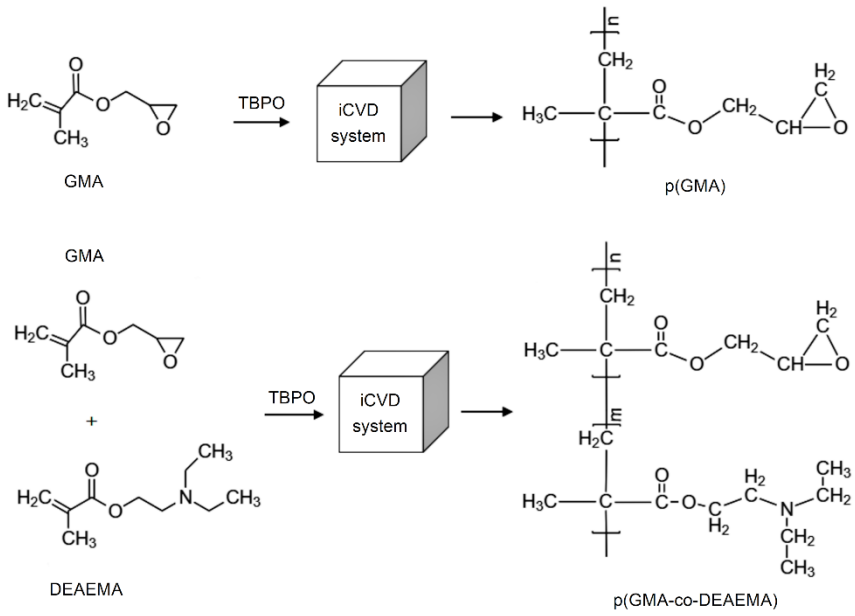

Figure 3.2. Synthesis of pGMA homopolymer (top) and p(GMA-co-DEAEMA) copolymer (bottom) via iCVD.

The formation of donor–acceptor complex interactions via a polymer with electron donor groups in its structure has a complex mechanism (T.Drzal 1986). Donor–acceptor complex interaction between the electron donor groups in the polymer which is tertiary amine group in DEAEMA and acceptor group which is hydroxyl-containing compound (water) enables epoxy ring opening and attachment of amine groups in the environment with the formation of both intramolecular and intermolecular interactions. The general view of the mechanism is given in Figure 3.3.

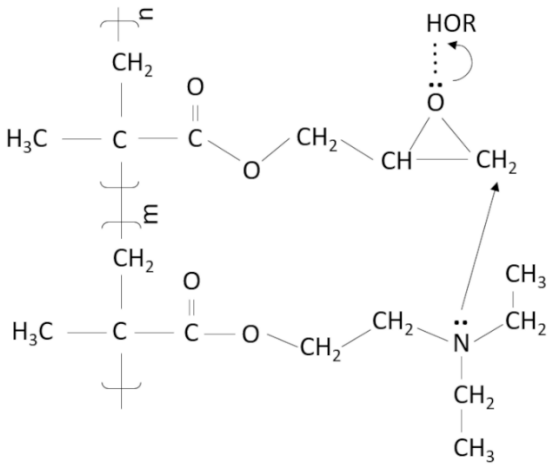

Figure 3.3. Epoxy ring opening reaction mechanism in p(GMA-co-DEAEMA) copolymer.

3.2.2.2. Procedure 2: pGMA Homopolymer Amine Functionalization

Homopolymer pGMA films fabricated via iCVD were functionalized using a slightly different process than copolymer functionalization. Ethanol solution was used as a catalyst for the epoxy ring opening reaction in the absence of DEAEMA monomer. pGMA homopolymer coatings were immersed into 1 M ethanol solutions of aniline, propylamine and Et_3N separately and stirred at 60°C for 2 h. After ring opening reaction, homopolymer films were rinsed with ethanol and dried at 60°C for 1 h under vacuum.

During the reaction, donor–acceptor complex interactions occur between the amine and the hydroxyl-containing compound (HOR). The general mechanism of addition of amines to the epoxy ring of pGMA is shown in Figure 3.4.

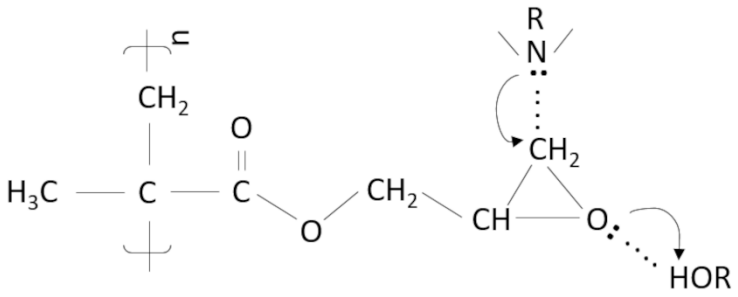

Figure 3.4. Epoxy ring opening reaction mechanism in pGMA homopolymer.

The addition of amines proceeds through a preliminary formation of fairly stable donor–acceptor complexes of the epoxy compound with ethanol, and then with a subsequent nucleophilic attack of the amine on this complex (T.Drzal 1986; Allmér, Hult, and Rånby 1989). In this way, the bonding of the amine group to the open epoxy ring takes place. After the amine group is attached to opened epoxy ring, other unbound amine molecules take on the role of forming donor–acceptor complexes with the hydroxyl-containing compound (HOR) to bind to other opened epoxy rings in the polymer film.

3.2.3. QD Attachment to Functionalized Thin Films

There are many studies in the literature reporting the binding of QDs to the polymer surface via the amine groups. Binding of QDs to the polymer surface generally occurs as a result of amide bond formation between the -COOH group of QDs and the amine groups on the polymer surface (Lee and Kennedy 2007; Xu and Gleason 2010b; Shen 2011; Rizvi S 2014). It is generally preferred that carbodiimide compound should be present in the reaction medium because it enables QD activation (Xu and Gleason 2010b; Shen 2011). The most commonly used carbodiimide compounds in literature are N, N'-dicyclohexylcarbodiimide (DCC) (Lee and Kennedy 2007; Xu and Gleason 2010b) and N-(3-dimethylaminopropyl)-N'-ethylcarbodiimide (EDC) (Shen 2011; Rizvi S 2014).

In the first part of this study, DCC was used to activate QDs in order to bind them on polymer surface by amine groups with formation of amide bond. One milligram of carboxylic acid functionalized CdTe QD (Sigma Aldrich, λ_{em} = 520 nm) was dispersed in 20 ml deionized water and was ultrasonicated for 30 min to obtain a uniform dispersion. A small amount of DCC (Sigma Aldrich, C 99.0%) (<1 mg) was added to the dispersion. Functionalized homo and copolymers were immersed into QD dispersion at 60°C for 2 h. The films then were rinsed with deionized water to remove unbound QDs from the surface and dried at 60°C for 1 h under vacuum. 60°C was used instead of room temperature to enhance DCC solubility in water. However, in the literature studies, it was observed that the same process could also be performed using EDC at room temperature (Alice Lee and Kennedy 2007; Rizvi S 2014). Due to lower reaction temperature, EDC/N-hydroxysuccinimide (NHS) was used in the binding of QD to the polymer surface in the second part of the study which is related with QD-4AT nanoprobe integration on polymer surface by interaction of QDs and amine groups of polymer. The bonding mechanism between QD and amine group of polymer is shown in Figure 3.5. Amide bond formation can be performed successfully with the presence of EDC and NHS in reaction medium. As a result, –NH groups along the polymer chain can easily react with –COOH functionalized QDs through EDC/NHS chemistry.

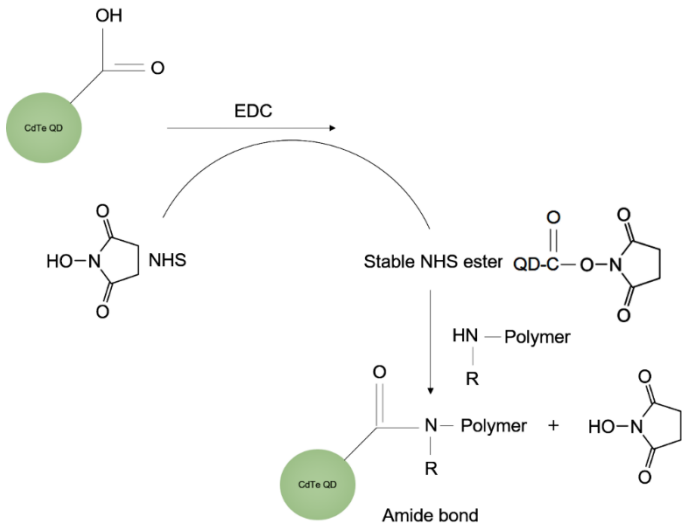

Figure 3.5. Carbodiimide-based coupling reaction. The –COOH groups on the QD surface are activated by EDC and addition of NHS yields a stable reactive NHS ester intermediate that reacts with NH groups on the polymer film to yield a stable amide bond.

3.2.4. Preparation of CdTe QD-4AT nanoprobe

CdTe QD-4AT nanoprobe was synthesized by binding 4-Amino TEMPO (4AT) molecules (as shown in Figure 3.1) to CdTe QDs. Two procedures with different QD activation and binding process times were followed to investigate the effect of QDs and 4AT interaction time on binding to the QD surface. All other conditions were kept the same. CdTe QD dispersion was prepared using deionized water with ultrasonication for 30 min at 25°C. A solution containing excess amount of EDC and NHS was prepared with phosphate buffered saline (PBS) (10 mM and pH: 7.4) and added to QDs dispersion to activate -COOH groups on QDs in PBS buffer (pH: 7.4). Continuous gentle stirring was applied to the mixture for 30 min (for procedure A) and 2 h (for procedure B) at 25°C. Next, 4AT solution was prepared using PBS buffer (pH: 7.4) and then added to activated QDs mixture. Continuous gentle stirring for 4 h (for procedure A) and for ~24 h (for procedure B) at 25°C was applied. Figure 3.6 describes the preparation of -COOH functionalized CdTe QD-4AT nanoprobe. Figure 3.7 shows experimental steps for CdTe QD-4AT complex preparation procedure and EPR analysis of the complex.

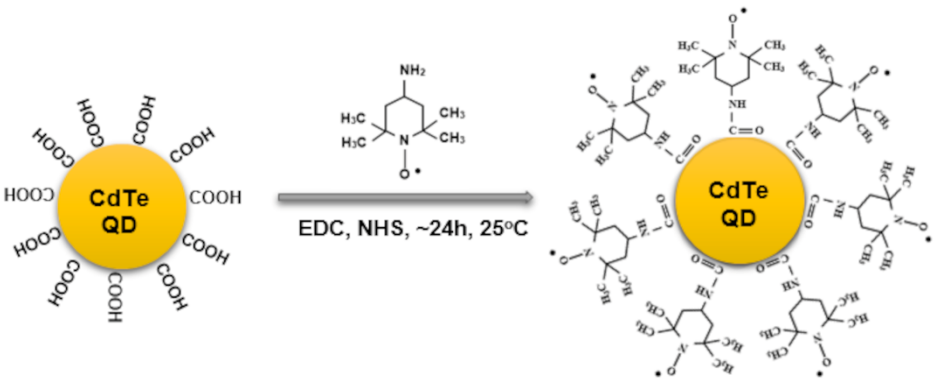

Figure 3.6. COOH functionalized CdTe QD-4AT nanoprobe.

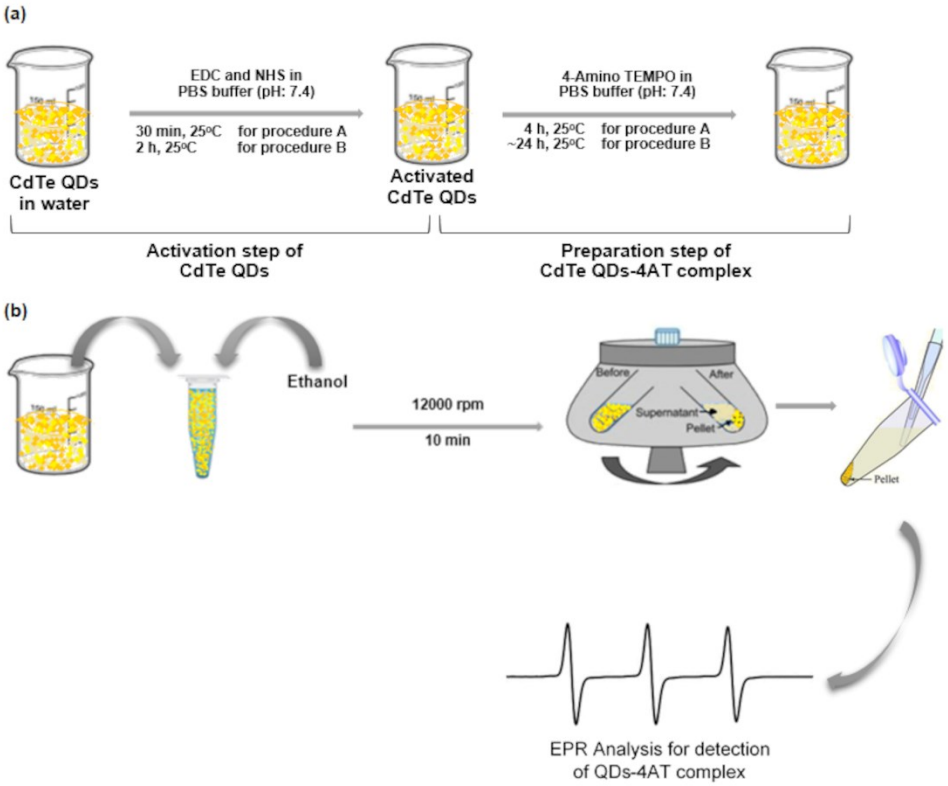

Figure 3.7. a) CdTe QD-4AT complex preparation procedure and b) EPR analysis for the detection of QD-4AT complex.

3.2.5. Attachment of QD-4AT Nanoprobes to Polymer Surface

To attach QD-4AT nanoprobes to the surface of iCVD polymers, thin-film polymer was immersed into the solution for 2 h, while QD-4AT nanoprobe formation procedure, as shown in Figure 3.7a, was being carried out. In addition, a reference solution was also prepared containing only 4AT without QDs by using the same procedure and iCVD polymers were dipped into this reference solution for comparison. EPR spectroscopy was used to confirm binding of QDs to the polymer surface.

3.2.6. Characterization

Thickness measurements of iCVD polymer films were performed using a Mprobe-Vis20 reflectometer with a spectral range between 400 and 1100 nm. FTIR analysis was used to investigate chemical composition and quality of polymer films. FTIR spectra of samples were taken using a PerkinElmer-UATR Two Spectrometer between 450 and 4000 cm-1 with 4 cm^{-1} resolution. In addition to FTIR analysis, energy-dispersive X-ray spectroscopy (EDX) (FEI QUANTA 250 FEG:EDX) was used to investigate chemical composition of the polymer films before and after epoxy ring opening reactions. Water contact angle (WCA) measurements were performed using a Theta Optical Tensiometer. Static contact angle measurements were performed for 1 min by dropping 5 µl water on sample surface. To examine QD and 4AT nitroxide radical interaction both in solution and on the polymer surface, electron paramagnetic resonance spectroscopy (EPR) analysis was performed using a CMS 8400 EPR Spectrometer. Fluorescence spectroscopy (Zeiss-Observer Z1 fluorescence microscope and PerkinElmer LS 55) was used to confirm the attachment of quantum dots onto the film surface and for fluorescence quenching measurements. Excitation and emission wavelength ranges of 300–350 nm and 500–550 nm, respectively, were used for CdTe QDs.

3.3. Results and Discussion

3.3.1. Polymer Synthesis and Amine Functionalization

In order to find optimum process conditions, initial experiments were carried out for homopolymers by varying monomer/initiator flow rate ratio, reactor pressure, filament and substrate temperatures. Similarly, copolymer films with various composition were fabricated using different monomer flow rates (F_{DEAEMA}: F_{GMA} ranging from 0.12 to 1), reactor pressures and substrate temperatures. Table 3.1 shows optimized iCVD process conditions, thicknesses and deposition rates for pGMA and pDEAEMA

homopolymers, and p(GMA-co-DEAEMA) copolymer used in this study. For all depositions, substrate temperature, T_s, and reactor pressure, P, were kept constant at 35ºC and 250mTorr, respectively. Resulting film deposition rates varied between 10 and 13 nm/min.

Table 3.1. iCVD process conditions for pGMA and pDEAEMA homopolymers, and p(GMA-co-DEAEMA) copolymer thin films.

Process Conditions	**pGMA**	**pDEAEMA**	**p(GMA-co-DEAEMA)**
F_{GMA} (sccm)	1.5		1
F_{DEAEMA} (sccm)		1.2	0.5
F_{TBPO} (sccm)	1	0.8	0.65
T_f (ºC)	330	300	300
T_{sub}(ºC)	35	35	35
P_{dep} (mTorr)	250	250	250
Thickness (nm)	378±4	312±1	390±4

FTIR analysis is a useful tool for evaluation of the quality and chemical composition of polymer films and also confirming complete polymerization that is no monomer is present on the surface of the substrate after deposition in iCVD. FTIR spectra of iCVD deposited pGMA, pDEAEMA homopolymers and p(GMA-co-DEAEMA) copolymer films are given in Figure 3.8.

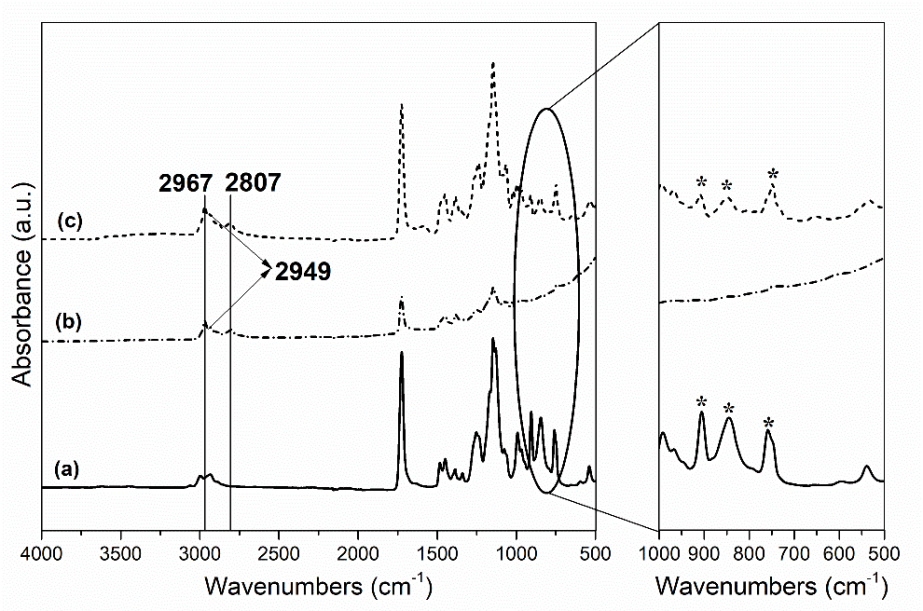

Figure 3.8. FTIR spectra of a) pGMA, b) pDEAEMA, c) p(GMA-co-DEAEMA) thin films. (*) represent epoxy group peaks.

The characteristic absorbance peaks that belong to methacrylates are clearly observed in FTIR spectra of all samples (H. Gunzler and Gremlich 2002; Mao and Gleason 2004, 2006; Bakker et al. 2007; Barbey and Klok 2010; Karaman and Çabuk 2012; Mohammed Safiullah, Abdul Wasi, and Anver Basha 2014; Sarıipek and Karaman 2014). Prominent characteristic peaks between 3000 and 2800cm^{-1} are assigned to C-H symmetry and asymmetry stretching caused by CH_3 and CH_2 groups; the peak at 1730cm^{-1} is related to carbonyl group (C=O) stretching vibration. Peaks related to C=C bonds belonging to monomers, like significant peak is at 1640cm^{-1}, are not observed in iCVD deposited polymers' spectra indicating complete consumption of adsorbed monomers (Bakker et al. 2007; Karaman and Çabuk 2012; Sarıipek and Karaman 2014). The characteristic peaks at 906, 846 and 760cm^{-1} which are belong to epoxy group stretching, are clearly seen in pGMA FTIR spectrum (Mao and Gleason 2004, 2006; Bakker et al. 2007; Mohammed Safiullah, Abdul Wasi, and Anver Basha 2014). The peaks at 2967, 2949 and 2807cm^{-1} are attributed to different C-H vibrations, and $–N(C_2H_5)_2$ functional group (Barbey and Klok 2010; Karaman and Çabuk 2012; Sarıipek and Karaman 2014). The characteristic peaks of both epoxy and tertiary amine groups are observed in copolymer spectrum confirming successful deposition of p(GMA-co-DEAEMA).

In addition to FTIR analysis, chemical composition of iCVD fabricated films was also investigated before and after epoxy ring opening reactions via EDX analysis. Table 3.2 shows elemental composition of as deposited iCVD polymer films.

Table 3.2. EDX analysis of iCVD deposited pGMA, pDEAEMA homopolymers and p(GMA-co-DEAEMA) copolymer films.

Element	pGMA		pDEAEMA		p(GMA-co-DEAEMA)	
	Wt%	Atomic%	Wt%	Atomic%	Wt%	Atomic%
C	60.0	66.7	62.2	67.7	51.8	58.7
O	40.0	33.3	26.2	21.4	46.0	39.1
N			11.6	10.9	2.2	2.20
Total	100.0	100.0	100.0	100.0	100.0	100.0

EDX analysis can detect elements with concentrations between 1 and 10wt % but cannot be used for detection of trace elements. Therefore, it is a useful tool for quick elemental analysis of polymer films before and after ring opening reactions but not for detection of CdTe QDs. For EDX analysis, the signal coming from c-Si substrate was removed and the composition was calculated based on carbon, nitrogen and oxygen elements. In Table 3.2, the presence of amine groups belonging to DEAEMA in copolymer films was confirmed via EDX analysis.

Table 3.3 shows elemental composition of pGMA and p(GMA-co-DEAEMA) films after ring opening reactions with aniline, propylamine and Et_3N. The highest nitrogen content was found in propylamine functionalized copolymers (12.10%) when compared with aniline (6.12%) and Et_3N (4.20%) functionalized copolymers. Similarly, propylamine-functionalized pGMA homopolymer showed higher nitrogen concentration (9.08%) than aniline (6.25%) and Et_3N (2.60%) functionalized pGMA.

Table 3.3. EDX results after p(GMA-co-DEAEMA) copolymer and pGMA homopolymer functionalizations with aniline, propylamine and Et_3N.

	Aniline		Propylamine		Et_3N	
Element	Wt %	Atomic %	Wt %	Atomic %	Wt %	Atomic %
	p(GMA-co-DEAEMA) functionalization					
C	53.2	59.8	50.6	56.9	65.8	71.6
O	40.4	34.1	36.8	31.0	29.7	24.2
N	6.4	6.1	12.6	12.1	4.5	4.2
Total	100.0	100.0	100.0	100.0	100.0	100.0
	pGMA functionalization					
C	54.0	60.5	52.8	59.1	54.0	60.8
O	39.5	33.2	37.8	31.8	43.3	36.6
N	6.5	6.3	9.4	9.1	2.7	2.6
Total	100.0	100.0	100.0	100.0	100.0	100.0

According to the EDX results, propylamine reactivity in the epoxy ring opening reaction is higher than aniline and Et_3N. For p(GMA-co-DEAEMA), amine containing DEAEMA monomer and for pGMA, ethanol act as catalyst during epoxy ring opening reaction. As expected, the reactions were successfully catalyzed by both routes (Yu and Lowe 2009; Sarıipek and Karaman 2014).

The purpose of using amine groups in this study is to ensure bonding of QD nanoparticles onto pGMA polymer via epoxy ring opening reaction. CdTe QDs can be attached to polymer surface over amine groups via formation of bond between amine groups and QDs' -COOH groups (Xu and Gleason 2010a; Sarıipek and Karaman 2014). WCA measurements were performed to investigate whether the polymer surfaces are successfully functionalized with amine groups in the epoxy ring opening reaction and to confirm the previous EDX and FTIR analysis results. It is well known that both pGMA and pDEAEMA homopolymers are hydrophilic in nature (Allmér, Hult, and Rånby 1989; Sarıipek and Karaman 2014). For this purpose, in the analysis, the change in hydrophilicity of polymer surfaces after ring opening reactions with different amine groups was examined. WCA values and changes in the water droplets after 1 min are shown in Figure 3.9.

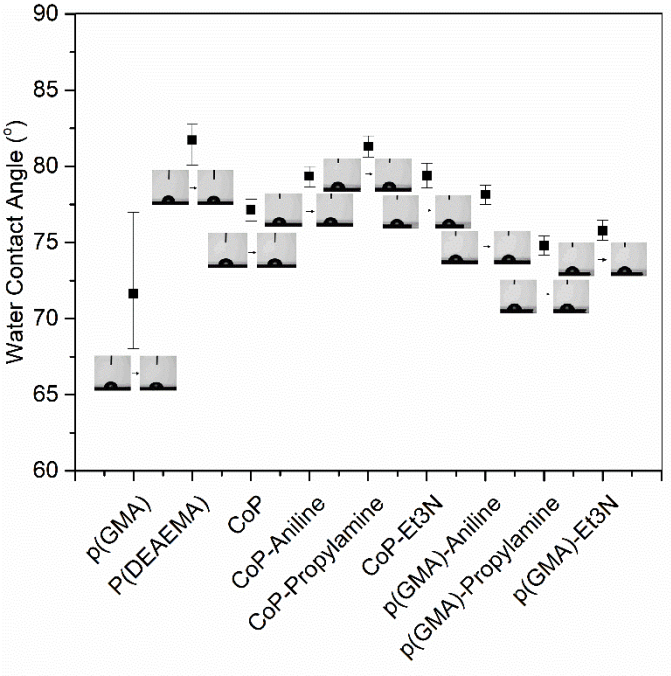

Figure 3.9. Water contact angle measurements for pGMA, pDEAEMA, their copolymer (CoP), functionalized CoP and pGMA after epoxy ring opening reaction with aniline, propylamine and Et_3N, respectively.

WCAs of iCVD deposited pGMA and pDEAEMA homopolymers were measured as 71.6 ± 4° and 81.7 ± 1°, respectively. These results are in good agreement with studies in the literature as pGMA is more hydrophilic than amine group polymers (Allmér, Hult, and Rånby 1989; Sarıipek and Karaman 2014). As expected, p(GMA-co-DEAEMA) copolymer was found to have a WCA of 77.1 ± 0.7°. WCA measurements of pGMA homopolymer and p(GMA-co-DEAEMA) copolymer were also taken after epoxy ring opening reactions. Homo- and copolymer films exhibited different WCAs depending on the presence of functional groups. For ring opening reactions, very reactive primary aliphatic amine (propylamine) and tertiary aliphatic amine (triethylamine (Et_3N)), and less reactive primary aromatic amine (aniline) were used. It was observed that ring opening reaction with amines reduces hydrophilicity of pGMA and p(GMA-co-DEAEMA) copolymer films. This was expected since amine functional groups are low surface energy components (Bayramoglu et al. 2013; Sarıipek and Karaman 2014; D'Ischia and Ruiz-Molina 2017). For p(GMA-co-DEAEMA) copolymer, the highest WCA was obtained with propylamine reaction. Triethylamine and aniline resulted in slightly lower WCAs. For pGMA homopolymers, the highest WCA was observed with

aniline. Slightly lower WCAs with aliphatic amine group sources, propylamine and Et_3N were observed. Similar to aromatic amines, aliphatic amines directly bond to epoxy ring, but the presence of unreacted amine tail ends in the aliphatic amines increases surface wettability. Therefore, lower WCAs were observed with propylamine and Et_3N compared to aniline in pGMA homopolymer (Bayramoglu et al. 2013; Shanmugharaj et al. 2013; D'Ischia and Ruiz-Molina 2017).

However, this behavior was not observed in p(GMA-co-DEAEMA) copolymers. To examine whether the amine groups maintain their reactivity and to evaluate the effectiveness of CdTe QD attachment procedure, fluorescence microscopy analysis was performed as shown in Figure 3.10.

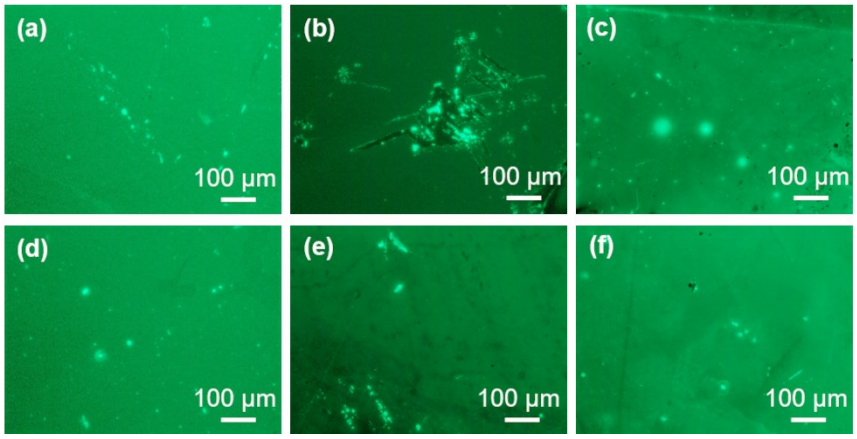

Figure 3.10. Fluorescence microscopy images of CdTe QD attached surfaces of (a–c) aniline, propylamine and Et_3N functionalized p(GMA-co-DEAEMA), and (d–f) aniline, propylamine and Et_3N functionalized pGMA, respectively. Excitation and emission wavelength ranges were 300–350 nm and 500–550 nm, respectively.

Linearly stretched fluorescence microscopy images showed relatively uniform emission over the entire sample surface for both pGMA homopolymer and p(GMA-co-DEAEMA) copolymers regardless of the amine groups used. The bright spots that exist in images are either CdTe QD agglomerates or impurities that scatter the emission from QDs. Some of these bright spots are distributed randomly over large areas, but most of them are concentrated on or near surface defects such as cracks on the film surface or

physical damage seen in Figure 3.10b due to mishandling of the samples and around surface impurities (dust and other particles) as seen in Figure 3.10c and d. However, fluorescence microscopy images are still useful to evaluate the effectiveness of QD attachment procedure and reveal that QD attachment was performed successfully for both homo- and copolymer films.

Considering the EDX, WCA and fluorescence microscopy analysis results, it is reasonable to state that epoxy ring opening routes where ethanol was used as catalyst for homopolymer and DEAEMA monomer was used as catalyst for copolymer coating are successful and QD attachment procedure was effective for both homo and copolymer films. The results obtained in the first part of this study are consistent with literature studies. It was reported that aliphatic primary or secondary amines can catalyze ring opening reactions of epoxides successfully while primary and secondary aromatic amines are not capable of catalyzing epoxide polymerization. The studies also indicated that tertiary amines can be used by themselves as catalysts of epoxide polymerizations and curing agents (Enikolopiyan 1976). Besides, tertiary amine containing copolymer coatings increase the reactivity of the epoxide reactions when compared with amine-free coatings. It was also reported that the presence of alcohols also leads to high reaction rates in polymerization of epoxides (Enikolopiyan 1976; Barbey and Klok 2010; Sarıipek and Karaman 2014).

3.3.2. Characterizations of QD-4AT Nanoprobe

In the second part of the study, the synthesis of QD- 4AT nanoprobe, its attachment to functionalized polymer thin films and evaluation of the feasibility of polymer-bonded QD-4AT nanoprobe as fluorescent sensor structure were investigated using pGMA homopolymer. The nanoprobe was synthesized either by the formation of a covalent or weak bond between QD and 4AT. QD-4AT nanoprobe complex before and after binding to iCVD deposited pGMA films was characterized via EPR analysis to investigate the bonding of nanoprobes to the polymer surface by comparing the EPR data.

The effect of QD and 4AT interaction time was examined by comparing EPR spectrum of the reference study and EPR spectra after procedures A and B which have 4

and 24 h interaction times, respectively. In addition, the effect of initial 4AT concentration on QD-4AT complex formation was investigated. The effect of QD and 4AT interaction time was evaluated based on the change in the amount of bound nitroxide to CdTe QDs for procedures A and B with comparison to free 4AT as shown in EPR spectra of samples in Figure 3.11.

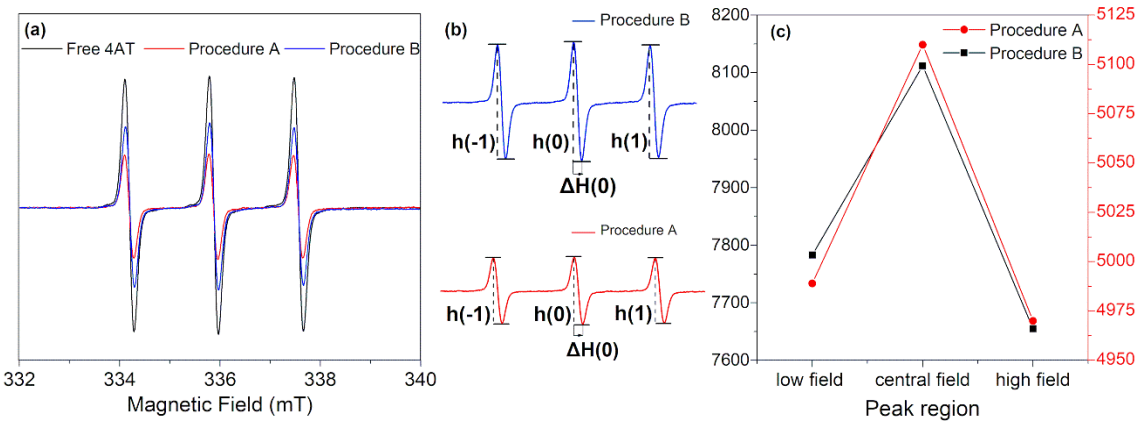

Figure 3.11. a) EPR spectra of procedure A (4 h interaction of QDs and 4AT), procedure B (24 h interaction of QDs and 4AT), and free 4AT, b) parameters (h(-1); h(0); h(1); ΔH(0)) of an EPR spectrum necessary to calculate the effective rotational correlation time (τR), c) peak to peak height changes for both procedure A and B.

In Figure 3.11, EPR spectra of free 4AT reference study illustrates the three characteristic ^{14}N hyperfine splitting as black line, which is consistent with previously reported studies in literature (Maurel et al. 2006; Tansakul et al. 2010; Adegoke et al. 2012). In both procedures A and B, the same amount of CdTe QDs was added to 4AT solution. In literature studies, it has been observed that the ratio [4AT]/([4AT]+[QD]) affects line broadening. With a ratio greater than 0.5, sharp peaks are observed as in free 4AT, no line broadening (Maurel et al. 2006). In this study, [4AT]/([4AT]+[QD]) ratio is greater than 0.9, since the 4AT concentration was much higher than the concentration of CdTe QD. As expected, line broadening was not observed in either procedure as seen in Figure 3.11a. However, peak intensities in procedure B were higher when compared with procedure A. Although the same amounts of QD and 4AT were used in both procedures, the interaction of the QD-4AT nanoprobe increased as time increased, which allowed

more nitroxide radicals to attach to the QD surface in procedure B. As the amount of 4AT interacting with QD increased, the amount of 4AT detected by EPR also increased. Also, the peak-to-peak height at the high-field peak in EPR signal is slightly less than those at central and low fields for both procedures (Figure 3.11b and c). The distortion of high field peak occurs as a result of the interaction between QD and 4AT proving that the nitroxide radical is bound to QD surface (Lin et al. 2012). The attachment of 4AT to QD surface causes a slowdown in rotational motion of spin labels. The motion of a nitroxide side-chain is characterized by the effective correlation time, τR (Schreier et al. 1978; Lin et al. 2012; Blaskó et al. 2017). In EPR, the molecular freedom of movement is quantitatively related to the rotational correlation time of the nitroxide spin-labeled molecule, and the rotational correlation time is described as (Lin et al. 2012);

$$\tau_R = 6.51x10^{-10}x\Delta H(0)\left[\sqrt{\frac{h(0)}{h(-1)}} + \sqrt{\frac{h(0)}{h(1)}} - 2\right] \quad (3.1)$$

where ΔH(0) is the peak-to-peak line width of the mid-field line and the peak-to-peak amplitude of the lateral lines of the peaks from low field to high field are referred to as h(-1), h(0) and h(1), respectively (Figure 3.11b).

Accordingly, the rotational correlation time can be useful to evaluate in which procedure more nitroxide radicals are attached to QD surface. The larger rotational correlation time indicates a slower motional regime after the attachment (Schreier et al. 1978; Lin et al. 2012; Blaskó et al. 2017). The rotational correlation time, τR, for procedures A and B was found as $3.018x10^{-12}$ s and $5.914x10^{-12}$ s, respectively; therefore, more nitroxide radicals were bound to QD surface in procedure B. Based on this result, procedure B with longer interaction time was selected as main QD-4AT nanoprobe complex formation procedure for the rest of the study.

The effect of initial radical concentration on the formation of QD-4AT complex was evaluated following procedure B. The concentration of 4AT was increased 10x and 50x compared to the CdTe QDs concentration in the solution, and EPR analysis was performed as shown in Figure 3.12.

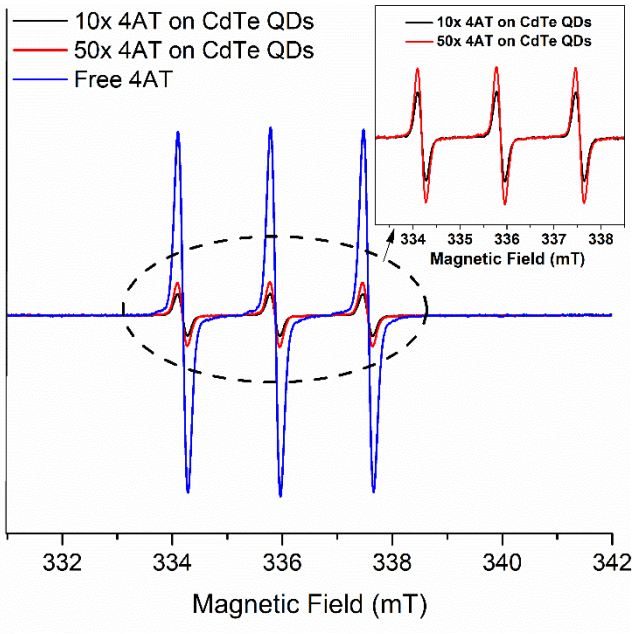

Figure 3.12. EPR spectra of 4AT at 10x and 50x concentration compared with CdTe QDs.

As expected, EPR peak intensities of QD-4AT complex are lower than peak intensity of free 4AT due to bonding on QD surface as seen in Figure 3.12. Increasing the concentration of 4AT from 10x to 50x resulted in an increase in the EPR peak intensity due to higher amount of 4AT molecules which are bonded to QDs. Similar to time studies described in Figure 3.11, 4AT concentration was much higher than that of CdTe QD. For 10x and 50x of 4AT concentrations used, [4AT]/([4AT]+[QD]) ratios were 0.91 and 0.98, respectively; therefore, no significant peak broadening was observed with the formation of QD-4AT nanoprobe complex (Maurel et al. 2006).

To examine whether a covalent or weak bond interaction occurs between 4AT and QD, QD-4AT nanoprobe synthesis procedure was carried out with and without EDC. EPR spectra obtained from the pellet and supernatant samples after centrifugation are given in Figure 3.13.

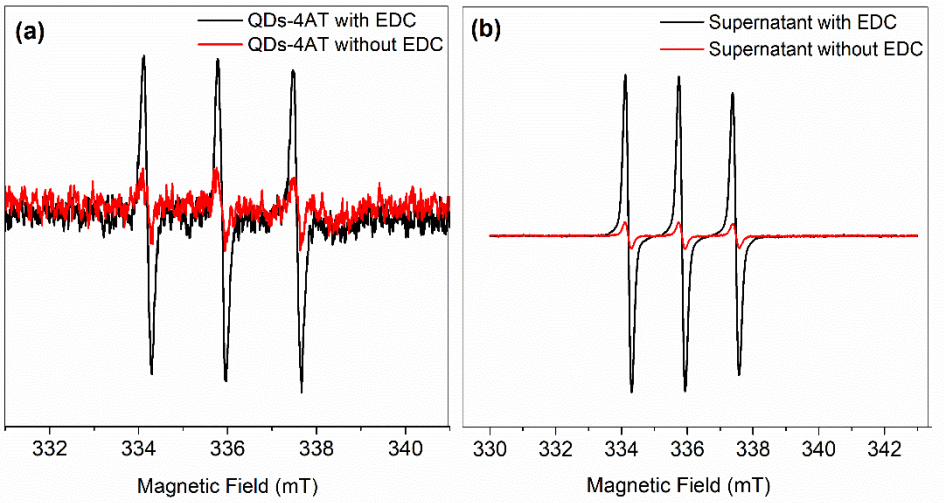

Figure 3.13. EPR spectra of a) pellet samples and b) supernatant samples with and without EDC.

As seen in EPR spectra from pellet samples (Figure 3.13a), EPR signals of QD-4AT with EDC are easily identified with three characteristic ^{14}N hyperfine splitting peaks when compared with QD-4AT without EDC. This is a clear validation of formation of QD-4AT complex by covalent bonding of nitroxides to the QD surface activated with EDC. EPR spectra shown in Figure 3.13b belong to the supernatant samples of EDC and EDC-free experiments, respectively. Similar to pellet samples, peak intensities are much higher for samples with EDC; however, samples without EDC also show three characteristic peaks with much lower intensities. Therefore, it is reasonable to assume that when EDC was added to the solution, QD activation and the formation of QD-4AT complex occurred with a covalent bond. Without EDC, free TEMPO radicals were not seen in the supernatant medium because EPR intensities were very low, so complex formation may have also occurred with weak bond interaction between QDs and 4AT.

Also, the EPR signals of EDC-free experiment of the supernatant samples were obtained lower than expected when compared with the results of the pellet samples. This may be due to electrostatic bonds. Because electrostatic bonds are more flexible than covalent bonds, 4AT radicals may come closer to the QD surface with electrostatic bonds compared to covalent bonds (Maurel et al. 2006; Scaiano et al. 2006; Tansakul et al. 2010; Lin et al. 2012). It is expected that the EPR signal intensity should be high if covalent bonds are formed between QD and 4AT due to the certain distance between the ligaments, and lower EPR signal should be obtained with weak bonds since the proximity between

the QD and 4AT increases due to flexibility in the weak bonds. Based on these results, it can be stated that the formation of QD-4AT complex by weak bonds in the experiments without EDC and existence of covalent bond with the use of EDC were observed in this study.

In addition to the interactions between QD and 4AT in the liquid phase, fluorescence quenching was investigated by attaching QD-4AT complex into pGMA homopolymer thin film for fluorescent sensor operation.

3.3.3. Attachment of QD-4AT nanoprobes to pGMA homopolymer

Polymer-QD-4AT nanoprobe complex generation procedure was performed following the procedure described in previous section. EPR spectra of pGMA thin-film coatings immersed in reference solution containing only 4AT molecule and QD-4AT nanoprobe solution are given in Figure 3.14.

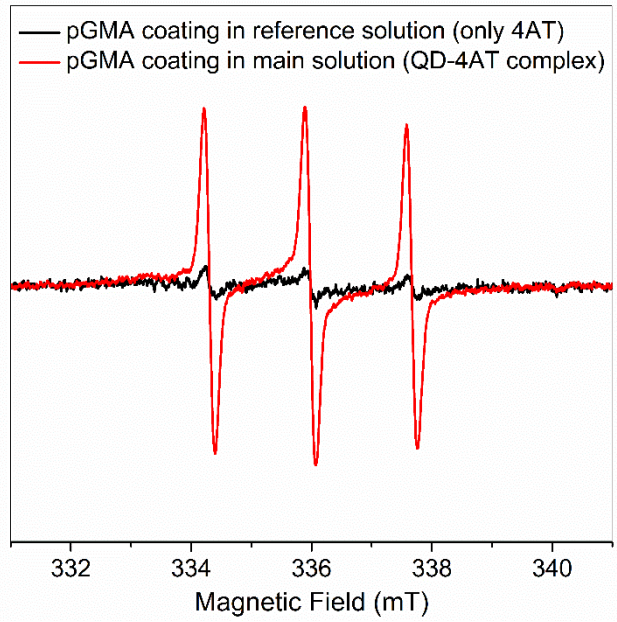

Figure 3.14. EPR spectra of pGMA homopolymer thin films processed with only 4AT and QD-4AT nanoprobe solutions.

EPR spectra of pGMA homopolymer coatings given above illustrate that in the absence of QDs, 4ATs could not bind to polymer surface on their own as indicated with a very weak spectrum (black line), as expected. However, when QDs are introduced to 4AT solution for the formation of nanoprobe complex, QD-4AT complex attached to polymer as indicated by the three characteristic ^{14}N hyperfine splitting peaks in EPR spectrum (red line) in Figure 3.14.

In order to examine the variation of the spectrum after nanoprobe bonding to the polymer surface, a comparison was made between spectra of 4AT in water and pGMA homopolymer coating after immersed into the QD-4AT complex. EPR spectra were normalized, and then, difference between the signals was examined (Figure 3.15).

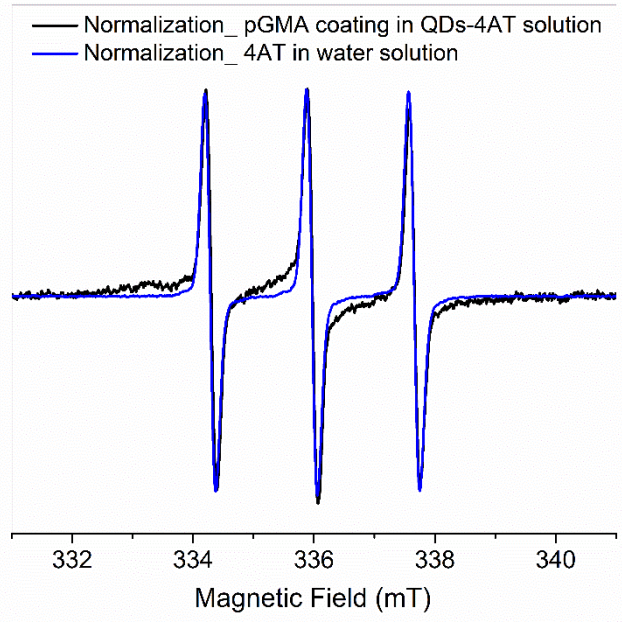

Figure 3.15. Normalized EPR spectra of pGMA homopolymer thin film in QD-4AT solution and 4AT in water.

As seen in Figure 3.15, EPR spectra of 4AT in water (blue line) exhibit three very sharp ^{14}N hyperfine splitting peaks. EPR spectrum of pGMA polymer in QD-4AT solution (black line) also shows these three peaks, but a significant broadening at peak bases is observed. The peak broadening is a result of restricted motion of the spin labels (Göksel and Akdogan 2019; Yildiz et al. 2020) indicating that QD-4AT nanoprobe is bound to polymer surface. However, clearly identified three distinct and sharp peaks of

pGMA polymer in QD-4AT solution also indicate that the radicals are not very close to each other on the polymer surface since more densely packing on the polymer surface would result in very broad peaks. Since the pGMA polymer samples were thoroughly dried, it is not possible to relate sharp peaks to remaining water that may have contain free 4AT radicals. Therefore, EPR analysis shown in Figure 3.15 proves that QD-4AT nanoprobes are homogeneously distributed on the polymer surface without any agglomeration. Binding of the QD-4AT nanoprobe to the polymer surface performed with the formation of amide bonds between the QD and the amine group on the polymer surface in the EDC/NHS reaction medium. The relevant mechanism is given in Sect. ‘‘QD attachment to functionalized thin films’’.

3.3.4. Fluorescence quenching mechanism

Tansakul et al. studied the examination of quenching efficiency by using different nitroxide radicals and reported that the nitroxide quenching efficiency depends on both the binding affinity and the proximity of the nitroxide moiety to the QD surface (Tansakul et al. 2010). As a result of the study, it was seen that the proximity effect was dominant while the hydrogen bond also contributed to the quenching effect. The quenching efficiency is highly dependent on distance to QD surface; therefore, an electron exchange mechanism is more possible. This mechanism necessitates close proximity with the excited electron in the conduction band and should be favored for smaller nanoparticles (Chen et al. 2008). Based on CdTe QDs used in this study (~ 2 to 3 nm), the electron exchange mechanism can be seen as the main mechanism for quenching, but more experiments are needed to evaluate the dependence of nitroxide fluorescence quenching on QD size.

To investigate fluorescence quenching of QD-4AT nanoprobes, fluorescence microscopy and spectroscopy analysis were performed. Fluorescence microscopy images of pGMA homopolymer films after QD and QD-4AT nanoprobe complex attachment process are shown in Figure 3.16.

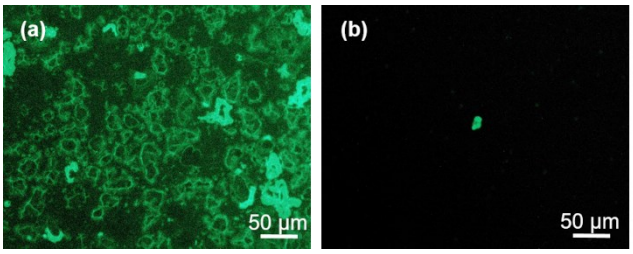

Figure 3.16. Fluorescence microscopy images of a) CdTe QD attached pGMA homopolymer thin film surface and b) QD-4AT attached pGMA homopolymer thin film surface.

Fluorescence microscopy image shown in Figure 3.16a shows pGMA homopolymer film after QD attachment procedure and the green emission of CdTe QDs indicates the QD attachment process was successful. On the other hand, Figure 3.16b shows fluorescence microscopy image of pGMA film after QD-4AT nanoprobe complex attachment process. This image also indicates successful bonding of QD-4AT complex to polymer surface due to lack of typical green emission due to fluorescence quenching caused by 4AT. These observations agree well with the results of EPR analysis. Additionally, fluorescence spectroscopy analysis was performed using QD-4AT complex solution to investigate the effect of time on the fluorescence quenching. Fluorescence intensity vs wavelength plot of QD-4AT complex solution is shown in Figure 3.17.

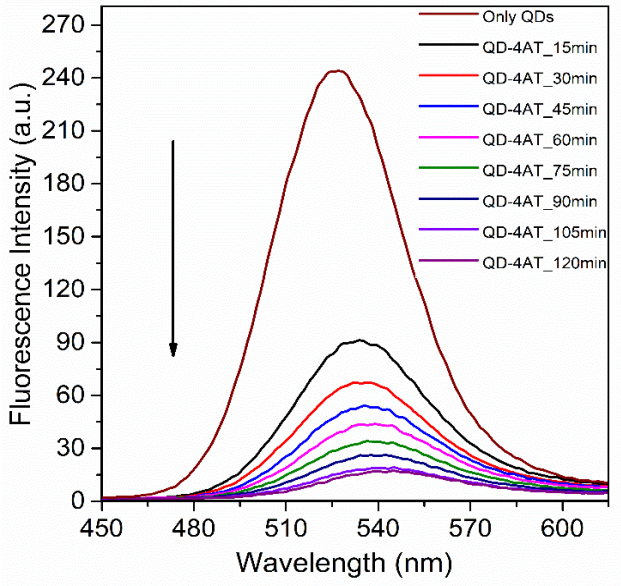

Figure 3.17. Fluorescence spectra of QD-4AT nanoprobe in water.

As expected, fluorescence spectra of QD-4AT complex solution shows a decrease in fluorescence intensity as more nitroxides bond to QD surface as time increases. Due to high 4AT concentration, the quenching rate was higher compared to similar studies in the literature (Diaz et al. 1999; Jin et al. 2004; Laferrière et al. 2006). It was observed that more than 50% quenching occurs in 15 min and after 120 min the fluorescence intensity does not decrease significantly. In addition, after formation of the QD-4AT complex, small red shift was observed compared with the only QDs fluorescence. This is related to surface modification of QD after interaction with 4AT and higher concentration of 4AT used for QD-4AT complex (Diaz et al. 1999; Jin et al. 2004; Laferrière et al. 2006). Fluorescence quenching can be also observed visually. The difference in fluorescence intensities between two samples one containing only CdTe QDs and other containing QD-4AT complex under UV light can be seen visually as shown in Figure 3.18.

Figure 3.18. Visual inspection of QDs in water (left) and QD-4AT complex (right) approximately 24 h after preparation.

The significant decrease in fluorescence observed visually and confirmed by fluorescence spectroscopy shows the potential of using polymer bond QD-radical sensors as multiple-use, cheap and easy to use fluorescent sensors in various applications. The results obtained in this study indicate that the demonstrated polymer-bonded nanoprobe structure can be used for target material detection in fluorescence sensor studies.

3.4. Conclusion

A novel functional polymer-based QDs-nitroxide radical complex was demonstrated as nanoprobe for fluorescent sensors. The study was carried out in two parts: in the first part synthesis of pGMA and p(GMA-co-DEAEMA) copolymer thin films via iCVD method, amine group functionalization of these thin films via epoxy ring opening reactions to achieve binding of CdTe QDs on the functionalized polymeric surfaces were demonstrated. Aromatic primary amine (aniline), aliphatic primary amine (propylamine) and aliphatic tertiary amine (Et_3N) were compared for nucleophilic epoxy ring opening reactions and QD attachment. Propylamine was found to be the most effective amine for functionalization of iCVD deposited pGMA and p(GMA-co-DEAEMA) thin-film surfaces and CdTe QD attachment to functionalized polymer surface.

In the second part of the study, the synthesis and attachment of QD-4AT nanoprobes to functionalized pGMA thin films and feasibility of using QD-4AT nanoprobes were investigated. In this part, study was carried out using only pGMA homopolymer since no significant difference was observed between homo and copolymers in terms of functionalization in the first part of the study. Characterization of QD-4AT nanoprobe was performed by EPR analysis by considering interaction time and initial 4AT concentration. It was found that high initial 4AT concentration and longer (24 h) interaction time are beneficial as more nitroxide radicals bond to QD surface compared to 4 h interaction time. EPR analysis also revealed the existence of covalent bond between QD and 4AT when EDC was used during nanoprobe synthesis, and weak bonds when EDC was not used. In both cases, QD-4AT nanoprobes were successfully synthesized. Further EPR analysis together with fluorescence microscopy investigation confirmed successful attachment of QD-4AT nanoprobes to pGMA surface. The feasibility of using QD-4AT nanoprobes for fluorescent sensor applications based on fluorescence quenching was demonstrated by fluorescence microscopy and spectroscopy analysis. Time-depended fluorescence quenching analysis revealed that more than 50% reduction in fluorescence intensity, which can also be observed visually, occurred within 15 min demonstrating the possibility of using polymer bonded QD-4AT nanoprobes as multiple-use and easy to use as sensor structure in various applications.

CHAPTER 4

CVD DEPOSITED EPOXY COPOLYMERS AS PROTECTIVE COATINGS FOR OPTICAL SURFACES

4.1. Introduction

Optical materials (glasses, mirrors, lenses, prisms, filters, etc.) are widely used in a variety of applications such as electronic and medical equipment, automotive and construction sector, aerospace industries, and various military and civilian electro-optic devices. Due to their widespread use, these materials may work in very harsh, unstable and corrosive conditions, and can be exposed to various solvents, dust and humidity, vibration, radiation, rapid temperature changes and physical abuse. Such conditions can reduce the performance and useful lifespan of these materials (Wilson and Hawkes 1998; Dakin and Brown 2006; Boentoro and Szyszka 2013; Ohring and Kasprzak 2015). Repairing damaged optical surfaces is usually expensive if not impossible, and protection of the materials is thus essential.

There are two basic requirements for coatings on optical surfaces. The coating material(s) should not interfere with the optical performance of the system, i.e., the coatings should be transparent in the respective wavelength ranges, and the coating should provide acceptable chemical and/or physical protection. In this regard, polymer films have attracted a lot of interest since they can provide physical and chemical protection to optical surfaces (Boentoro and Szyszka 2013). In the literature, a variety of polymeric materials as poly(methyl methacrylate) (PMMA) (Michaeli, Hessner, and Klaiber 2009), poly(carbonate) (PC) (Singh et al. 1996; Pazos, Baselga, and Bravo 2003), poly(styrene) (PS) (Gokan, Esho, and Ohnishi 1983), poly(urethane) (PU) (Ma, Jen, and Dalton 2002),

This chapter has been published as:
Karabıyık, Merve, Gizem Cihanoğlu, and Özgenç Ebil. 2023. "CVD Deposited Epoxy Copolymers as Protective Coatings for Optical Surfaces." Polymers 15 (3):652. https://doi.org/10.3390/polym15030652.

poly(ethylene terephthalate) (PET), poly(ethylene naphthalate) (PEN) (Zhao et al. 2021), benzocyclobutene (BCB) (Kane and Krchnavek 1995), perfluorovinyl ether cyclopolymer (CY-TOP) (Zhao et al. 2000), tetrafluoroethylene and perfluorovinyl ether copolymer (Teflon AF) (Resnick and Buck 1997), fluorinated poly(arylene ether sulfide) (FPAESI) (Kim et al. 2001), and fluorinated hyperbranched polymers (Pitois et al. 2001) were investigated as coatings on optical surfaces. Most of these studies suggest that homopolymer films do not exhibit the thermal and mechanical strength required for the protection of optical surfaces on their own (Pan et al. 2022; Sun, Rawat, and Chen 2022; Yin et al. 2022). To overcome this issue, crosslinking and combining polymeric materials (Zhao et al. 2019; Bhattacharjee et al. 2022; Pan et al. 2022; Shen et al. 2022) or modifying the polymer surface with inorganic coatings to improve thermal, mechanical and optical properties and adhesion between the coating and the substrate (Althues, Simon, and Kaskel 2007; Sun, Rawat, and Chen 2022; Yin et al. 2022) have been evaluated. Zhao et al. (2019) fabricated liquid-release polymeric gel films with a novel bilayer structure which consist of a slippery liquid-locked rough top layer and liquid-supplied bottom layer by one-pot casting (Zhao et al. 2019). Bhattacharjee et al. (2022) fabricated polymeric sheets by combining cationic amphiphilic water-soluble polyethylenimine derivative (QPEINH-C6) and poly(vinyl alcohol) (PVA). Polymeric sheets showed antimicrobial properties and high mechanical durability and were highly transparent (86−90% transmittance in visible spectrum) (Bhattacharjee et al. 2022). Sulfoxide biphenyl polyimide PI (TFSODA/BPDA) optical coatings prepared via a low-temperature process demonstrated high optical performance (88.5% between 380 and 780 nm) and good thermal properties (Shen et al. 2022). A polyimide composite membrane with SiO_2 antireflective layer prepared by a sol-gel method exhibited good thermal stability and up to 93% optical transmittance between 500 and 800 nm (Yin et al. 2022). Sun et al. (2022) combined oxygen plasma and pulse laser deposition to fabricate polycarbonate with nanoporous silica film. Silica coated polymer film exhibited high transparency (89.9% within 420–700 nm), excellent mechanical robustness, and excellent antifogging performance (Sun, Rawat, and Chen 2022). Althues (2007) et al. fabricated transparent nanocomposites consisting of europium doped yttrium vanadate (YVO4:Eu) nanoparticles in methyl methacrylate (MMA) and lauryl acrylate (LA) matrices with excellent optical properties (transmission >90% in visible spectrum) (Althues, Simon, and Kaskel 2007).

The commonly used methods for fabrication of polymeric films such as dip coating and spin coating are usually applied to flat surfaces, but issues related to solvent use (wetting of surface, solvent evaporation, etc.) and difficulty in accurate control of film thickness still exist. In addition, optical materials to be coated may be damaged due to substrate-solvent interactions. Since optical surfaces also vary greatly in shape and size, and may have micro-and nano-structured features, solventless processes such as physical vapor deposition (PVD) and chemical vapor deposition (CVD) should be considered despite a higher cost of fabrication due to vacuum requirements (Träger 2012; Boentoro and Szyszka 2013). A CVD process is similar to a PVD but at least one chemical reaction takes place for the deposition of the thin film (Piegari and Flory 2013). Initiated chemical vapor deposition (iCVD) is a well-established process for synthesis of thin polymeric films. Compared to other CVD methods, iCVD offers a lower thermal budget (low filament temperatures between 200–400ºC). The low deposition temperature enables use of a variety of substrates including plastics, inorganic materials, textiles, glass, membranes, carbon nanotubes, etc. The iCVD process can achieve high deposition rates with precise thickness and morphology control and without damaging functional groups of monomers (Lau et al. 2003; Gupta and Gleason 2006b, a; Lau and Gleason 2006a, b; Bakker et al. 2007; Lau and Gleason 2007b; Gupta et al. 2008b; Lau and Gleason 2008; Coclite et al. 2009; Parker, Baechle, and Demaree 2011; Aresta et al. 2012; Sarıipek and Karaman 2014; Gleason 2015). During iCVD polymerization, monomer units are sent to the reactor in the vapor phase where they are adsorbed on the cooled substrate surface (0–40ºC). The unsaturated bonds of the adsorbed monomers are activated by free radicals produced via thermal decomposition of an initiator molecule (typically 200–400ºC). Free radical polymerization takes place (including initiation, propagation and termination steps) on the substrate surface (Chan et al. 2006; Gupta and Gleason 2006b; Mao and Gleason 2006; Bakker et al. 2007; Martin et al. 2007; Gupta et al. 2008a; Tenhaeff and Gleason 2008; Coclite et al. 2009; Asatekin and Gleason 2010; Ozaydin-Ince and Gleason 2010; Parker, Baechle, and Demaree 2011; Gleason 2015; Chen et al. 2016). In recent years, iCVD has emerged as an attractive alternative for fabrication of polymer thin films to protect surfaces against aggressive media. Employing a transparent and very adhesive polymer thin film such as poly(glycidyl methacrylate) (poly(GMA)) can lead to enhanced chemical and mechanical properties due to the epoxy ring ($-C_2H_3O$) which provides a good binding site (Bakker et al. 2007; Xu and Gleason 2010b; Jeevendrakumar, Pascual, and Bergkvist 2015). In addition, poly(GMA) is a promising candidate for coatings on

optical surfaces requiring transparent and durable protective layers (Lee et al. 1996; Yang, Kang, and Neoh 2000).

Here, we report the fabrication of robust cross-linked copolymer thin films of GMA with ethylene glycol dimethacrylate (EGDMA) and 2,4,6,8-tetramethyl-2,4,6,8-tetravinylcyclotetrasiloxane (V4D4) via iCVD as protective coatings for optical surfaces. Cross-linked copolymers can improve chemical and mechanical durability while maintaining high optical transmittance in the visible spectrum. To the best of our knowledge, this is the first study in the literature where the effect of cross-linkers on poly(GMA) based polymer thin films are investigated as protective coatings. This work also demonstrates the feasibility of non-fluorinated polymers to protect optical surfaces. Another goal of this contribution is to demonstrate the effectiveness of the iCVD process to tailor properties of polymer films by crosslinking during polymerization without losing functional groups.

4.2. Materials and Methods

4.2.1. Materials

Homopolymers of glycidyl methacrylate (poly(GMA)), ethylene glycol dimethacrylate (poly(EGDMA)) and 2,4,6,8-tetramethyl-2,4,6,8 tetravinylcyclotetrasiloxane (poly(V4D4)), and copolymers poly(GMA-co-EDMA) and poly(GMA-co-V4D4) were fabricated as thin films on crystalline silicon (c-Si) and glass substrates. Analytical grade chemicals, GMA (Sigma Aldrich, USA, 97%) as monomer, EGDMA (Sigma Aldrich, Burlington, MA, USA, 98%) and V4D4 (SigmaAldrich, USA, 97%) as crosslinkers and tert-butyl peroxide (TBPO, Sigma Aldrich, USA, 98%) as the initiator were used for the synthesis of thin film coatings. Various organic solvents such as toluene (Sigma-Aldrich, ≥99.5%), dichloromethane (DCM, Sigma Aldrich, USA), ethanol (Sigma Aldrich, USA, ≥99.8%), 1-propanol (Sigma-Aldrich, USA, ≥99.8%), acetone (Sigma Aldrich, USA, ≥99.5%), tetrahydrofuran (THF, Sigma Aldrich, USA,

99.9%), and N,N-dimethylformamide (DMF, Sigma Aldrich, USA) were used for the chemical durability tests.

4.2.2. Fabrication of Polymer Coatings

Polymer coatings were fabricated using a custom-built iCVD system. The square reactor chamber was 32 cm by 32 cm in size and had a height of 4 cm. A nichrome filament array suspended 2.5 cm above the substrate was used to provide thermal energy for the decomposition of the initiator. The filament temperature was measured with a type-K (Omega Engineering) thermocouple attached to the filaments. The temperature of the substrate was controlled by an external circulator (WiseCircu WCR-P8) connected to the bottom of the reactor. The vacuum was provided via a rotary vane pump (BSV10, Baosi). The reactor pressure was controlled with a throttling butterfly valve (MKS Model 253) connected to a pressure controller (MKS Type 651C). Poly(GMA), poly(EGDMA), poly(V4D4) homopolymers and poly(GMA-co-EGDMA) and poly(GMA-co-V4D4) copolymers were deposited on crystalline silicon (c-Si) wafers and BK7 optical glass substrates. In order to obtain sufficient vapor pressure, GMA, EGDMA and V4D4 monomers were heated to 65, 85 and 90ºC, respectively. For homopolymer coatings, monomers were fed into the chamber through a special mass-flow controller (MKS1150C). TBPO was metered into the reactor at room temperature through a mass-flow controller (MKS 1479A). Reactor pressure was maintained at 250 or 515 mTorr during this study. The average thickness of polymer coatings was 350 nm ± 50 nm. The deposition conditions for homopolymers and copolymers are summarized in Table 4.1.

Table 4.1. Summary of iCVD process conditions for copolymers.

iCVD Sample	Substrate Temp. ºC	Filament Temp. ºC	Pressure mTorr	Flow rate (sccm)				Flow Ratio Crosslinker/ GMA
				TBPO	GMA	EGDMA	V4D4	
pGMA	25 or 35	300	250	0.8	0.4			
ECOP-1					1.6			0.25
ECOP-2	25	330	515	2	0.8	0.4		0.5
ECOP-3					0.4			1

(cont. on next page)

Table 4.1 (cont.)

pEGDMA	25	330	515	2		0.4		
VCOP-1							0.1	0.25
VCOP-2	35	300	250	0.8	0.4		0.2	0.5
VCOP-3							0.4	1
pV4D4	35	300	250	0.8			0.4	

4.2.3. Film Characterization

Mprobe-Vis20 reflectometer system with a spectral range of 400–1100 nm and 2 nm measurement accuracy was used to measure the thicknesses of fabricated films. For the evaluation of the quality and chemical composition of fabricated polymer films a Perkin Elmer Inc. (Shelton, CT) BX FTIR (Fourier Transform Infrared Spectroscopy) Spectrometer was used. The spectra of the polymer films were measured from 4000 to 650 cm^{-1}. All spectra were baseline corrected and thickness normalized. Surface morphologies of fabricated iCVD polymer coatings were investigated using a Scanning Electron Microscope (SEM) (FEI Quanta250, Hillsboro, OR). Surface roughness was measured by Atomic-force Microscopy (AFM) using a Nanosurf-Flex Axiom system. A BEL MPL-2 polarization microscope was employed to evaluate the surface of the films before and after the adhesion tests. Thermogravimetric Analysis (TGA) was performed using a Shimadzu TGA-51 system.

4.2.4. Chemical Stability and Durability Tests

The durability of fabricated homopolymer and copolymer coatings was investigated by solubility, adhesions, and thermal tests. Solubility tests were performed by immersing coatings into various solvents for 30 min. The immersed samples were then dried at 70^{o}C for 1 h to remove excess solvent from the surface. Salt resistance tests were performed in 5 wt. % NaCl solutions at room temperature for 1 day. Film thicknesses were measured before and after the immersion. The experiments were carried out at least

three times, and the standard deviation was ± 5%. The adhesion tests of polymer coatings to silicon substrates were performed by following the procedure described previously in the literature (Özpirin and Ebil 2018; Cihanoğlu and Ebil 2021). A cellophane adhesive tape was placed on the film surface and then rapidly removed from the surface at the angle that was normal to the surface. The percentage of delamination was calculated by dividing the test surface into equally spaced grids. The coating adhesion was evaluated by optical microscope analysis. The thermal durability was evaluated by annealing the coatings at temperatures up to 250ºC for 4 h (10ºC min^{-1} heating rate) in a furnace. Thermogravimetric analysis of samples (ca. 10 mg) was performed at a constant heating rate of 10ºC min^{-1}, from room temperature to 1000ºC, under a nitrogen flow.

4.3. Results and Discussion

4.3.1. Deposition Rate

For copolymer depositions, the flow rates of monomers were varied to obtain copolymers with different compositions, as shown in Table 4.1. Although the iCVD process can achieve extremely high deposition rates (of the order of nm min^{-1}), the process parameters were carefully selected to yield much lower deposition rates (<10 nm min^{-1}) to accurately control film thickness and uniformity. In the iCVD process, the deposition rate is inversely proportional to the substrate temperature. Lower substrate temperature leads to increased monomer adsorption on the surface resulting in a higher deposition rate (Lau and Gleason 2006a, b). However, a low substrate temperature might also lead to condensation due to excessive monomer concentration on the substrate surface (Gleason 2015). For the deposition of poly(GMA-co-V4D4) (VCOP) copolymer, the substrate temperature was increased to 35ºC from 25ºC to avoid condensation. Poly(GMA-co-EGDMA) (ECOP) copolymer depositions were performed at 25ºC. Copolymer deposition rates for ECOP and VCOP copolymers are shown in Figure 4.1. The deposition rate of poly(GMA-co-EGDMA) copolymers decreased as the flow rate ratio of EGDMA/GMA increased from 0.25 to 1. For the poly(GMA-co-V4D4)

copolymers, higher deposition rates were observed as the flow rate ratio of V4D4/GMA increased.

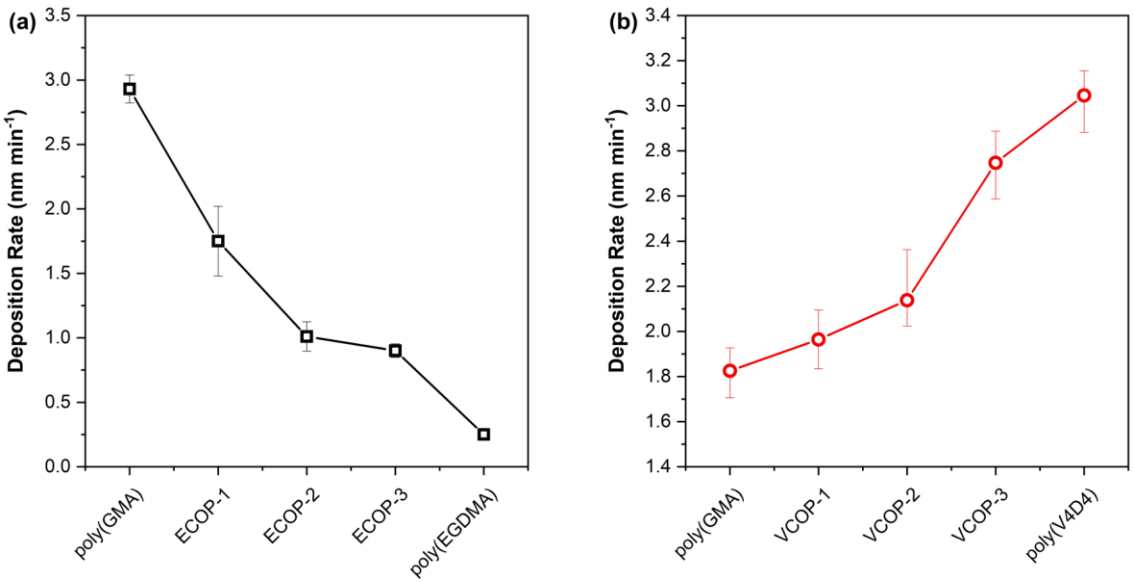

Figure 4.1. Deposition rates of (a) poly(GMA), poly(EGDMA) and ECOP (black squares), and (b) poly(GMA), poly(V4D4) and VCOP (red circles).

4.3.2. Chemical Composition

Chemical compositions of monomers and homopolymers were investigated via FTIR analysis as shown in Figure 4.2.

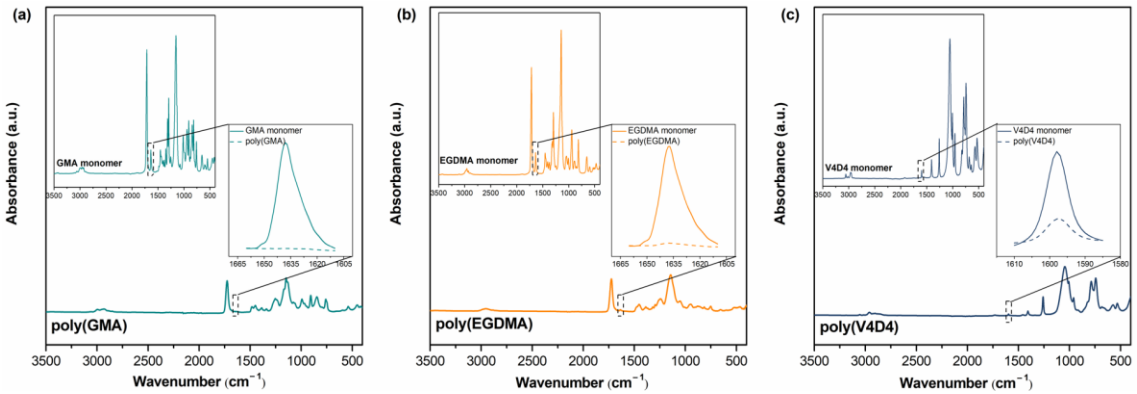

Figure 4.2. FTIR spectra of (a) GMA (green), (b) EGDMA (orange) and (c) V4D4 (blue) monomers and their polymers.

The characteristic peaks of C-O-C epoxy ring vibrations at 758, 845 and 906 cm^{-1} are clearly shown in poly(GMA) (Marinović et al. 2011). The symmetric epoxy ring deformation, asymmetric epoxy ring deformation, and the epoxy ring breathing vibration for poly(GMA) are seen in the region of 840–853 cm^{-1}, 912–920 cm^{-1}, and near 1241–1251 cm^{-1}, respectively. The strong absorption from C-O-C asymmetric and symmetric stretching vibrations in the region of 883–912 cm^{-1} and 1246–1322 cm^{-1} also masks the epoxy ring deformation and breathing vibrations, respectively (Nyquist 2001). The region of the infrared spectrum from 1200 to 700 cm^{-1} belongs to the fingerprint region. Many different vibrations, including C-O, C-C and C-N single bond stretches and C-H bending vibrations are found in this region, therefore stretching and bending vibrations of various groups overlap with that of the epoxy group (Nyquist 2001; Marinović et al. 2011). For poly(EGDMA) homopolymer, the peak formed at 1716 cm^{-1} belongs to the valence vibration of the ester group (C=O) (Haoue et al. 2020). For poly(GMA) and poly(EGDMA) homopolymers, the peaks at 1161, 1252 and 1727 cm^{-1} show C-O, C-C and C=O stretching vibrations, respectively (Stefanović et al. 2015; Zhao et al. 2018). The band around 1630–1640 cm^{-1} in both monomer GMA and EGDMA represents the vinyl group and the absence of this peak in both homopolymer spectra indicates complete polymerization of all monomers on the substrate surface (Iqbal et al. 2009). Figure 4.2c shows that the vinyl (CH_2=CH–) group peak intensity of V4D4 monomer at 1598 cm^{-1} decreased to a certain extent in poly(V4D4) spectrum, indicating that polymerization of V4D4 monomer was successfully achieved by consuming vinyl functionality; however,

a significant amount of vinyl group still remained in the final polymer. A V4D4 monomer molecule contains 4 vinyl groups and the complete consumption of the vinyl group by free radical polymerization was shown to be impossible due to the steric hindrance (Yoo et al. 2013; Seok et al. 2018; Abessolo Ondo et al. 2019). The existence of monomer-specific wagging of Si-$(CH_2)_x$-Si (963 cm^{-1}), asymmetric Si-O-Si stretching (1075 cm^{-1}), Si-CH_3 symmetric bending (1260 cm^{-1}), and the bending in Si-CH_2 (1410 cm^{-1}) in poly(V4D4) spectrum also indicate the preservation of functional groups of the monomer (Shokuhfar and Arab 2013; Yoo et al. 2013; Seok et al. 2018; Abessolo Ondo et al. 2019).

Poly(GMA-co-EGDMA) and poly(GMA-co-V4D4) polymerizations in iCVD are shown in Figure 4.3. It should be noted that in Figure 4.3c, poly(GMA-co-V4D4) copolymer structure does not represent the real structure since not all vinyl bonds in V4D4 monomer participate in cross-linking, as discussed above.

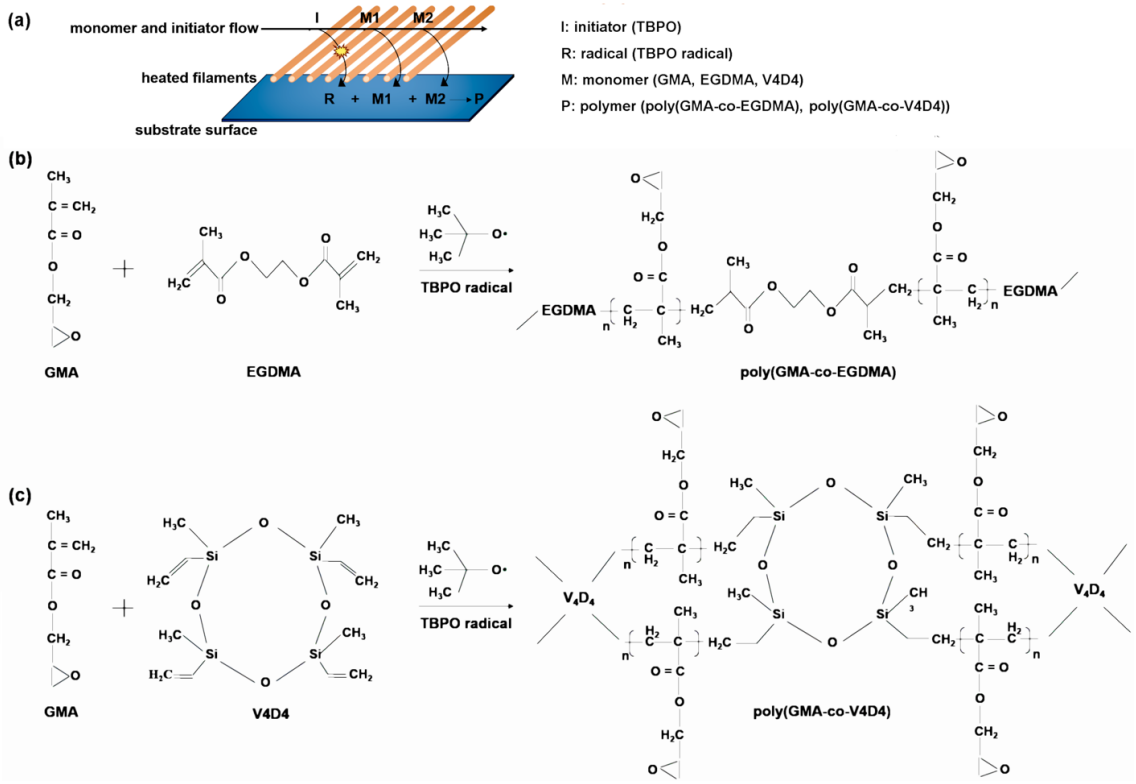

Figure 4.3. Schematics of (a) iCVD process, (b) poly(GMA-co-EGDMA) and (c) poly(GMA-co-V4D4) copolymer film synthesis.

Figure 4.4 shows FTIR spectra of homopolymers and copolymers deposited via iCVD.

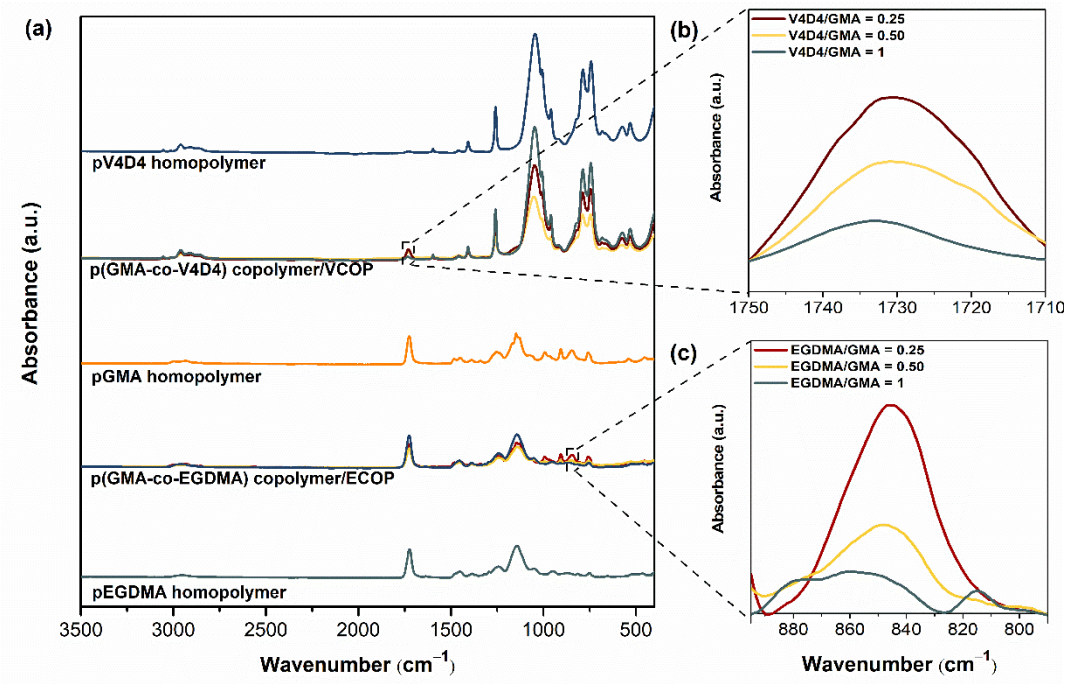

Figure 4.4. FTIR spectra of (a) GMA, EGDMA and V4D4 homopolymers and their copolymers, (b) poly(GMA-co-V4D4) copolymers, and (c) poly(GMA-co-EGDMA) copolymers.

Figure 4.4b shows the enlargement of a portion of Figure 4.4a emphasizing the absorption peak from 1710 and 1750 cm^{-1} where the specific peaks of GMA are located. Peak intensities related to C=O stretching decreased as the V4D4/GMA flow rate ratio was increased gradually from 0.25 to 1. Figure 4.4c shows the enlargements of a portion of Figure 4.4a, indicating the epoxy peak (the C-O-C vibration) of GMA at 846 cm^{-1}. The composition of copolymer coatings can be controlled by adjusting the monomer flow rates. The highest peak intensity was observed when the EGDMA/GMA flow rate ratio was 0.25 and declined with decreasing GMA in copolymer composition. However, the decrease in the peak intensity (peak area) does not necessarily correspond to feed composition due to difference in monomer adsorption rates on the surface (Gleason 2015).

4.3.3. Chemical Stability

Chemical stability of homopolymers and copolymers was evaluated by immersion of samples in various organic solvents. The relative changes in thicknesses of homo and copolymer coatings before and after immersion in organic solvents (DCM, acetone, THF, DMF, IPA and ethanol) are shown in Figure 4.5. The Hildebrand solubility parameter (δ) is a good way to determine whether a substance is a good solvent or nonsolvent for a polymer (Venkatram et al. 2019). When the difference between the Hildebrand solubility parameters of the polymer (δp) and solvent (δs) is low ($|\delta p - \delta s| \leq 2$), the solvent may be considered a good solvent (or solvating solvent) of that polymer. On the other hand, when this difference is high ($|\delta p - \delta s| \geq 2$), this solvent is considered a thermodynamically poor solvent of the polymer. According to the literature data, DCM can be considered as good (δs = 19.8) (J. Brandrup 1999), and ethanol is a poor solvent (δs = 26.6) (J. Brandrup 1999) of the epoxy polymer (δp = 17.8) (Tao and Anthamatten 2016). Unlike poly(EGDMA) homopolymer, poly(GMA) homopolymer is not usually resistant to organic solvents. As expected, poly(GMA-co-EGDMA) copolymers with higher EGDMA content (ECOP-2 and ECOP-3) exhibited better resistance than poly(GMA) with less than 10% thickness loss. Poly(V4D4) homopolymer showed better resistance to organic solvents compared to poly(GMA) with a maximum 15% thickness loss. Among poly(GMA-co-V4D4) copolymer coatings, VCOP-1 demonstrated the best resistance against organic solvents with a maximum 5% thickness loss. The difference in resistivity to organic solvents between poly(GMA-co-V4D4) and poly(GMA-co-EGDMA) coatings is related to the difference in the number of reactive sites per monomer. V4D4 monomer provides two more reactive groups for cross-linking compared to EGDMA monomer. Therefore, it is expected that poly(GMA-co-V4D4) copolymers should be more resistant to organic solvents (Shokuhfar and Arab 2013). However, we did not observe substantial difference in performances of poly(GMA-co-V4D4) and poly(GMA-co-EGDMA) copolymers (except ECOP-1) which might be related to the partial polymerization of vinyl groups in V4D4 due to steric hindrance.

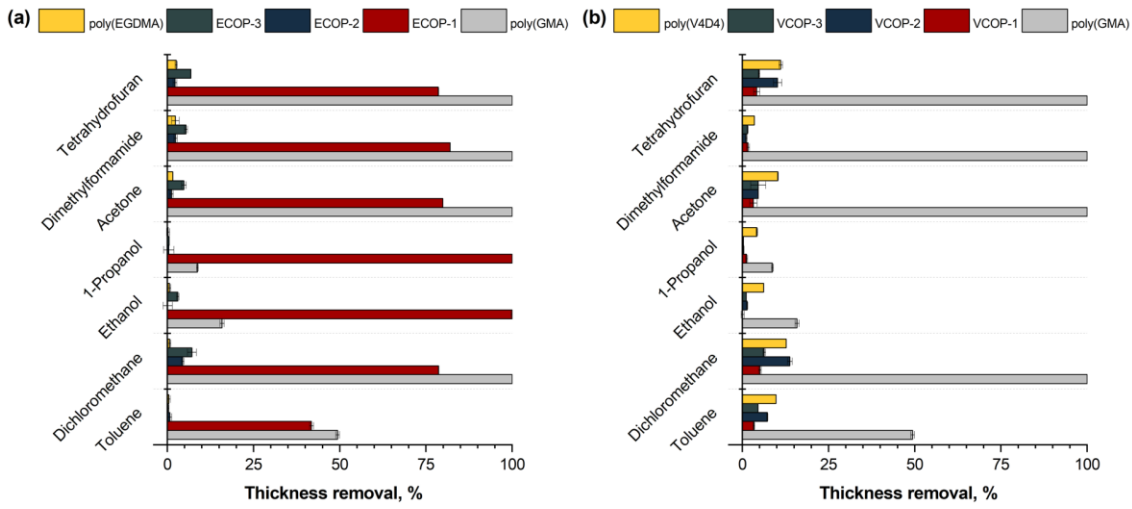

Figure 4.5. Relative change in film thickness of (a) poly(GMA), poly(EGDMA) homopolymers and their copolymers, and (b) poly(GMA), poly(V4D4) homopolymers and their copolymers in various solvents.

FTIR analysis was repeated after immersion in solvents. Figure 4.6 shows FTIR spectra of ECOP-2 and VCOP-1 copolymer coatings which were found to be the most durable copolymer films in organic solvents. All characteristic peaks of poly(GMA-co-EGDMA) and poly(GMA-co-V4D4) copolymers remained visible after immersion in THF, DCM, DMF, acetone, ethanol, toluene, and 1-propanol for 30 min. However, the reduction in peak intensities was much less for ECOP-2 and VCOP-1 compared to other copolymers. VCOP-1 exhibited very slight peak intensity reduction in only DCM which was one of the strongest solvents used in this study.

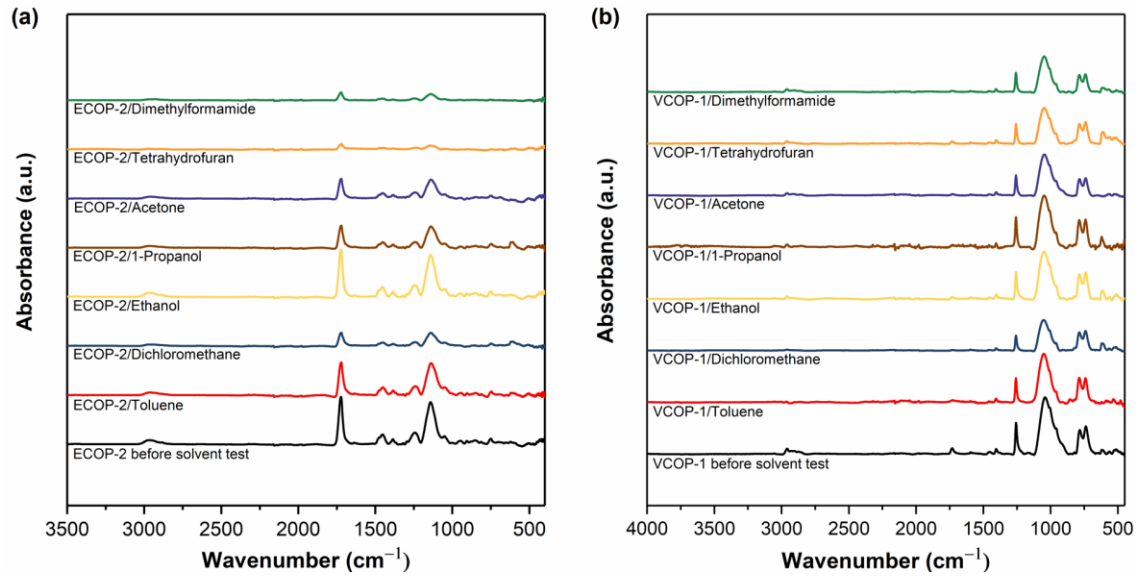

Figure 4.6. FTIR spectra of (a) ECOP-2 and (b) VCOP-1 copolymers before and after immersion in organic solvents.

To further evaluate the chemical durability of ECOP-2 and VCOP-1 copolymer coatings, samples were immersed in DCM and ethanol (a weaker solvent) for 30 days. The relative changes in film thicknesses after 30 days are shown in Figure 4.7.

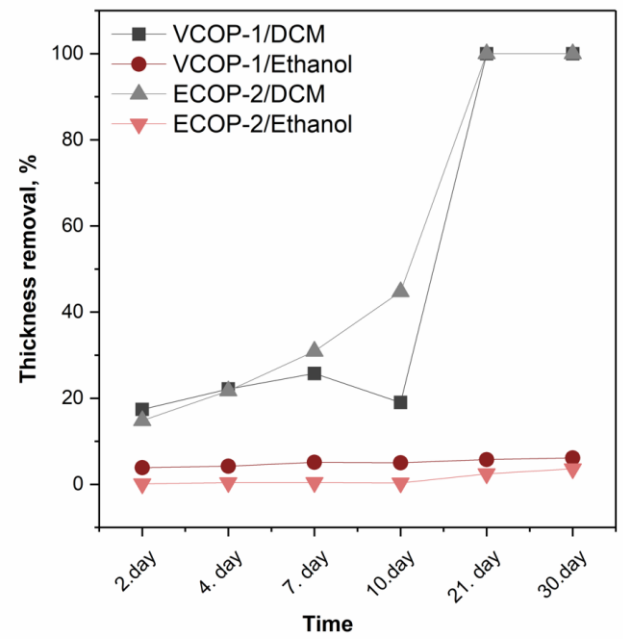

Figure 4.7. Relative change in film thickness for copolymers after immersion in DCM and ethanol.

Immersion in ethanol did not lead to a significant thickness loss for the copolymers. However, ECOP-2 and VCOP-1 coatings were dissolved in DCM completely after 20 days. Still, the results indicate that these copolymers can act as effective protective coatings against accidental exposure to very strong solvents and can serve as protective barriers very long times in weak solvents.

SEM images of ECOP-2 and VCOP-1 copolymer coatings before and after immersion in DCM and ethanol are shown in Figure 4.8. ECOP-2 copolymer showed a slight increase in surface roughness after immersion in ethanol while VCOP-1 copolymer showed no change in surface morphology. Both copolymers showed wrinkling leading to crack formation, and eventually complete delamination from the surface after immersion in DCM. It is suspected that immersion in DCM solvent weakens the adhesion of coatings to c-Si substrate and coatings are released from the substrates in pieces. The difference in the amount of delamination for ECOP-2 and VCOP-1 coatings can be clearly seen in SEM images which also supports FTIR analysis and thickness measurements after the tests.

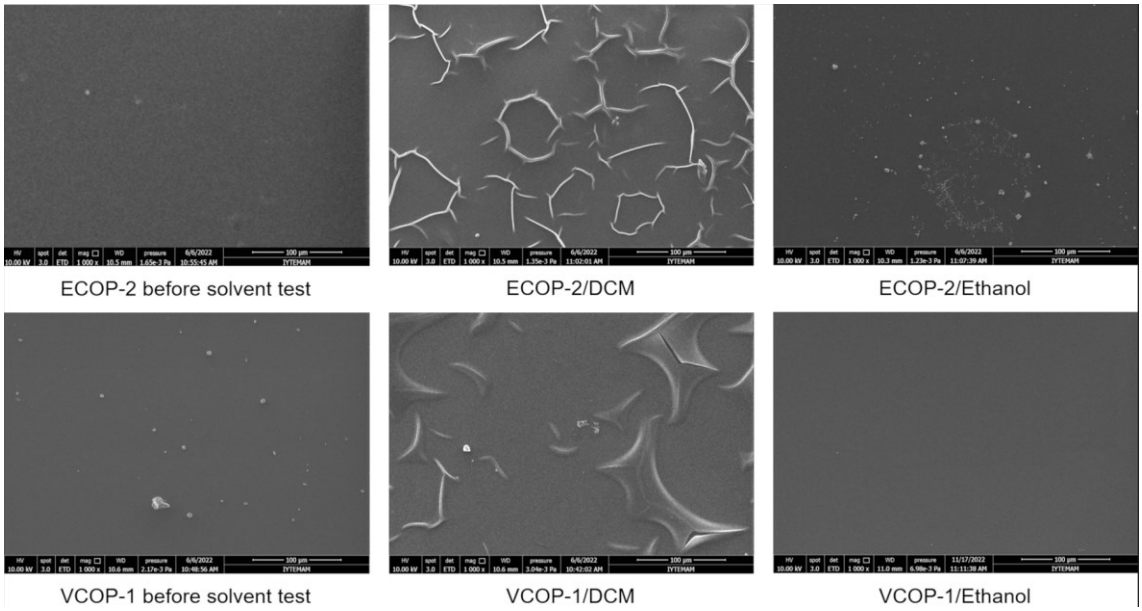

Figure 4.8. SEM images of ECOP-2 and VCOP-1 copolymers before and after immersion in DCM and ethanol for 30 min.

Figure 4.9 shows AFM images of ECOP-2 and VCOP-1 copolymers before and after immersion in DCM and ethanol which support SEM analysis. For clarity, image scales are different as the VCOP-1 copolymer coating has a smoother surface. While the coatings had different surface morphologies, the change in surface roughness was clear for ECOP-2 copolymer while VCOP-1 copolymer showed no change in morphology in ethanol and exhibited the first signs of delamination in DCM.

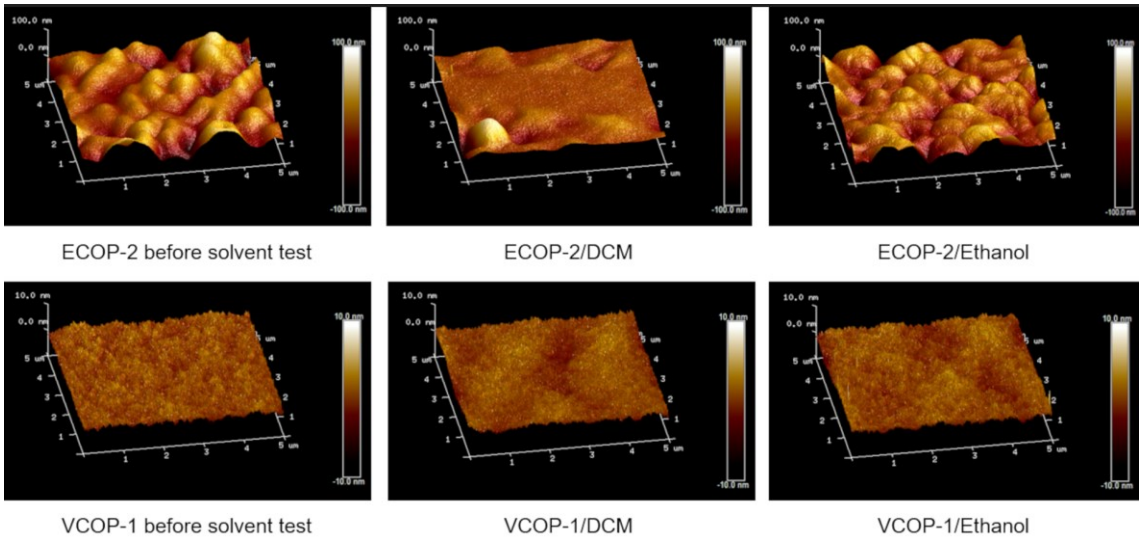

Figure 4.9. AFM surface analysis of copolymers before and after immersion in DCM and ethanol for 30 min.

The mean roughness (R_a) and root-mean-square roughness (R_q) values are also given in Table 4.2 below. As seen in Figure 4.9, the surface roughness of the ECOP-2 copolymer, both before and after the solvent test, is considerably higher than VCOP-1. In the literature, the existence of spherical structures leading to increased surface roughness on iCVD poly(GMA) films were reported (Bakker et al. 2007; Özpirin and Ebil 2018). However, both VCOP-1 and ECOP-2 copolymers contain GMA, and the VCOP-1 copolymer exhibits a very smooth surface. The difference between surface morphologies may be related solely to crosslinking monomer (EGDMA vs. V4D4). After immersion in solvents, surface roughness gradually decreases due to removal of ECOP-2 from the surface (Christian, Coclite, and J. 2017). The VCOP-1 copolymer exhibited no significant change in surface roughness before the complete removal from the surface after 20 days.

Table 4.2. Surface roughness changes for ECOP-2 and VCOP-1 copolymer coatings.

Sample	R_q	R_a
ECOP-2	23.1	17.3
ECOP-2/Ethanol	17	12.4
ECOP-2/DCM	9.46	7.25
VCOP-1	0.807	0.646
VCOP-1/Ethanol	0.756	0.6
VCOP-1/DCM	0.931	0.743

4.3.4. Water and Saltwater Resistance

Protective coatings play a vital role in electronic and optical devices providing a physical barrier between substrates and aggressive media. Electronic and optical devices can be exposed to water either by accident or intentionally due to the operational environment. iCVD polymers with some degree of crosslinking usually exhibit low solubility in water (Martin et al. 2007; Cihanoğlu and Ebil 2021). Water solubility tests were performed by immersion of iCVD homo- and copolymers in deionized water for 48 h. Thickness measurements performed before and after the water solubility test are given in Figure 4.10. Both poly(GMA) and poly(EGDMA) homopolymers showed around 2% thickness loss. Interestingly, only ECOP-3 copolymer showed significantly more resistance to immersion in water with less than 0.5% thickness loss. While poly(V4D4) homopolymer is resistant to immersion in water (around 0.5% thickness loss), all poly(GMA-co-V4D4) copolymers exhibited better resistance than homopolymers and ECOP copolymers.

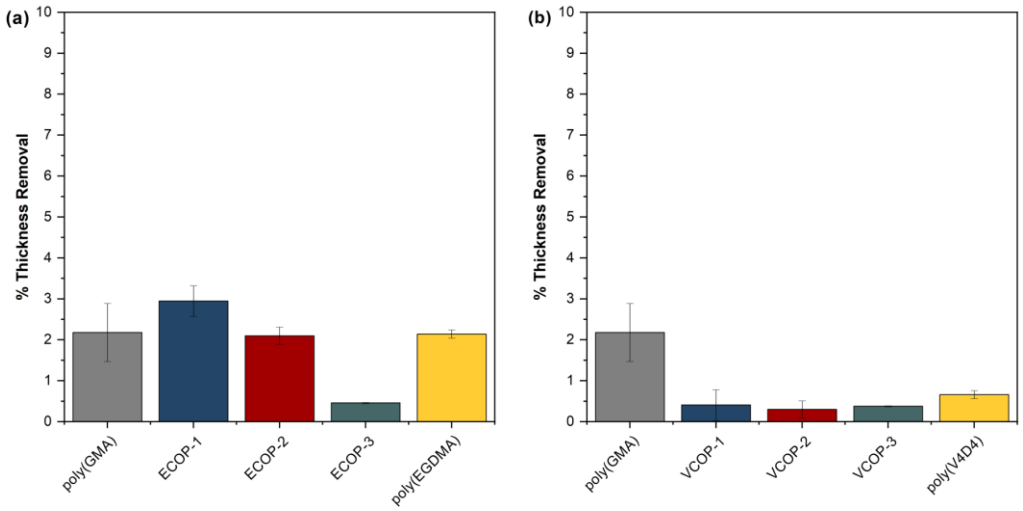

Figure 4.10. Relative change in film thickness for homo and (a) poly(GMA-co EGDMA) (b) poly(GMA-co-V4D4) copolymer coatings immersed in water for 48h.

Since optical surfaces can also be exposed to sea water, saltwater resistance tests of iCVD coatings on c-Si substrates were also performed. Coatings were immersed in 5 wt. % NaCl solution for 24 h. No significant changes in film thicknesses were observed, as shown in Figure 4.11. All coatings were quite resistant to the salt resistance test. All copolymers showed better saltwater resistance compared to homopolymer coatings with less than 2% thickness loss, demonstrating the effectiveness of crosslinking.

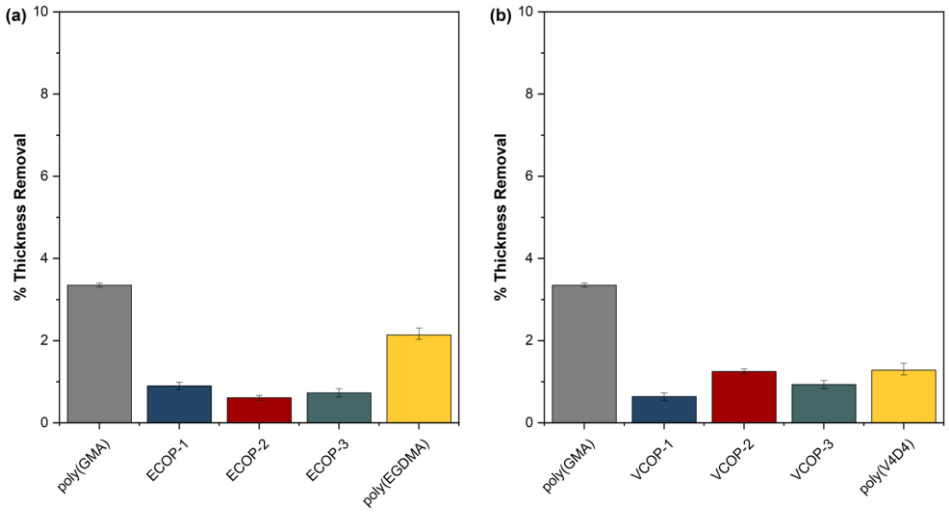

Figure 4.11. Relative change in film thickness of homo and (a) poly(GMA-co-EGDMA) (b) poly(GMAco-V4D4) copolymer coatings immersed in 5 wt. % NaCl solution for 24h.

4.3.5. Adhesion Test

An ideal protective coating should have excellent chemical durability and good adhesion to the surface. To evaluate the adhesion of homo and copolymer iCVD coatings, standard adhesion tests were performed. Figure 4.12 shows the optical microscope images of coatings before and after an adhesion test.

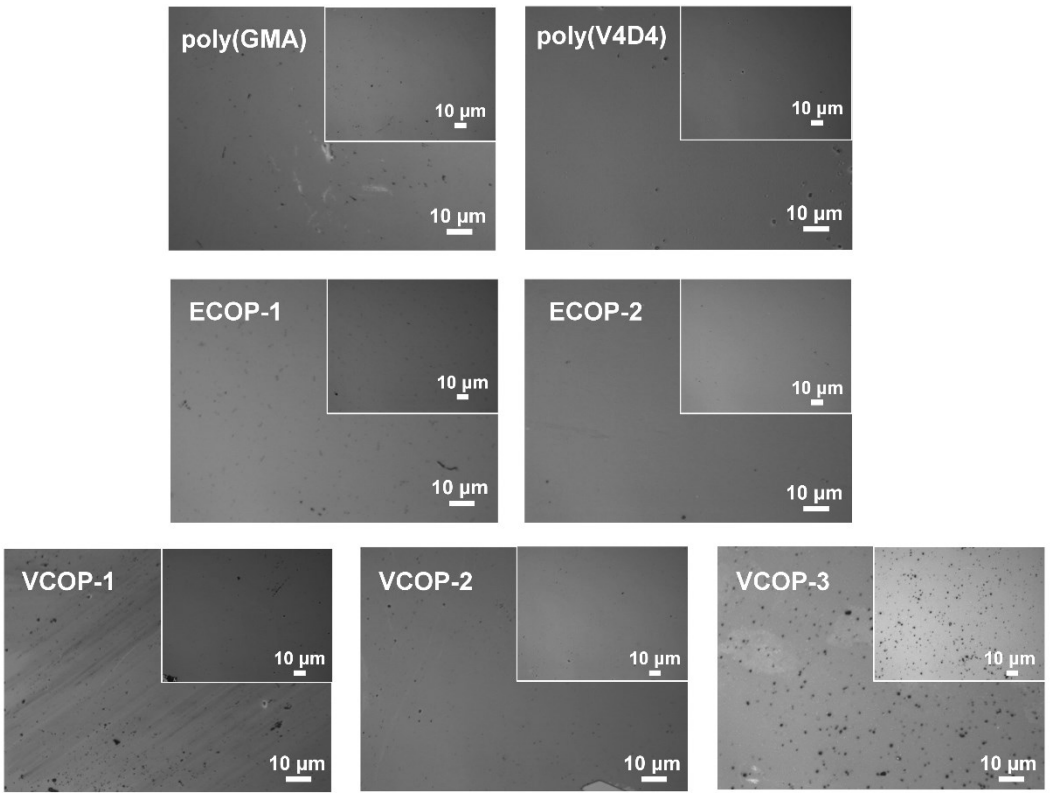

Figure 4.12. Optical microscopy images of homo and cross-linked copolymer films before (inset) and after (onset) adhesion test.

The large images (onset) in Figure 4.12 show the coating surface after the test with images in the upper right corner (inset) showing the pristine coatings. Cross-linked polymer coatings are known to have very good adhesion to most surfaces (Cihanoğlu and Ebil 2021). No defects or delamination were observed under optical microscope analysis of the surfaces for poly(GMA), ECOP-1 and ECOP-2. However, all sections of poly(EGDMA) and ECOP-3 coatings were removed by the cellophane tape from the

surface during adhesion tests; hence, the optical microscope images of poly(EGDMA) and ECOP-3 are not given in Figure 4.12. MIL-F-1 48616 and MIL-C-48497A standards cover adhesion tests for optical coatings and consider the removal of less than 5% of the sample area acceptable. For poly(GMA), ECOP-1 and ECOP-2 coatings, the area removed during the test was less than 0.5% which is still within the acceptable range according to the test protocols followed, except for ECOP-3 and poly(EGDMA). Poly(V4D4) homopolymer and poly(GMA-co-V4D4) copolymer coatings successfully passed the adhesion tests. The only exception was VCOP-2 coating with a small area detaching from the surface. However, the area removed was less than 0.1% of the sample which is still less than the adhesion test limit of 5%. Relative change in film thickness of homo and copolymer coatings after the adhesion test are shown in Figure 4.13. Optical microscopy evaluation of the samples supports chemical durability test results indicating that poly(GMA-co-V4D4) copolymer coatings exhibit slightly better durability and adhesion than homopolymers and poly(GMA-co-EGDMA) copolymers.

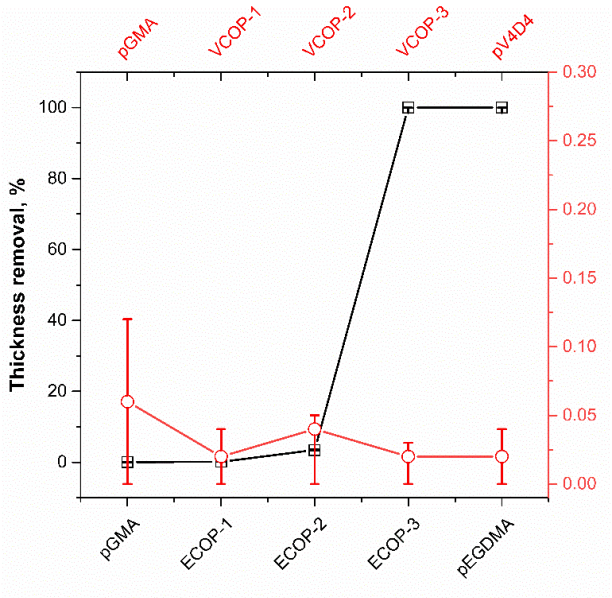

Figure 4.13 . Relative change in film thickness of homo and copolymer coatings after the adhesion test (black squares-poly(GMA), poly(EGDMA) and ECOP copolymers; red circles-poly(GMA), poly(V4D4) and VCOP copolymers).

Optical devices are also exposed to temperature variations during operation. Coatings for optical surfaces should be stable in a wide temperature range. It has been

shown that poly(GMA) thin films can be cross-linked via epoxy ring opening reaction by thermal annealing above 120°C in air (Jeevendrakumar, Pascual, and Bergkvist 2015). Thermal degradation and decomposition of poly(GMA) homopolymer film starts above 200°C (Özpirin and Ebil 2018). Cross-linking poly(GMA) polymers with a suitable monomer should increase chemical stability at higher temperatures. To evaluate temperature stability, VCOP-1 copolymer coatings were annealed at 250°C. Although VCOP-1 copolymer exhibited up to 28% thickness loss during annealing, FTIR analysis revealed almost identical spectra before and after the test, indicating good chemical stability, as seen in Figure 4.14.

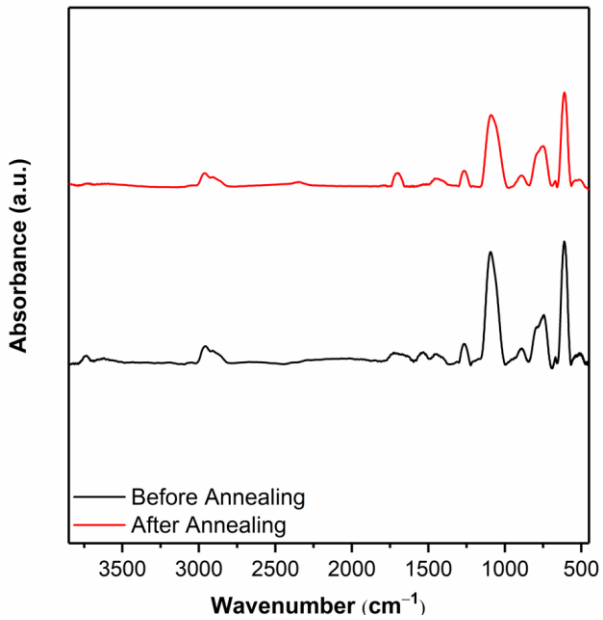

Figure 4.14. FTIR spectra of VCOP-1 films on c-Si substrate before and after annealing at 250ºC.

The peaks assigned to asymmetric Si-O-Si stretching at 1090 cm^{-1} and C-O-C epoxy ring vibrations at 760 cm^{-1} remained clearly visible after the annealing test. However, the peak intensities of VCOP-1 coating slightly decreased after the test which might be related to the change in film thickness. The change in the film thickness may be partially related to relaxation of the copolymer film. Optical microscopy analysis of the coating surface after the analysis did not reveal significant changes, defects, or damage

to the coating after annealing, confirming that crosslinked poly(GMA-co-V4D4) copolymer coatings are stable at temperatures up to 250°C without any degradation.

The thermal stability and degradation profiles of VCOP-1 were also evaluated by thermogravimetric analysis under nitrogen atmosphere, as shown in Figure 4.15. Siloxanes have high thermal stability due to the strength of their Si-O bond (Hao, Xu, and An 2014; García-Garrido et al. 2016). Therefore, the thermal stability of the copolymer produced using cross-linker (V4D4) is expected to be better than that of homopolymer poly(GMA) (Çaykara, Çakar, and Demirci 2008; Haloi, Mandal, and Singha 2013; Faria et al. 2019).

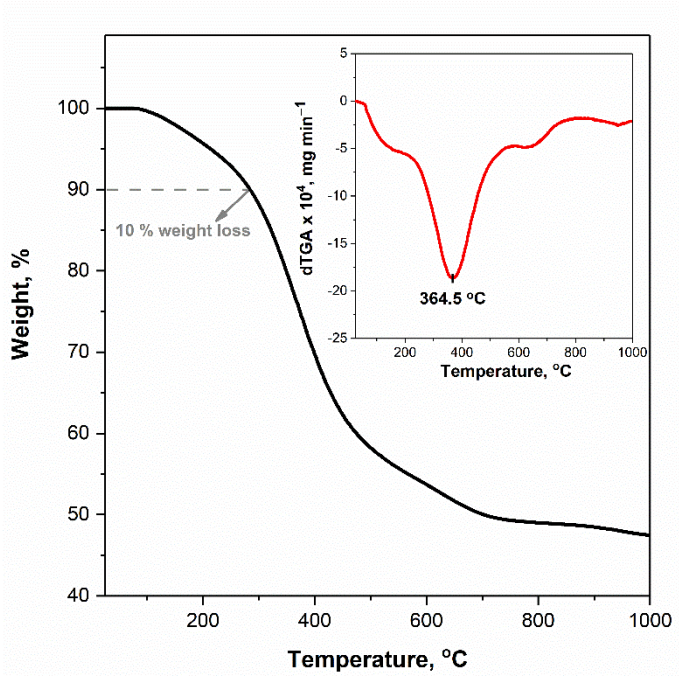

Figure 4.15. Experimental weight loss vs. T curves for thermal decomposition of VCOP-1 copolymer, black curve (insert, dTGA vs. T, red curve).

TGA curves shown in Figure 4.15 indicate that cross-linked VCOP-1 exhibits a degradation profile with three temperature zones which occur between room temperature to 177.8ºC, 285.7–473.4ºC and 580.6–709.3ºC, respectively. The first zone may be attributed to the loss of unreacted molecules during polymerization while the second and third weight losses correspond to the decomposition of the copolymer. Cross-linked VCOP-1 copolymer starts to decompose close to 285ºC and reaches the maximum

decomposition temperature at 364.5°C, and it has a second lower decomposition temperature at about 650.7°C. The results are in good agreement with data for other GMA-based cross-linked copolymers in the literature (Çaykara, Çakar, and Demirci 2008; Faria et al. 2019). TGA data show that the 10% weight loss temperature (T10%) is 285.7°C which is considered to represent the beginning of degradation of the copolymer. When compared with the reported TGA data of homopolymers poly(GMA) (Haloi, Mandal, and Singha 2013) and poly(V4D4) (García-Garrido et al. 2016) in the literature, crosslinked VCOP-1 has better thermal stability than uncrosslinked poly(GMA) homopolymer.

4.3.6. Optical Transmittance

Unlike most protective coatings used in a variety of substrates such as metals, plastics, electronic components, etc., protective coatings for optical surfaces must be transparent in the wavelength of interest and they must not affect the optical performance of the coated surface.

Optical transmittance of selected iCVD copolymers on BK7 glass substrates was modeled using TF Companion software between 300 and 1000 nm range. BK7 is a high-quality optical glass with high optical transmittance and near IR spectrum and is the most commonly used glass for optical windows, lenses, and prisms. In previous studies, it was shown that a coating with a thickness of less than 1000 nm would not significantly affect the optical transmittance of BK7 glass substrate in the visible region (Özpirin and Ebil 2018). The simulated optical transmittance of 1 μm thick ECOP-2 and VCOP-1 copolymer on BK7 glass substrates are shown in Figure 4.16. Simulated optical transmittance of ECOP-2 was slightly lower than VCOP-1 due to its higher refractive index (n=1.495) of VCOP-1 (n=1.487) however, the difference is negligible. Simulation results show that both copolymer coatings should not change the optical transmittance of BK7 glass substrate.

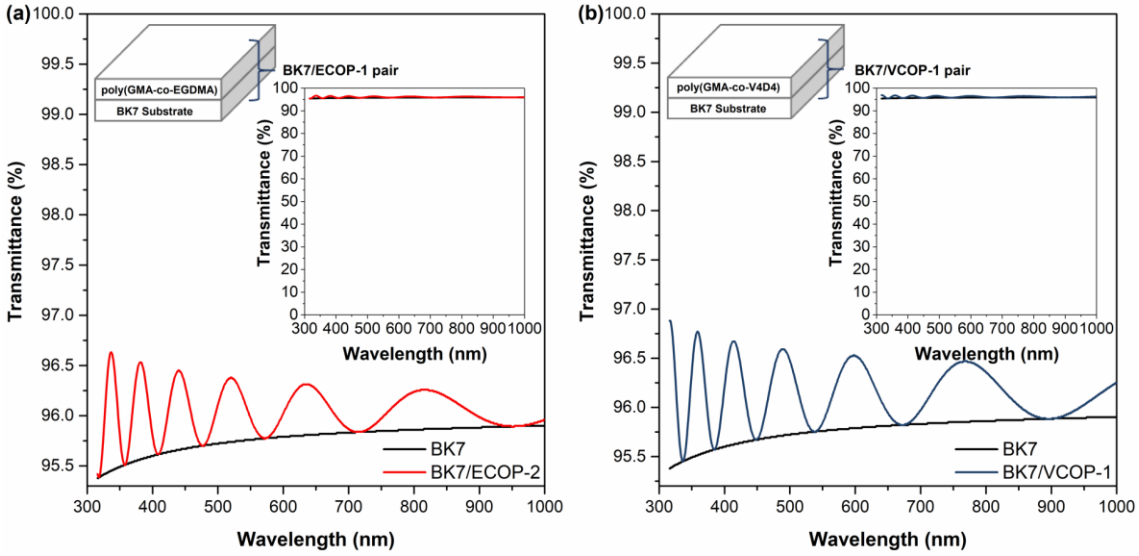

Figure 4.16. Modeled optical transmittance of (a) BK7/ECOP-2 and (b) BK7/VCOP-1 copolymer coatings.

To confirm the simulation results, 400nm thick VCOP-1 copolymers were deposited on optical glass substrates via iCVD using the conditions given in Table 4.1. The optical transmittance of VCOP-1 coated, and uncoated BK7 glass substrates are shown in Figure 4.17.

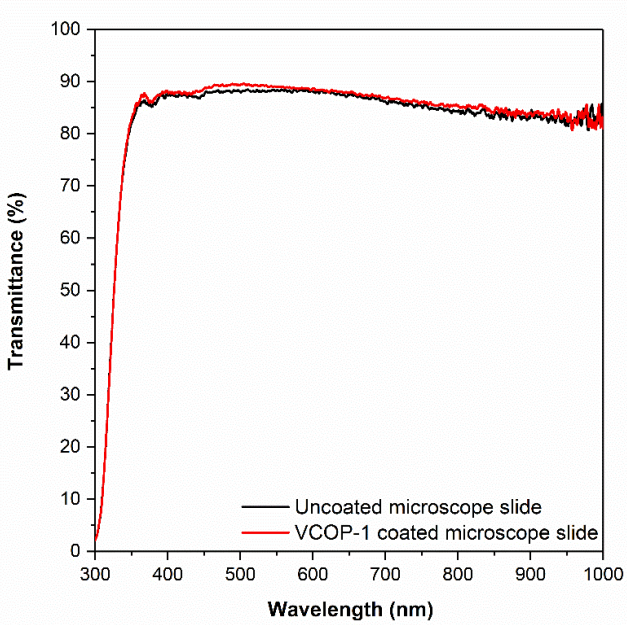

Figure 4.17. Measured optical transmittance of uncoated and VCOP-1 coated glass substrates.

Experimental measurements confirm simulation results. Although uncoated BK7 glass showed much lower optical transmittance (>85% in visible spectrum) compared to simulated transmittance (~95–96%), 400 nm VCOP-1 copolymer coating did not reduce the optical transmittance, it increased the transmittance very slightly between 450 and 600nm. The difference between simulated and measured optical transmittance for uncoated and coated glass substrates is mainly due to the quality of glass substrates used in the experimental study.

It should be noted that in the iCVD process the deposition rate of the polymer film strongly depends on the substrate temperature and does not depend on the substrate material; however, the final film morphology is affected by the substrate surface and film thickness. No measurable differences between chemical stability, optical transmittance and adhesion were observed between 350–400 nm thick iCVD copolymers deposited on glass and c-Si.

4.4. Conclusions

In this work, thin (350–400 nm) poly(GMA), poly(EGDMA), poly(V4D4) homopolymers and copolymers of poly(GMA-co-EGDMA) (ECOP series) and poly(GMA-co-V4D4) (VCOP series) with varying compositions were synthesized via the iCVD process on c-Si and glass substrates. The chemical durability, thermal stability, optical transmittance, and adhesion of coatings were evaluated for protection of optical surfaces used in a variety of applications. A comparative study has been carried out between ECOP and VCOP series of copolymer coatings. FTIR analysis confirmed that cross-linked copolymer thin films with the desired chemical composition can be obtained simply by changing the monomer flow rates during the polymerization process. It was also confirmed that functional groups of monomers are preserved in the process. ECOP-2 and VCOP-1 coatings were found to be the better performing coatings after chemical durability tests performed using various solvents. The durability of VCOP-1 coating was better than ECOP-2, especially in organic solvent immersion, water solubility and long-term stability tests, due to V4D4 crosslinker. VCOP-1 copolymer showed high thermal resistance and it was chemically stable at 250^{o}C. 400 nm thick VCOP-1 copolymer

coating on glass exhibited excellent optical transparency in the visible spectrum and did not affect the optical performance of the glass substrate. The results also show that non-fluorinated polymers can be tailored via iCVD copolymerization to fabricate protective transparent coatings for optical surfaces. The findings indicate that poly(GMA-co-EGDMA) and poly(GMA-co-V4D4) copolymer thin film coatings can provide excellent chemical and physical protection from the elements for optical surfaces without sacrificing optical performance. In theory, the chemical durability of the coatings could be further improved with addition of a fluorinated monomer, if necessary. The iCVD process also enables the preservation of functional groups during polymerization, so additional functionalities can be further activated. The possibility of removing the copolymer coatings using a suitable solvent and re-coating the surface is a big advantage of iCVD polymer coatings over inorganic coatings that are currently being used. In addition, the advantage of scalability, the ability to control film morphology and the ability to conformal coat complex non flat optical surfaces make the iCVD process an excellent candidate for fabrication of protective coatings at low cost.

CHAPTER 5

REUSABLE POLYMER-BASED FLUORESCENT SENSOR NANOPROBE FOR SELECTIVE DETECTION OF CD^{2+} ION IN REAL WATER SOURCES

5.1. Introduction

Heavy metal pollution has become one of the important environmental problems due to quick increase in global population associated with science and technology (Chen et al. 2020; García-Miranda Ferrari et al. 2020). Heavy metals are toxic even at low concentrations, therefore, releasing of them into the environment in any way such as leaching from the existing water infrastructure, agricultural, mining and industrial activities etc. creates a serious threat for surrounding environment and human health (Chen et al. 2019; De Acha et al. 2019; Chen et al. 2020; García-Miranda Ferrari et al. 2020). Some of these heavy metals are known as essential nutrients like iron (Fe), zinc (Zn), and cobalt (Co) but they can be toxic at higher concentrations (De Acha et al. 2019; García-Miranda Ferrari et al. 2020). According to the World Health Organization (WHO), cadmium (Cd), lead (Pb), mercury (Hg) and arsenic (As) are elements classified as highly toxic substances and contaminants which are not essential for plants and animals. They are also non-biodegradable; they can gradually accumulate in human body with different ways in which water plays a key role (Chithiraikumar, Balakrishnan, and Neelakantan 2017; Hemmati, Rajabi, and Asghari 2018; Chen et al. 2019). Among these toxic heavy metals, especially long term and high exposure to cadmium (Cd^{2+}), which has been widely used in industry and agriculture, has lead serious environmental and health problems including cardiovascular diseases and different types of cancers (Chithiraikumar, Balakrishnan, and Neelakantan 2017; Lin et al. 2019; Balali-Mood et al. 2021; Es-said et al. 2021). World Health Organization and Environmental Protection Agency fixed the

concentration limits of Cd^{2+} ion in drinking water as 0.003 mg/L (Chithiraikumar, Balakrishnan, and Neelakantan 2017; Chen et al. 2020). Therefore, sensitive and selective detection of Cd^{2+} ion at the early stage with low concentrations has attracted interest to prevent diseases and reduce its environmental impact (Chithiraikumar, Balakrishnan, and Neelakantan 2017; De Acha et al. 2019; Es-said et al. 2021). Although some of Cd^{2+} ion sensing probes have been reported in literature, the detection limits were not at sufficient levels. In addition, these sensing probes could only be used in liquid media rendering them single-use only.

Traditional approaches such as atomic absorption spectrometry (AAS), atomic emission spectrometry (AES), inductively coupled plasma mass spectrometry (ICP-MS) that have high sensitivity and accuracy, have been used for heavy metal ion detection in aqueous solutions (Suvarapu and Baek 2015). However, their implementation has been limited due to complex operations required in terms of complicated sample pretreatment or large sample volumes. As a result, various new sensing platforms were developed based on relatively lower cost and simple operational routes that include electrochemical (EC) methods, surface plasmon resonance (SPR) detections, quartz crystal microbalance (QCM), chemiluminescence (CL) and fluorescence methods (Wing Fen and Mahmood Mat Yunus 2013; Yang Shen 2019; Khanmohammadi et al. 2020). Fluorescence methods have attracted great interest due to high sensitivity, high accuracy, and relative simplicity (Li and Wang 2008; Koneswaran and Narayanaswamy 2009). The sensitivity, reliability, dynamic range and repeatability of fluorescence sensors relies upon the selection of the suitable fluorophore (Chen et al. 2020). When compared with the other fluorophores as small organic dyes, metal-ligand complexes, metal-organic frameworks (MOFs) and silica nanoparticles (Oliveira et al. 2015; Kumar et al. 2017; Rasheed et al. 2018; Samanta et al. 2020), semiconductor quantum dots (QDs) have advantages over others with regards to high quantum efficiency, large stokes shift, narrow emission spectra, long fluorescence lifetime and better optical stability properties. In addition, QDs are generally preferred for the detection of ions, as they maintain stability between the ions and functional groups interacting with target ions (Medintz et al. 2005; Wang et al. 2009; Zhang, Qi, and Wu 2010; Gan et al. 2012; Kim et al. 2012; Mandal, Dandapat, and De 2012; Pei et al. 2012; Wu et al. 2014; Zhou, Yang, and Zhang 2015; Gong et al. 2016; Chen et al. 2017; Hu et al. 2017). The most preferred quantum dots are CdTe QDs in sensor applications and particularly QDs that have carboxylic acid ligands can easily interact with functional

groups (Medintz et al. 2005; Xu and Gleason 2010b; Prabhakaran et al. 2012; McElroy et al. 2014; Zhou et al. 2016).

In literature, there are many studies on QD based sensors used to detect different ions. Simple QDs have disadvantages when used as sensor nanoprobe, such as non-specific binding with metal ions. In that case, the detection mechanism is generally based on quenching the luminescence intensity (Banerjee, Kar, and Santra 2008; Chen et al. 2017). In these studies, QDs either do not respond to certain ions like Li^{+}, Na^{+}, Zn^{2+}, Cd^{2+} or show luminescence quenching in the presence of various transition and heavy metal ions as Cu^{2+}, Fe^{2+}, Ni^{2+}, Hg^{2+} (Banerjee, Kar, and Santra 2008). Therefore, using only QDs cannot achieve selective detection of metal ions. On the other hand, using nanoprobes with ligands bonded to QDs have shown great promise for successful metal ion detection (Banerjee, Kar, and Santra 2008). Unlike previous approaches to detect metal ions by fluorescent quenching mechanism, detection with QD-ligand probes is usually accomplished by fluorescence enhancement (Banerjee, Kar, and Santra 2008; Gong et al. 2016; Elmizadeh et al. 2019; Zhang, Sun, and Wu 2019; Khan, Mitra, and Sahoo 2020). In addition to the target analyte, different factors in the environment can also cause photoluminescence (PL) quenching of the QDs reducing the accuracy of the detection of the target analyte. Therefore, the PL enhancement (PL “on” mode) seems more preferable. This is mainly because the PL "off-on" conversion in "on" mode can reduce the probability of false positives and is also more suitable for multiplexing. For instance, even if several detectors are used simultaneously, they can respond specifically to various analytes (Xu, Miao, et al. 2011).

Due to above mentioned factors, and considering studies of these nanoprobe types are quite rare in literature, the development of a QD-ligand-based sensor structure was determined as the first step in this study.

Controlled fluorescent quenching of QDs with ligands has led to development of custom fluorescent nanoprobes for different sensor applications (Chen et al. 2008; Tansakul et al. 2010). In literature, the most effective quenchers of fluorescence of small organic fluorophore were found to be nitroxide radicals (Chen et al. 2008; Tansakul et al. 2010; Xu, Chen, et al. 2011; Adegoke et al. 2012). Specifically, functionalized 2,2,6,6 tetramethylpiperidine-Noxide (TEMPO) radicals interact more with the QDs’ surface leading to strong binding (Maurel et al. 2006; Scaiano et al. 2006; Tansakul et al. 2010; Lin et al. 2012). In quenching efficiency studies, 4-Amino TEMPO (4AT) showed three times more effectiveness as a quencher compared with the other functionalized TEMPO

radicals such as amino pyrrolidine, carboxylic acid and bisamino (Tansakul et al. 2010). It was found to be a very suitable structure as a ligand in terms of sensor operations in detecting target materials (Chen et al. 2008; Tansakul et al. 2010; Adegoke et al. 2012).

The main aim of this study is to develop a multi-use polymer-based fluorescent sensor nanoprobe, contrary to disposable, single use sensor studies in liquid-phase demonstrated in literature. For polymer fabrication, initiated chemical vapor deposition (iCVD) system was used as main coating technique. The fact that no heavy metal detection studies in literature have been conducted with the QD-4AT nanoprobe structure until now also adds a unique value to this study.

5.2. Materials and Methods

This study was separated into three main sections: (i) the synthesis of CdTe QD-4Amino TEMPO nanoprobe and heavy metal ion detection via the nanoprobe; (ii) the fabrication of cross-linked copolymer thin films via Initiated Chemical Vapor Deposition (iCVD), and attachment of QD-4AT nanoprobes to polymer surface; (iii) heavy metal ion detection with this new polymer-based QD-4AT nanoprobe in real water sources and demonstration of multi-use operation.

5.2.1. Heavy Metal Ion Detection with CdTe QD-4AT Nanoprobe

CdTe QD-4AT nanoprobes were developed in this part of the study by following previously published protocol (Karabiyik and Ebil 2022). CdTe QD solution was prepared using deionized water and homogeneous distribution of QDs in water was ensured by applying ultra-sonication at 25^{o}C for 10 minutes. Then, a solution of 1-ethyl-3-(3dimethylaminopropyl) carbodiimide (EDC) and N hydroxysuccinimide (NHS) was prepared with phosphate buffered saline (PBS) buffer (50 mM and pH: 7.4) and added to the QD solution to activate the -COOH groups on the QDs. This solution was stirred at 25^{o}C for 30 minutes. After this process, 4AT solution was prepared again using PBS

buffer (pH: 7.4) and combined with the activated QD solution and stirred at 25ºC for 2 hours. Free 4AT and other unreacted molecules were removed from the nanoprobe solution via centrifugation (~7000 rpm for 20 minutes).

In literature studies, photoluminescence density has been linked to the solution pH, the nature of the buffer, and QDs-4AT concentration. Maximum and stable fluorescence values were generally obtained between pH 5.2 and 9 (Adegoke et al. 2012) by using PBS buffer; therefore, a pH range of 7-7.5 was chosen for the experiments as a first step in this study. The effects of solvent type, nanoprobe and solvent concentration, pH of the solution were also studied.

For heavy metal ion detection, solutions of each Cd^{2+}, Zn^{2+}, Hg^{2+}, Cr^{3+}, Mg^{2+}, Cu^{2+}, Al^{3+}, Fe^{3+} ions were prepared from chloride salts ($CdCl_2$, $ZnCl_2$, $HgCl_2$, $CrCl_3$, $MgCl_2$, $CuCl_2$, $AlCl_3$, $FeCl_3$) with PBS buffer. Sulfate salts ($MnSO_4.H_2O$, $CoSO_4.7H_2O$, $NiSO_4.6H_2O$) and nitrate salts ($AgNO_3$, $Pb(NO_3)_2$) were also used to obtain Mn^{2+}, Co^{2+}, Ni^{2+}, Ag^{+} and Pb^{2+} ions, respectively. These solutions were added to the nanoprobe solution separately. A continuous gentle mixing was applied at 25ºC for at least 10 minutes for each solution. The selectivity of QD-4AT nanoprobe to particular ions was determined using fluorescence spectroscopy.

5.2.1.1. Mechanism of Nanoprobe Formation and Heavy Metal Ion Detection

Semiconductor band theory can be used to describe QDs' fluorescence operation (Ramírez-Herrera et al. 2019). According to this theory, when an electron in the valence band (VB) of QDs is excited to the conduction band (CB), it creates a hole with opposite charge to the excited electron. The electron-hole pair attracts each other, and the structure known as an exciton (an electron and an electron hole bonded together by the electrostatic Coulombic force) is formed. Returning the excited electron to the valence band is called recombination and a fluorescence emission is produced by the release of a photon. If the surface of QDs is changed due to interaction with molecules or ions in the environment, the efficiency of the electron hole recombination process is influenced leading to a decrease in the fluorescence intensity of QDs. This process is called fluorescence

quenching (Ramírez-Herrera et al. 2019). In literature studies, the quenching of the fluorescence of QDs by nitroxide radicals has been generally explained with electron exchange mechanism (Laferrière et al. 2006; Maurel et al. 2006; Chen et al. 2008; Tansakul et al. 2010). In this mechanism, proximity between the donor and acceptor is the most important parameter (Scaiano et al. 2006; Chen et al. 2008; Tansakul et al. 2010). Reversible electron transfer, which is called as the electron shuttle mechanism, involves the transfer of electrons from the conduction band of QDs to the half-filled single occupied molecular orbital (SOMO) of nitroxides, where the nitroxyl radical plays the role of electron and hole carrier, and from the nitroxide to the valence band of QDs containing back electron transfer (relaxation) as shown in the Figure 5.1.

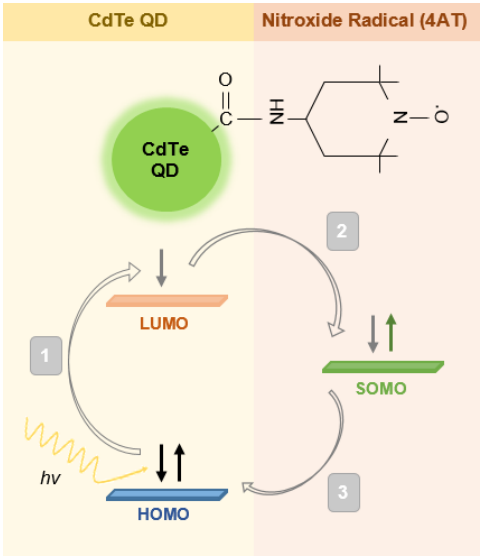

Figure 5.1. Schematic representation of shuttle mechanism for electron transfer between the nanoparticle and the nitroxyl radical: (1) excitation; (2) transfer of e−; (3) relaxation.

Considering that the redox potential of the conduction band of CdTe QDs (~2.8 nm in diameter) (Muñoz et al. 2019) is -1.0V (compared to the standard hydrogen electrode (SHE)) (Poznyak et al. 2005), the redox potential of 4AT (0.895V vs. SHE) can be said to be high enough to induce thermodynamic electron transfer from the conduction band of CdTe QDs to the vacant 4AT band (Zhou et al. 2020). Thus, half-filled SOMO of 4AT will act as a shuttle for electron transfer from conduction band (CB) to valence

band (VB) of CdTe QDs in aqueous solution (electron shuttle mechanism). Looking at this cycle, it is clear that the quenching of fluorescence of QDs is due to paramagnetic half-filled SOMO, which provides a more efficient non-radiative relaxation channel that can compete with radiative recombination of photo-induced electrons and holes (Lin et al. 2012).

A nitroxide radical can accept an electron to be reduced to its diamagnetic counterpart, hydroxylamine, or donate an electron to be converted into another diamagnetic counterpart, oxammonium cation (Figure 5.2). During the formation of the QD-4AT nanoprobe, fluorescence quenching mechanism occurs. If there are ions or molecules in the environment, nitroxide part of the fluorescent nanoprobe may react with them to produce a diamagnetic form and thus electron transfer pathway between the SOMO of 4AT and VB of QD is blocked. As a result, 4AT can no longer quench the QD fluorescence and fluorescence restoring occurs (Maurel et al. 2006; Chen et al. 2008; Tansakul et al. 2010; Adegoke et al. 2012; Lin et al. 2012). Fluorescence enhancement in heavy metal ion detection with this nanoprobe can be explained in this manner. This mechanism has been described in the literature as a fluorescence recovery mechanism (Maurel et al. 2006; Chen et al. 2008; Lin et al. 2012; Maiti et al. 2015).

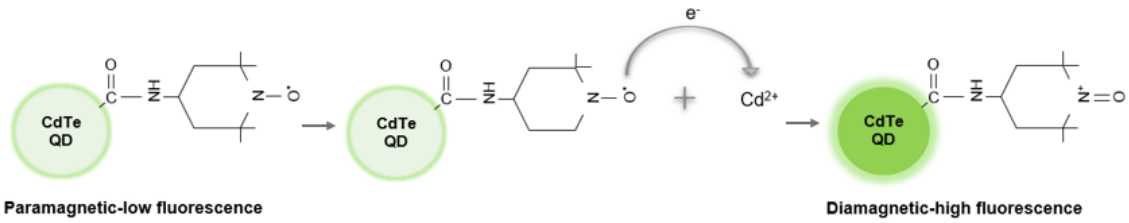

Figure 5.2. The proposed sensing mechanism of reaction between 4AT and Cd^{2+}.

5.2.2. Cross-linked Copolymer Deposition via iCVD system and Epoxy Ring Opening Reaction

In iCVD process, free radical polymerization reaction in which the unsaturated bonds of the monomer unit are activated by free radicals produced during the thermal

decomposition of an initiator molecule (typically at low filament temperatures of 200–400°C) takes place. This process is performed in both vapor and solid phase without any solvent. The main advantage of iCVD process is low substrate temperature enabling the use of temperature sensitive materials such as paper, polymer, membrane etc. (Lau et al. 2003; Lau and Gleason 2006b, a; Lau and Gleason 2007b). In addition, the functional groups of the monomers are successfully transferred to the polymeric film due to gentle process conditions (Coclite et al. 2009; Aresta et al. 2012; Sarıipek and Karaman 2014; Gleason 2015). iCVD fabricated thin polymeric films for physical and chemical protection of a variety of substrates were also demonstrated. (Lau and Gleason 2007a).

The main purposes of this study are to produce robust cross-linked copolymer films via iCVD, attach the developed QD-4AT nanoprobe structure to this film, and evaluate the detection of heavy metal ions in real water sources with this new polymer-based fluorescent sensor nanoprobe, a first in literature.

Tert-butyl peroxide (TBPO) was used as initiator. Glycidyl methacrylate (GMA) and 2,4,6,8-tetramethyl- 2,4,6,8tetravinylcyclotetrasiloxane (V4D4) were used as monomers. GMA is one of the most studied monomers due to its epoxy group that can be converted into different functionalities via ring-opening reactions (Kim et al. 1996; Lee et al. 1996; Li et al. 2005; Labbé et al. 2011; Sarıipek and Karaman 2014; Gleason 2015; Muzammil, Khan, and Stuparu 2017; Irzhak, Uflyand, and Dzhardimalieva 2022). A variety of chemical groups such as primary amine, sulfhydryl, or hydroxyl group can be covalently bonded to pGMA through the ring-opening reactions leading to further functionalization and modifications of polymeric or inorganic surfaces (Allmér, Hult, and Rånby 1989; Mori, Uyama, and Ikada 1994; Zhang et al. 1995; Tarducci et al. 2000; Allcock, Lampe, and Mark 2003; Lau and Gleason 2006c; Baxamusa, Im, and Gleason 2009; Alf et al. 2010; Xu and Gleason 2010b; Kimmins, Wyman, and Cameron 2014; Sarıipek and Karaman 2014). Especially, cross-linked pGMA is both physically and chemically highly durable in harsh environments making it suitable for protective coating applications (Mao and Gleason 2004; Chan and Gleason 2006; Mao and Gleason 2006). Therefore, for a robust cross-linked polymer film GMA was selected in this study. V4D4 monomer enables the production of films with high mechanical strength due to cross-linking during polymerization. It also acts as a barrier against moisture making it a preferred material for protective coatings for sensor structures. In literature, cross-linked copolymers have been formed with both acrylate monomers and fluoro-monomers with V4D4 with good mechanical and chemical properties (Yoo et al. 2013; Lee et al. 2019).

Cross-linked copolymer film depositions were performed in a custom built iCVD system. The surface on which the substrate is placed was kept at a fixed temperature (35°C) via an external cooler. A filament array (Nichrome, 80% Ni/20%Cr) was used to decompose the initiator. GMA (SigmaAldrich, 97%) and V4D4 (Sigma-Aldrich) were used without further purification. GMA and V4D4 monomers were heated to 65°C and 85°C, respectively, in stainless steel containers. TBPO (Sigma-Aldrich, 98%) was used as initiator at room temperature. All depositions were performed on crystalline silicon (c-Si) substrates. Process conditions for homopolymers of pGMA and pV4D4, and copolymer p(GMA-co-V4D4) including flow rates of the monomers and initiator, substrate and filament temperatures, and reactor pressure are given Table 5.1.

Table 5.1. Details of GMA and V4D4 Homo and Copolymer Depositions.

iCVD sample	Substrate Temp (°C)	Filament Temp (°C)	Pressure (mTorr)	Flow rate (sccm)			Flow Ratio (V4D4/GMA)	Deposition time (min)	Thickness (nm)
				V4D4	GMA	TBPO			
Homo pGMA					0.4				219.0±0.6
cop-1				0.1	0.4		0.25		235.7±0.4
cop-2				0.2	0.4		0.5		256.6±0.2
cop-3				0.3	0.4		0.75		320.5±0.4
cop-4	35	300	250	0.4	0.4	0.8	1.0	120	329.6±0.5
cop-5				0.4	0.3		1.33		339.5±0.3
cop-6				0.4	0.2		2.0		342.4±0.4
cop-7				0.4	0.1		4.0		346.8±0.4
Homo pV4D4				0.4					365.5±0.3

After fabrication of copolymer films in iCVD system, chemical and mechanical tests (durability in organic solvent, salt resistance, water resistance and adhesion) were carried out by following previously published procedures (Karabıyık, Cihanoğlu, and Ebil 2023) to determine the optimum process conditions with respect to chemical and mechanical properties of the polymers.

After selecting the best cross-linked copolymer film for this study, surface functionalization via epoxy ring opening reaction was carried out by following again the previously published procedure (Karabiyik and Ebil 2022). Two different aliphatic amine groups were used in epoxy ring opening process. Coatings were immersed separately into ethanol solutions of aliphatic primary amines which are propylamine (Sigma-Aldrich, 98%) and ethylenediamine (Sigma-Aldrich, >99%), then stirred at 60°C for 2 h. This reaction provides the necessary time for interaction between the amine and the hydroxyl-

containing compound (HOR) (ethanol in this study). The formation of donor–acceptor complexes of the epoxy compound is supported with the solution including amine and ethanol, and nucleophilic attack on this complex is made by amine (T.Drzal 1986; Allmér, Hult, and Rånby 1989). In this way, the bonding of the amine group to the open epoxy ring takes place. After the ring opening reaction, copolymer films were rinsed with ethanol and dried at 60ºC for 1 h under vacuum.

5.2.3. Nanoprobe Attachment to Functionalized Copolymer Thin Films and Heavy Metal Ion Detection

Binding of QD-4AT nanoprobe to the polymer surface generally occurs as a result of amide bond formation between -COOH groups of QDs and the primary or secondary amine groups on the polymer surface (Alice Lee and Kennedy 2007; Xu and Gleason 2010b; Shen 2011; Rizvi S 2014). It is usually preferred that carbodiimide compound should be present in the reaction medium to enable QDs' activation. Due to lower reaction temperature, N-(3-dimethylaminopropyl)-N'-ethylcarbodiimide (EDC)/N hydroxysuccinimide (NHS) was used because $–NH_2$ groups along the polymer chain can easily react with –COOH functionalized QDs through EDC/NHS chemistry (Alice Lee and Kennedy 2007; Shen 2011; Rizvi S 2014). To attach QD-4AT nanoprobes to the surface of iCVD polymers, thin-film copolymers were immersed into the solution for 2 h while QD-4AT nanoprobe formation procedure was being carried out. After drying in vacuum oven at room temperature for 24 h, copolymer bonded QD-4AT nanoprobes were immersed into the solution containing heavy metal ion at certain pH and a continuous gentle mixing was performed for at least 10 minutes at 25ºC, before drying in vacuum oven at room temperature (25ºC). Fluorescence spectroscopy analysis was carried out to determine whether the QD-4AT nanoprobe went into the "on" mode, which is the recovery of QD emission, meaning the ion was detected by the nanoprobe.

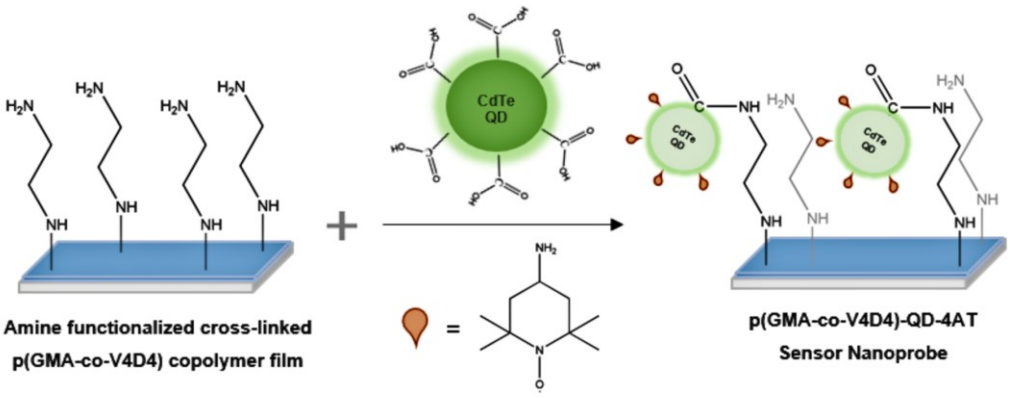

Figure 5.3. Schematic representation of cross-linked p(GMA-co-V4D4) copolymer-QD-4AT sensor nanoprobe formation with amide bond.

5.2.3.1. Target Heavy Metal Ion Detection in Real Samples and Multi-Use Study

As a final part, the feasibility of polymer-based QD-4AT nanoprobe as an effective fluorescent sensor for detection of target heavy metal ion (Cd^{2+} ions) in real water sources was evaluated. Regular tap water, commercial bottled water and sea water were used as water source. Tap water and sea water were filtered using a membrane filter (0.22 μm) before the experiments. Standard addition method (spike method) has been used to detect different ions in real samples in the literature (Xu, Miao, et al. 2011; Afkhami et al. 2015; Gong et al. 2016; Elmizadeh et al. 2019; Ramírez-Herrera et al. 2019; Chen et al. 2020; Preeyanka and Sarkar 2021). In this study, in addition to the standard addition method, Inductively Coupled Plasma Mass Spectrometer (ICP-MS) was used to evaluate the accuracy of the results. In standard addition method, real samples were used as solvents to prepare target ion solutions with different concentrations. For the evaluation of multi-use of nanoprobe sensors, the target ions interacting with the nanoprobe were removed from the structure by increasing the pH of the solution (from 8.0 to 12) while keeping all other experimental conditions fixed, before repeating the experiments. Since multiple use sensors similar to nanoprobes developed in this study have never been studied or demonstrated before, this part of the study add a unique value to this work.

5.2.4. Characterizations

Fluorescent spectroscopy, a PerkinElmer LS 55 spectrometer, was used to examine the interaction between QD and 4AT and to investigate whether the detection of target heavy metal ion was achieved. Fluorescent spectroscopy was used to determine how and to what extent the emission given by QDs at a certain wavelength (λem: 520 nm for CdTe QD used in this study) changes after interaction of QD-4AT with heavy metal ions. Thickness measurements of iCVD fabricated polymer films were performed by using Mprobe-Vis20 reflectometer with a spectral range between 400-1100 nm. Fourier transform infrared spectroscopy (FTIR) analysis was carried out using a Perkin Elmer – UATR Two Spectrometer to investigate chemical composition and quality of polymer films. FTIR spectra of samples were taken between 450-4000 cm^{-1} scan range and at 4 cm^{-1} resolution. Energy-dispersive X-ray spectroscopy (EDX) (FEI QUANTA 250 FEG:EDX) was used to investigate chemical composition of the polymer films before and after epoxy ring opening reactions.

The selectivity of copolymer-QD-4AT sensor nanoprobe to metal ions was also determined by fluorescent spectroscopy system. The fluorescence spectra were obtained in a range of emission wavelengths from 350 to 650 nm, at an excitation wavelength of 320 nm. A Zeiss-Observer Z1 fluorescence microscope was also used to verify the detection of heavy metal ion with polymer bonded sensor nanoprobe. A Perkin Elmer Lambda 45 UV-Vis Spectrophotometer was used to investigate QD-4AT nanoprobe structure and whether target ion could be detected with this nanoprobe. Data were taken with a wavelength range of 200-800 nm. A Freeze Dryer (Labconco-Freezone 18) was used to dry and obtain powder form of the solutions to examine the interaction between the QD-4AT nanoprobe and target ions. To examine 4AT nitroxide radical and target ion interactions, Electron Paramagnetic Resonance spectroscopy (EPR) analysis was performed using a CMS 8400 EPR Spectrometer. To investigate cadmium ions in tap water and treatment water at mg/L to ng/L levels Coupled Plasma Mass Spectrometer (ICP-MS) – (Agilent 7500ce) was used.

5.3. Results and Discussion

5.3.1. Part I: Heavy Metal Ion Detection with unattached (free) QD-4AT Nanoprobe

As a first part of this study, the detection of 13 different heavy metal ions (Cd^{2+}, Al^{3+}, Co^{2+}, Cu^{2+}, Mn^{2+}, Ag^{+}, Fe^{3+}, Ni^{2+}, Pb^{2+}, Cr^{3+}, Hg^{2+}, Mg^{2+}, Zn^{2+}) was carried out with developed QD-4AT nanoprobe structure. The procedure described in previous sections was followed separately for each heavy metal ion and fluorescence spectroscopy analysis was performed at the end of the experiments. The results of the analysis are shown in Figure 5.4. An acceptable average error of ±5.0% in relative fluorescence intensity was obtained.

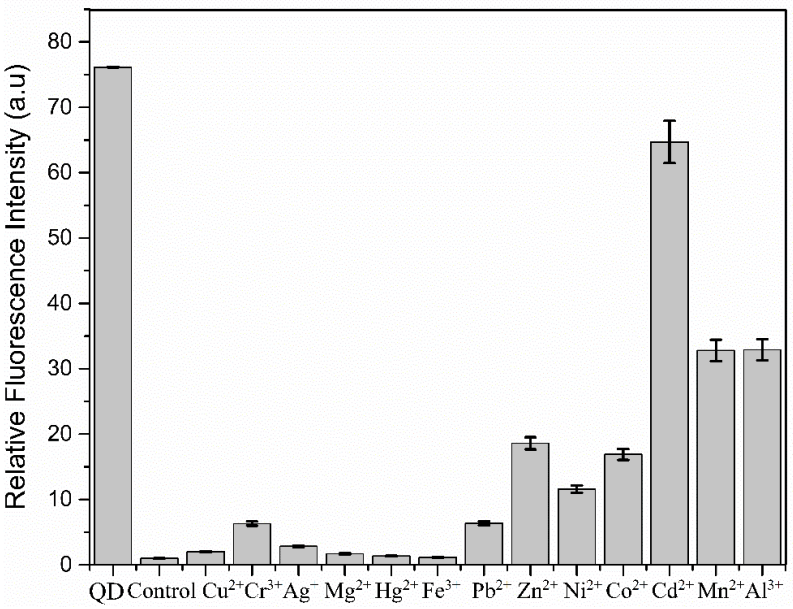

Figure 5.4. Fluorescence intensities of QDs-4AT nanoprobe obtained in the presence of 13 different metal ions in pH=7.4, 50 mM PBS. (Data of the "control" belongs to QD-4AT).

According to Figure 5.4, after the interaction of QDs with 4AT, fluorescence quenching successfully observed as the photoluminescence (PL) intensity of QD-4AT (control) nanoprobe was obtained as very low. This nanoprobe was used for detection of heavy metal ions and results indicated that PL intensity of QD-4AT nanoprobe changed insignificantly with Cu^{2+}, Cr^{3+}, Ag^{+}, Mg^{2+}, Hg^{2+}, Fe^{3+}, Pb^{2+}, Ni^{2+}, Co^{2+} and Zn^{2+}, while under the same conditions, in the presence of Mn^{2+} and Al^{3+} ions, an increase in fluorescence intensity was observed. However, considering the PL intensity for Cd^{2+} ion, it can be stated that QD-4AT nanoprobe does not show sufficient selectivity against other ions used in the experiment (including Mn^{2+} and Al^{3+} ions). Therefore, it can be concluded that the nanoprobe developed in this study is more sensitive and selective towards Cd^{2+} ion. The subsequent parametric studies were only conducted for Cd^{+2} ion.

5.3.1.1. Solvent Effect on Detection of Cd^{2+} Ion

In literature studies related to heavy metal ion detection, it was shown that the detection of ions was affected by the solvent. Therefore, three different solvents, de-ionized water (DI-W) (Maiti et al. 2015; Lin et al. 2019; Khan, Mitra, and Sahoo 2020) phosphate buffered saline (PBS) (Xu, Chen, et al. 2011; Ramírez-Herrera et al. 2019; Radhakrishnan, Sivanesan, and Panneerselvam 2020) and dimethylformamide (DMF) (Dijksman, Arends, and Sheldon 2003; Geißlmeir, Jary, and Falk 2005) which are the most preferred in the literature, were selected for heavy metal ion detection.

After synthesis of QD-4AT nanoprobe, salt solution was prepared with selected solvents. The solutions were then added separately to the medium of QD-4AT. The fluorescence analysis was performed to determine which solvents, or their mixture give the best result in terms of QD fluorescence restoring in Cd^{2+} ion detection.

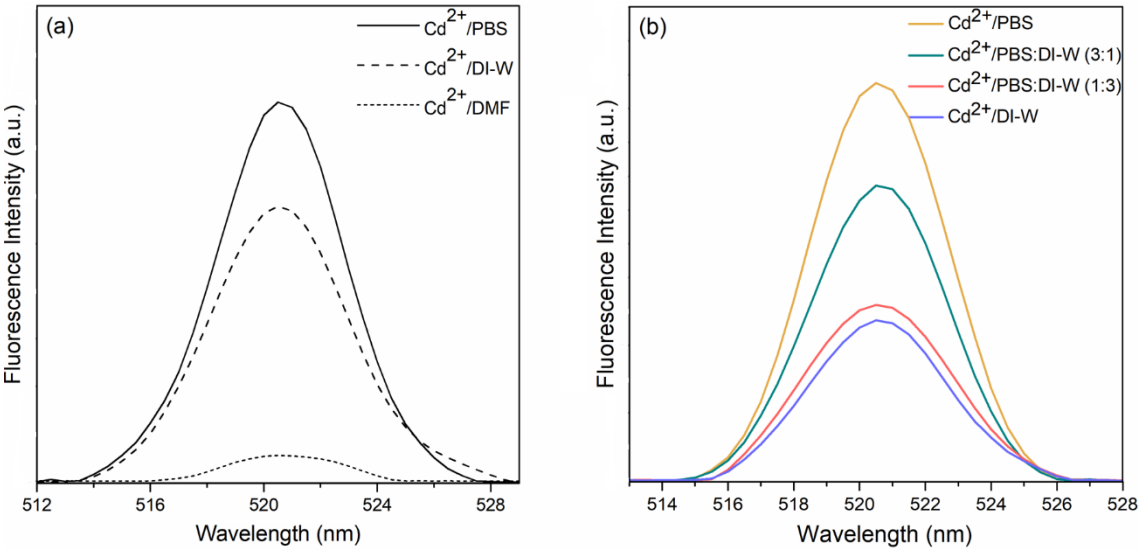

Figure 5.5. Detection results of Cd^{2+} ion with QD-4AT nanoprobe in (a) PBS, DI-W and DMF solvents, respectively and (b) PBS and DI-W solvent mixture.

Experimental results shown in Figure 5.5a show that higher fluorescence intensity was obtained in DI-W compared to DMF; however, the best result was obtained at 520 nm with PBS. PBS and DI-W mixtures with various ratios were also used (Figure 5.5b). It is clear that as the amount of water in the environment increases, the detection rate of Cd^{+2} ions decreases and the fluorescence recovery of QDs decreases also. Therefore, the best solvent for Cd^{+2} ion detection with QD-4AT nanoprobe was found as PBS.

The reason for achieving the better detection result with PBS can be briefly explained as follows: Buffers fulfill the function of stabilizing the pH of the solution and PBS has a higher ionic strength than the other solvents used in this study. Ionic strength of a solution is a measure of the concentration of ions in the solution. Ionic compounds (e.g salts) dissociate into ions when they are dissolved. The most common composition of PBS includes salts of NaCl, KCl, Na_2HPO_4 and KH_2PO_4 and when it dissolves in water, it dissociates into different ions like Na^+, K^+, Cl^-, HPO_4^{2-}, $H_2PO_4^-$ etc. How a solvent with high ionic strength (like PBS) has a positive effect on fluorescence recovery by increasing the interaction between Cd^{2+} and 4AT in this study can be explained by Debye–Hückel theory (Kennedy 1990; Atkins and de Paula 2006). Oppositely charged ions attract each other, and as a result, anions are more probable to be found near cations in solution and vice versa. Oppositely charged ions will be attracted to a region around each of the reacting ions in a solution in which any reaction between ions takes place. This

slows down the rate of approach of ions reacting in opposite directions and the rate of separation of ions of the same sign. Thus, reactions between ions with different charges slow down and reactions between ions with similar charges go faster than they would otherwise (Kennedy 1990; Atkins and de Paula 2006; Wu et al. 2017). As the ionic strength that is the concentration of ions in the solution increases, the occurrence of this situation also increases. Based on this theory, it is clear why PBS increased the interaction between Cd^{2+} ion and 4AT more than other solvents and led to higher fluorescence recovery.

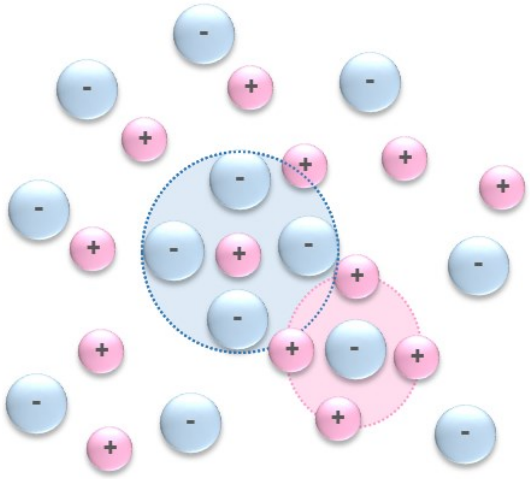

Figure 5.6. An idealized representation of ions in the solution (Debye-Hückel Theory).

5.3.1.2. QD-4AT Nanoprobe and PBS Concentration Effects on Detection of Cd^{2+} Ion

Another parameter that has an effect on the detection of Cd^{2+} ion is the concentrations of QD-4AT nanoprobe solution and PBS. Initially, the effect of QD-4AT nanoprobe concentration was examined by keeping PBS concentration fixed at 50mM. The concentration of the nanoprobe solution was varied as 0.25, 0.5, 1, 5, 20, 200 and 500 µM. Initially, 0.5 µM of Cd^{2+} ions were added into each solution and fluorescence analysis performed.

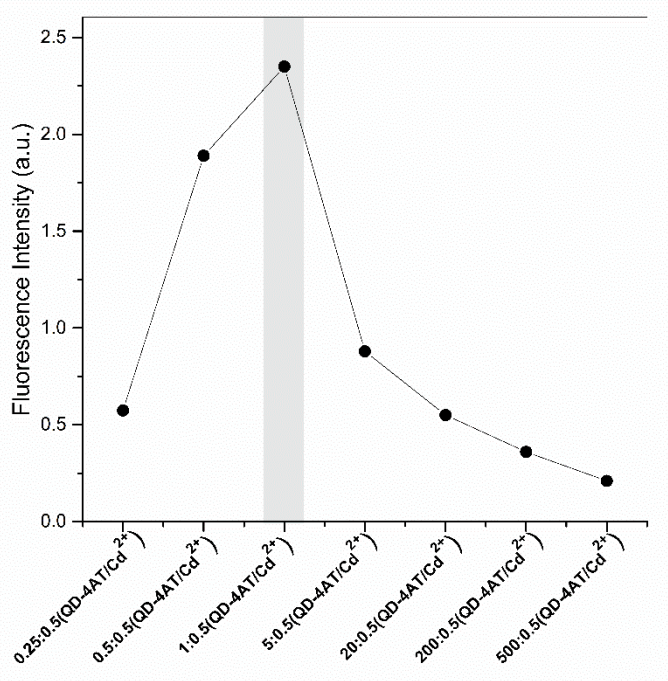

Figure 5.7. The fluorescence recovery responses with different concentration of QD-4AT nanoprobe (0.25, 0.5, 1, 5, 20, 200 and 500 μM) analyzed with 0.5 μM of Cd^{2+} ion.

As seen in Figure 5.7, 1 μM of nanoprobe solution showed better sensing response when compared with the others. Fluorescence intensity decreased significantly when the concentration of nanoprobe solution was higher than 1 μM. Based on this finding, 1 μM QD-4AT concentration was fixed while examining the effect of other parameters on detection of Cd^{2+} ion.

As explained previously, PBS was selected as a solvent utilized in the development of QD-4AT nanoprobe and for evaluation of the nanoprobe for the detection of Cd^{2+} ion. The reaction medium also plays an important role. The effect of buffer concentration on Cd^{2+} ion detection was investigated by using 1, 5, 10, 25, 50, 100 and 150 mM PBS buffer solutions.

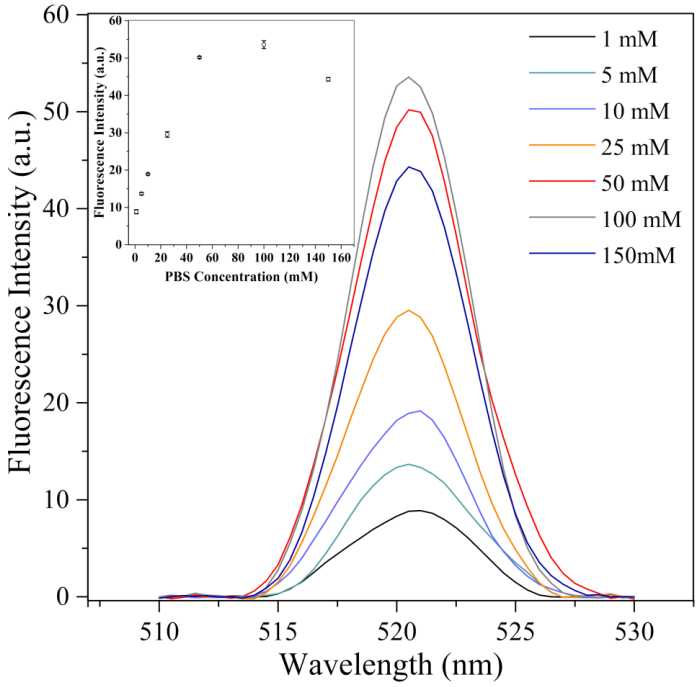

Figure 5.8. Effect of PBS buffer at 1, 5, 10, 25, 50, 100 and 150 mM concentrations on Cd^{2+} ion detection.

It can be clearly seen in Figure 5.8 that as the PBS concentration increased up to 100 mM, the fluorescence intensity enhanced as well. However, a reduction was observed when PBS concentration increased further. In addition, the difference in intensity between 50 mM and 100 mM was negligible. These results indicated that target ion could be detected better at sufficiently high PBS concentration like 50mM. This may be related to the ionic strength of the solution as described previously. The most frequently used definition of ionic strength, I, is (Kennedy 1990; Atkins and de Paula 2006; Wu et al. 2017);

$$I = \frac{1}{2}\sum_i c_i . z_i{}^2 \qquad (5.1)$$

where Σ is the sum of all ions in the solution, i is the total number of ion species, c and z are the molar concentration and charge, respectively, of each of the ions in the solution. According to this equation, increasing of the PBS concentration in the solution causes the increasing of the ionic strength of the solution proportionally. Increasing the concentration too much can negatively affect the detection of the ion as in 150 mM. Since

the change in fluorescence intensity was not affected much, despite a 2-fold increase in concentration (between 50 and 100 mM), 50 mM was chosen as the most appropriate PBS concentration value to be used in this study.

5.3.1.3. Effect of Solution pH on Detection of Cd^{2+} Ion

The effect of the pH of the reaction medium on the detection of Cd^{2+} ion with the QD-4AT nanoprobe was investigated to improve the selectivity of nanoprobe to this target heavy metal ion. The pH value of the reaction medium in the formation of QD-4AT nanoprobe and during the detection of Cd^{2+} ion is crucial. In literature it was shown that the pH values higher than 5.0 causes protonation of 4AT by generating the positive charges and deprotonation of the carboxyl (-COOH) group on the CdTe QD with formation of a negative surface charges on the particle. This enables the formation of the QD-4AT structure, which results in fluorescence quenching due to interaction between QD and 4AT as electron donor and acceptor, respectively (Xu, Miao, et al. 2011; Nutting, Rafiee, and Stahl 2018; Muñoz et al. 2019). The final solution pH where the detection process of Cd^{2+} ion takes place is also important since it affects the fraction of the 4AT existing at the protonated form and also affects the extent of ion-pair formation (Yager, Eaton, and Eaton 1979). Cd^{2+} ion takes an electron from 4AT in order to become more stable in the solution, causing an electron transfer. As a result, it plays a role in QD re-emission and recovery of fluorescence by converting 4AT to its diamagnetic counterpart. Therefore, during the experiments for detecting Cd^{2+} ion with QD-4AT nanoprobe, the pH of the medium was adjusted as 5, 6, 7, 8 and 9, respectively by adding certain amounts of sodium hydroxide (NaOH) or hydrochloric acid (HCl) solutions into the medium. At the end of the experiments, fluorescence spectroscopy analysis was performed to evaluate QD fluorescence recovery.

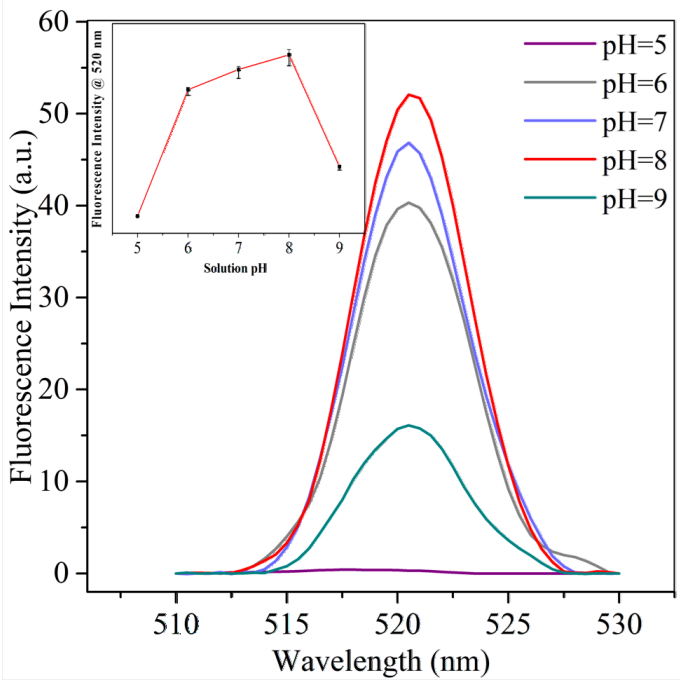

Figure 5.9. Influence of the final solution pH on fluorescence enhancement in detection of Cd^{2+} ion with QD-4AT nanoprobe.

As seen in Figure 5.9, the intensity of fluorescence emission increased considerably as the pH increased over 5 and reached its maximum value at the pH value of 8. The further increase in pH resulted in a decrease in fluorescence intensity, preventing the reaction from eventuating favorably. Too high pH values are not beneficial since Cd^{2+} ion would react with OH^- (high pH values mean high OH^- concentration in the solution) to form the corresponding metal hydroxides reducing the interaction with the nanoprobe. As a result, the highest fluorescence enhancement was obtained at pH=8. This is a confirmation that Cd^{2+} ions and 4AT in the nanoprobe interacted properly and QD fluorescence recovery was successfully obtained by converting 4AT into its diamagnetic counterpart. For these reasons, the pH value was chosen as pH=8 for the reaction medium.

5.3.1.4. Time Effect on Detection of Cd^{2+} Ion

Another parameter examined in this study was the effect of time on target ion detection. The time values were set as 10, 15, 20, 30 minutes, 1 hour and 1 day,

respectively. At the end of the experiments, fluorescence analysis was performed, and the results are shown in Figure 5.10.

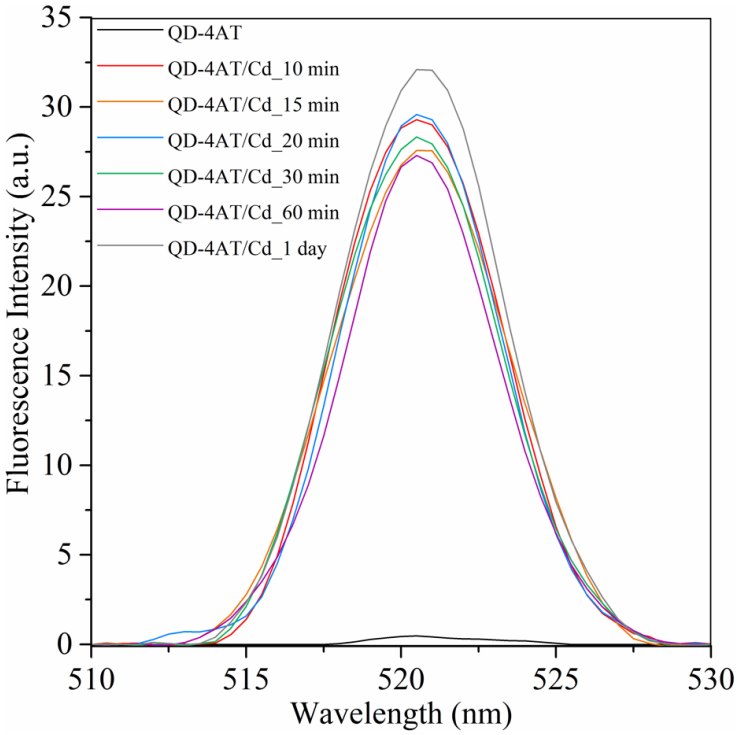

Figure 5.10. Time dependent fluorescence recovery with Cd^{2+} ion.

A very low fluorescence intensity due to fluorescence quenching caused by the binding of nitroxide radical to QD was seen (black line in Figure 5.10). The fluorescence analysis was performed 10 minutes after adding Cd^{2+} salt solution to the QD-4AT nanoprobe medium. The result clearly showed that there was a very significant fluorescence recovery. As the interaction time increased from 10 minutes to 60 minutes, the increase in fluorescence recovery was minimal. Although results showed that better fluorescence recovery was obtained after 1 day, the fact that there was not a big difference compared to the 10-minutes experiment indicates that a short interaction time is sufficient for sensing applications.

5.3.1.5. Investigation of Cd^{2+} ion Interaction with QD-4AT Nanoprobe

In order to investigate the interaction between the Cd^{2+} ion and QD-4AT nanoprobe developed in this study, UV-Vis and FTIR analyzes were performed. The results were shown in Figure 5.11 and 5.12, respectively.

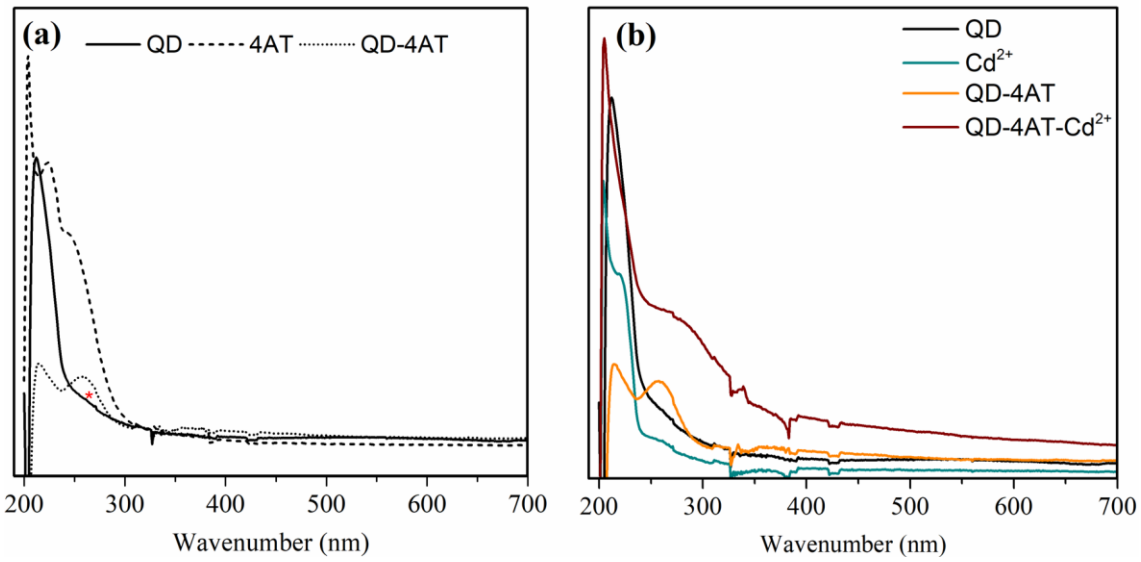

Figure 5.11. UV-Vis absorption spectra of (a) QD, 4AT and QD-4AT nanoprobe and (b) QD-4AT in the presence of Cd^{2+} ion in the medium.

CdTe QD absorption spectrum given in Figure 5.11a has a sharp peak between 200-240 nm due to the presence of the carboxyl functional group (–COOH) of CdTe QD (Pooja, Rana, and Chowdhury 2019; Pooja and Chowdhury 2020, 2021). As shown in Figure 5.11a, QDs exhibited one absorption peak as a weak shoulder at 261 nm, labeled with red star, belonging to π-π^*transition of C=O bond (Ellairaja et al. 2015; Radhakrishnan, Sivanesan, and Panneerselvam 2020; Yuan et al. 2022). It is clearly seen in QD-4AT spectrum that an increase in the intensity of the band at 261 nm (also exists as a weak and broad band in the CdTe QD spectrum) and the emergence of a new band at 362 nm, show evidence of a significant interaction between 4AT and QD (Wątły et al. 2019). As shown in Figure 5.11b, after the interaction of QD-4AT nanoprobe with Cd^{2+} ion, due to surface modification of the ligand, a broad peak was obtained between 250-

320 nm and a slight red shift occurred in the absorption of band-edge in UV–Vis spectrum of QD-4AT nanoprobe. The red shift in UV–Vis spectrum of QD-4AT confirms that detection of the Cd^{2+} ion with nanoprobe has been successful (Xu, Miao, et al. 2011; Manjumeena et al. 2015; Elmizadeh et al. 2019).

The FTIR spectra of CdTe QD, 4AT, QD-4AT and QD-4AT-Cd^{2+} are shown in the following Figure 5.12.

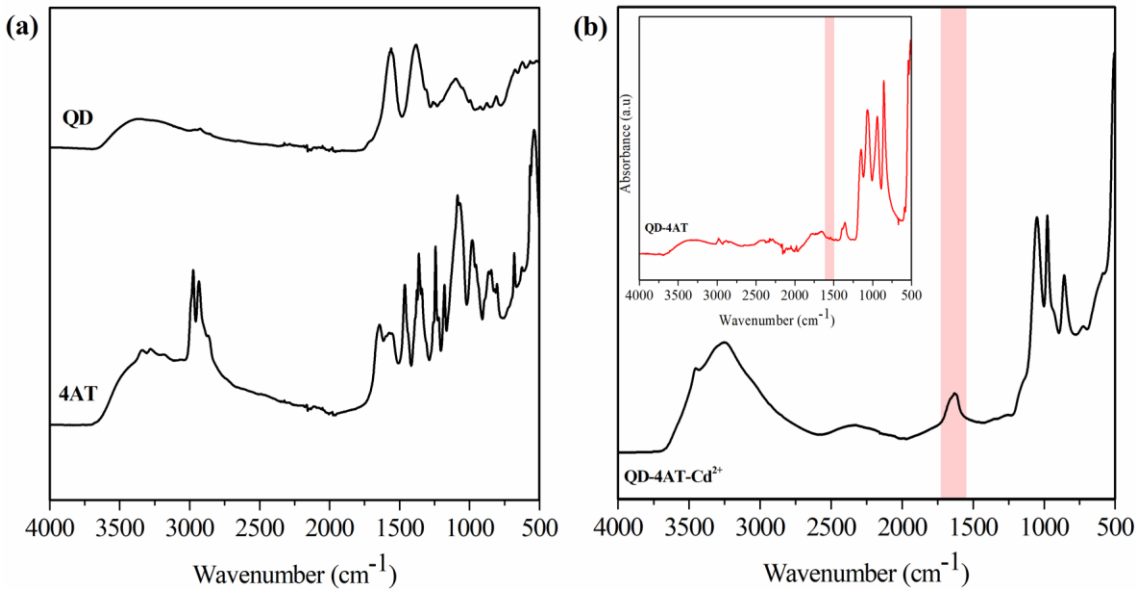

Figure 5.12. FTIR spectra of (a) QD and 4AT (b) QD-4AT-Cd^{2+} complex and inset FTIR spectrum of QD-4AT nanoprobe.

The broad absorption band observed around 3400 cm^{-1} in QD, 4AT and QD-4AT nanoprobe spectra was assigned to O–H vibrations of the PBS aqueous solution (Arivarasan, Sasikala, and Jayavel 2014; Rodríguez-Valencia et al. 2014; Achadu, Britton, and Nyokong 2016; Yuan et al. 2022). The bands around 3337-3180 cm^{-1} in 4AT spectrum are attributed to asymmetric and symmetric stretching vibrations of –NH bonds (Adegoke, Khene, and Nyokong 2013; Ribeiro et al. 2017; Yeo et al. 2022; Yuan et al. 2022) and this is supported by the presence of corresponding -NH bending at 1600 cm^{-1} of amine group (Adegoke, Khene, and Nyokong 2013; Yeo et al. 2022). C-H bending and stretching vibrations modes were found at 845 and 2934 cm^{-1}, respectively (Adegoke, Khene, and Nyokong 2013; Achadu, Britton, and Nyokong 2016; Yuan et al. 2022). The bands at around 1390 cm^{-1} and 1562 cm^{-1} were attributed to the symmetric and

asymmetric stretches of COO− in QD spectrum, respectively (Arivarasan, Sasikala, and Jayavel 2014; Achadu, Britton, and Nyokong 2016; Ribeiro et al. 2017; Yuan et al. 2022). The absorption peak at 1310 and 1100 cm^{-1} were ascribed to the oxygen-containing functional groups such as C–O stretching vibration peak in QD spectrum (Rodríguez-Valencia et al. 2014; Achadu, Britton, and Nyokong 2016; Yuan et al. 2022). The weak absorption band obtained at 3285 cm^{-1} (inset plot in Figure 5.12b) was attributed to the overlapping of two different absorptions corresponding to the asymmetric and symmetric –NH stretching vibrations (Ribeiro et al. 2017). The appearance of weak primary carbon amide band at 1657 cm^{-1} confirmed the formation of amide linkages in QD-4AT nanoprobe (Adegoke, Khene, and Nyokong 2013; Achadu, Britton, and Nyokong 2016). Also, the absorption peak at 1395 cm^{-1} belongs to the ionization form of the carbonyl group in CdTe QD (COO−) and peaks around 2850-2980 cm^{-1} could be ascribed to the C-H stretching vibrations in 4AT (Adegoke, Khene, and Nyokong 2013; Arivarasan, Sasikala, and Jayavel 2014; Achadu, Britton, and Nyokong 2016; Ribeiro et al. 2017; Yuan et al. 2022).The data obtained indicate that the QD-4AT nanoprobe was formed by the formation of both weak and covalent bonds between QD and 4AT. Additionally, the P-O stretching was observed at 1069, 1050 and 1068 cm^{-1} in 4AT, QD and QD-4AT nanoprobe spectra, respectively. Due to PBS treatment, P-OH out of the plane bending vibrations were appeared at 539, 530 and 542 cm^{-1} in 4AT, QD and QD-4AT nanoprobe spectra, respectively (Trivedi et al. 2015; Velásquez-Hernández et al. 2019).

FTIR analysis was repeated after performing Cd^{2+} ion detection with the QD-4AT nanoprobe as shown in extended graph in Figure 5.12b. Cadmium has ten electrons in its outermost shell and has a strong tendency to lose the electrons in 4s orbitals and thus, it exhibits the oxidation state of +2 in their compounds. Due to the interaction of $NO^{\cdot}$ radical and Cd^{2+} ion, 4AT turned into diamagnetic counterpart which is oxoammonium cation enabling fluorescence enhancement. As a result of this interaction, a new peak observed in QD-4AT-Cd^{2+} spectrum at 1630 cm^{-1} which is attributed to bent nitrosyl absorption ($^{+}N=O$) generally observed in the range between 1525–1690 cm^{-1} (Drouet, Alphonse, and Rousset 2001).

5.3.1.6. Selectivity of Proposed Nanoprobe for Cd^{2+} Ion over Other Heavy Metal Ions

A previously conducted experiment was conducted to investigate QD-4AT nanoprobe sensitivity to heavy metal ions showed that proposed probe exhibited good selectivity towards Cd^{2+} ion. However, especially in real environments, more than one ion may be present at the same time, and this may affect the selectivity of the sensor. In order to examine whether the QD-4AT nanoprobe shows selectivity towards Cd^{2+} ions in the presence of other heavy metal ions (Cu^{2+}, Cr^{3+}, A^{g+}, Mg^{2+}, Hg^{2+}, Fe^{3+}, Pb^{2+}, Ni^{2+}, Co^{2+}, Zn^{2+}, Mn^{2+} and Al^{3+}) fluorescence analysis was performed and PL responses were examined.

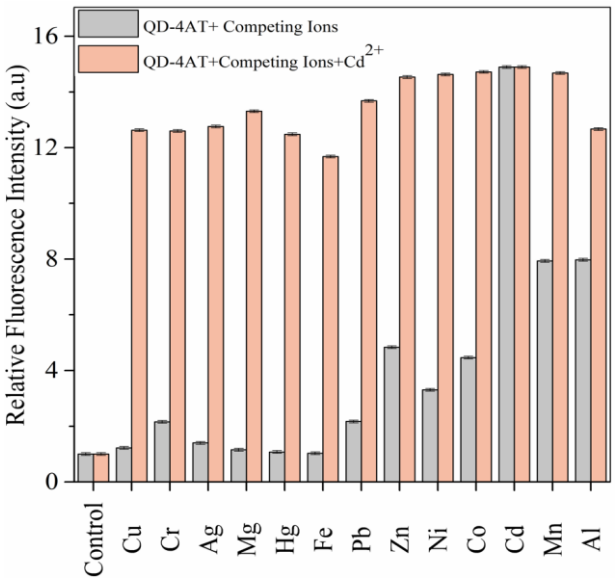

Figure 5.13. Fluorescence intensity of QD-4AT nanoprobe at 520 nm upon the addition of 500 µM Cd^{2+} ion in the presence of equivalent concentration of other heavy metal ions in the solution.

According to the PL responses, although heavy metal ions except for Cd^{2+} ion did not show a remarkable change in the fluorescence intensity of QD-4AT nanoprobe. Addition of an equivalent amount of Cd^{2+} ions to the medium with other heavy metal ions

under the same conditions led to a great increase of fluorescence intensity. These results indicate that proposed nanoprobe can serve as an "on-off-on" chemical sensor and exhibits an excellent selectivity towards Cd^{2+} ion by easily recognizing Cd^{2+} ion even if in the presence of other metal ions.

5.3.1.7. Control Experiments for Investigation of Cd^{2+} Ion Effects on QD Fluorescence

Three different control experiments were performed to investigate the effect of Cd^{2+} ion on QD fluorescence. The first control study is the investigation of Cd^{2+} ion source effect where cadmium nitrate tetrahydrate $Cd(NO_3)_2.4H_2O$ and $CdCl_2$ were used. The second study involves the addition of Cd^{2+} ion to a suspension of CdTe QDs in the absence of nitroxide (4AT) radical and the final control study involves the addition of Cd^{2+} ion to the 4AT suspension in the absence of QDs followed by mixing of 4AT and QDs. For control experiments, fluorescence spectroscopy analysis was used, and results are given below.

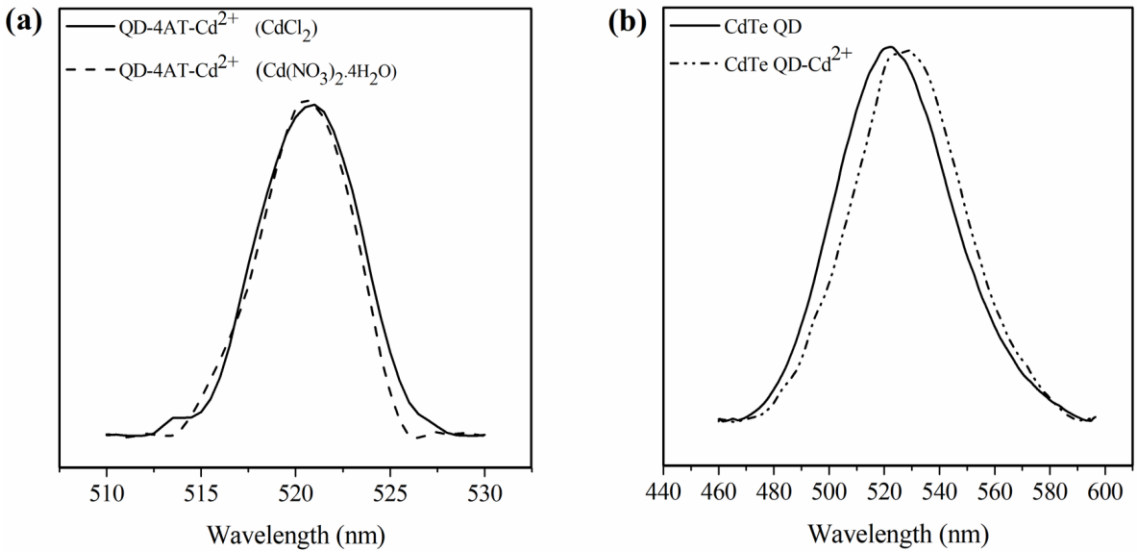

Figure 5.14. Fluorescence spectra of (a) Cd^{2+} ion detection with QD-4AT nanoprobe by using different Cd^{2+} ion sources and (b) Cd^{2+} ion effect on QD fluorescence in the absence of 4AT.

Figure 5.14a shows that the detection of Cd^{2+} ion was successfully achieved by QD-4AT nanoprobe by using two different cadmium salts. This result is a proof that regardless of the cadmium source, Cd^{2+} ion can be easily recognized by the developed nanoprobe. According to Figure 5.14b, the fluorescence intensity remained fairly stable over 24 h after the addition of 500 µM Cd^{2+} ion into the solution which only contains QDs. This is the evidence of Cd^{2+} ion does not directly affect the quenching or enhancement behavior of QD fluorescence. Only small red shift was observed in wavelength after the addition of Cd^{2+} ion, which is suspected to be related to the surface modification of QDs occurs due to its surface charge alteration with pH change in the solution.

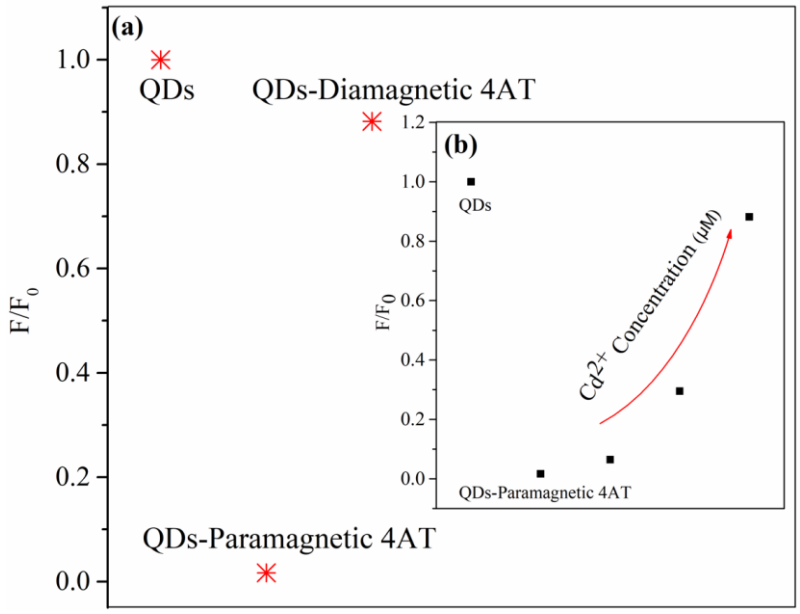

Figure 5.15. Fluorescence intensity of (a) QDs after addition of paramagnetic and diamagnetic 4AT (b) QDs after the addition of 4AT interacting with different concentrations of Cd^{2+} ions (50, 250 and 500 µM).

To understand the interaction between 4AT and Cd^{2+} ions, 4AT was mixed with Cd^{2+} ion. Then QDs were added to the medium and the fluorescence intensity was analyzed. Figure 5.15a shows that 4AT was reduced to diamagnetic form (oxammonium cation) due to electron transfer between 4AT and Cd^{2+} ions in PBS buffer (50 mM, pH=8) solution. No significant fluorescence quenching was observed when QDs were added to

the medium containing this reduced 4AT. However, fluorescence quenching was achieved when 4AT interacted directly with the QDs due to its paramagnetic structure having unpaired electrons. According to Figure 5.15b, as the Cd^{2+} ion concentration increases, the interaction with 4AT increases and thus the quenching effect on the fluorescence emission of the QDs added to the medium decreases.

These results confirm that the quenching of the fluorescence of QDs is due to the paramagnetic half-filled SOMO of 4AT and Cd^{2+} ion detection is achieved as a result of an electron transfer between Cd^{2+} ions and 4AT in the nanoprobe structure.

5.3.2. Part II: Fabrication of Cross-linked Copolymers via iCVD and Detection of Cd^{2+} Ion

Initial experiments were carried out for homopolymers by varying monomer/initiator flow rate ratio, reactor pressure, filament and substrate temperatures during iCVD process. After that, by changing the V4D4 (cross-linker)/GMA monomer flow rate ratio, seven copolymer films with varying compositions were fabricated. The aim here was to examine the effect of cross-linker density on copolymer film. Firstly, deposition rates were calculated by measuring final film thickness. All process conditions were kept fixed except for flow rates in copolymer depositions. Deposition rates for both homo and copolymer coatings were given in Figure 5.16.

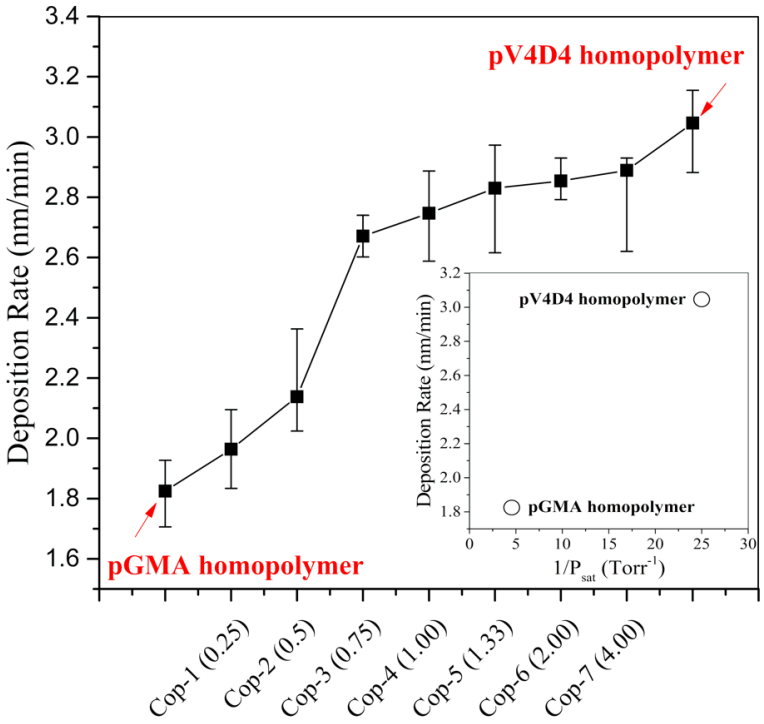

Figure 5.16. Deposition rate of pGMA, pV4D4 and their copolymers.

In order to investigate the effect of cross-linker on the polymer films, monomer flow rates in copolymer depositions were changed. To control film thickness and uniformity, the process parameters were selected to yield lower deposition rates (<10 nm/min) even high deposition rates (>1000 nm/min) can be obtained in iCVD process. In Figure 5.16, it can be seen that the deposition rate of homopolymer pV4D4 is higher than pGMA. In iCVD process, heavier monomers are adsorbed to the surface more, thus the deposition rate increment is observed (MW_{V4D4}: 344,66 g/mol and MW_{GMA}: 142,16 g/mol) (Chan and Gleason 2006; Lau and Gleason 2006b, a; Tao and Anthamatten 2016; Lee et al. 2019). In addition, for copolymer depositions, the flow rate ratio of V4D4/GMA was gradually increased from Cop-1 (0.25) to Cop-7 (4.0) sample. According to the Figure 5.16, the increase in cross-linker density caused an increase in the deposition rate as expected.

5.3.2.1. Chemical Composition of Homo- and Cross-linked Copolymer Films

In this study, FTIR analysis was used to confirm complete polymerization of monomers and evaluate the quality and chemical composition of the polymer films.

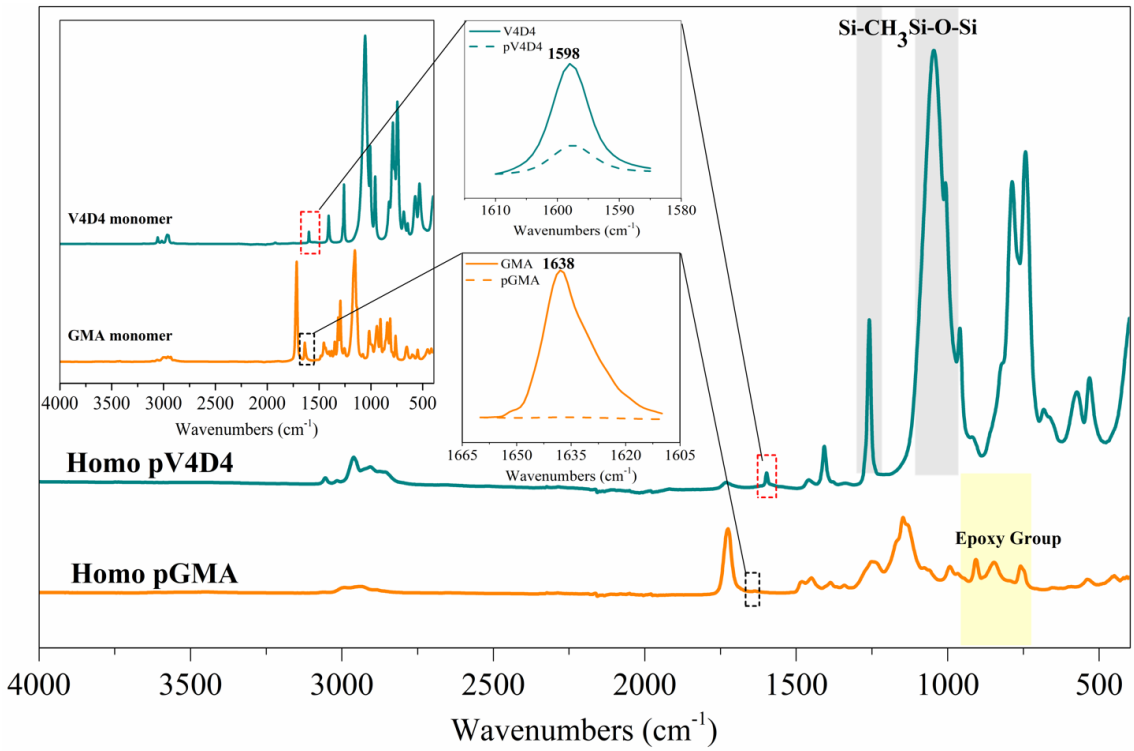

Figure 5.17. FTIR spectra of GMA and V4D4 monomers and their homopolymer films.

The peak intensity of V4D4 monomer at 1598 cm^{-1} attributed to vinyl (CH_2=CH) group decreased to a certain extent in pV4D4 spectrum. The decrease of the peak intensity demonstrates consumption vinyl functionality by polymerization of V4D4 monomer, but a significant amount of the vinyl group still remained in the polymer. A V4D4 monomer contains 4 vinyl groups and with free radical polymerization, complete consumption of the vinyl groups is unfeasible due to the steric hindrance (Yoo et al. 2013; Seok et al. 2018; Abessolo Ondo et al. 2019). Specific peaks of V4D4 monomer which are asymmetric Si-O-Si stretching (1075 cm^{-1}) and strong $SiCH_3$ symmetric bending (1260

cm^{-1}) were obtained in pV4D4 spectrum similarly and this is the indication of conserving the functionality of V4D4 monomer during deposition (Yoo et al. 2013; Seok et al. 2018; Abessolo Ondo et al. 2019).

The prominent characteristic peaks between 3000 and 2800 cm^{-1} assigned to C-H symmetry and asymmetry stretching caused by CH_3 and CH_2 groups and the peak at 1730 cm^{-1} related to carbonyl group (C=O) stretching vibration were explicitly observed in both GMA and pGMA spectra. The peak at 1640 cm^{-1} related to C=C bonds was not observed in iCVD deposited polymer's spectra and this is an indication of polymerization (Bakker et al. 2007; Karaman and Çabuk 2012; Sarıipek and Karaman 2014). The characteristic peaks at 906, 846 and 760 cm^{-1} which belong to epoxy group stretching was clearly seen in pGMA spectrum in addition to the monomer spectra (Mao and Gleason 2004, 2006; Mohammed Safiullah, Abdul Wasi, and Anver Basha 2014). This is a demonstration of preserving the functional properties of the monomer after deposition. After homopolymer films, FTIR analysis was also carried out for cross-linked copolymer films to investigate the effect of cross-linker density on the films (Figure 5.18).

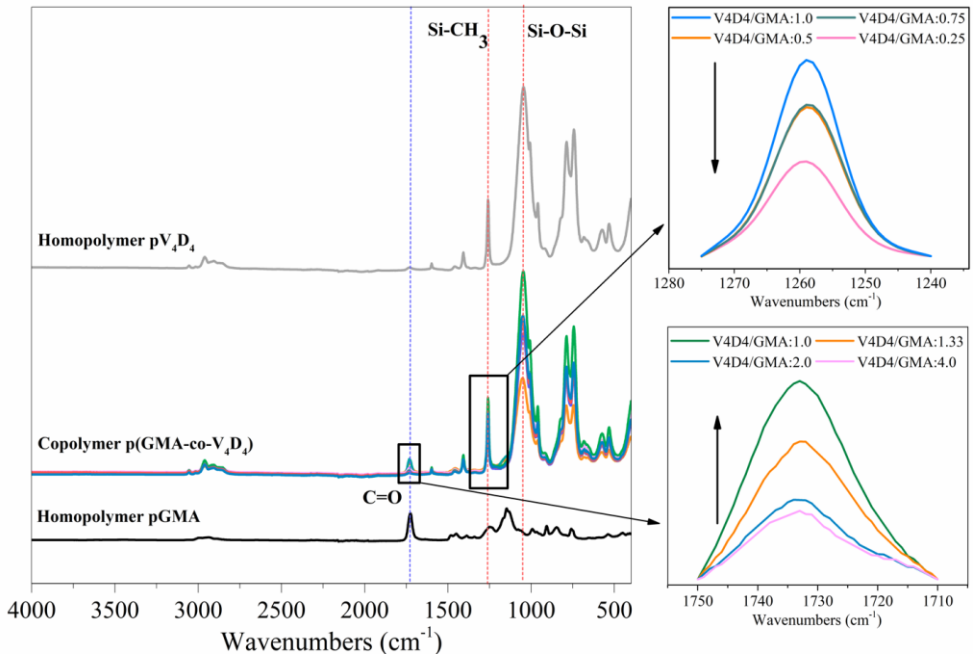

Figure 5.19. FTIR spectra of pGMA and pV4D4 homopolymers and their copolymers.

In copolymer FTIR spectra, all characteristic peaks of pV4D4 and pGMA homopolymers including asymmetric Si-O-Si stretching (1075 cm^{-1}), strong Si-CH_3

symmetric bending (1260 cm^{-1}) and C=O stretching (1730 cm^{-1}) were clearly observed. This is the evidence of successful fabrication of cross-linked copolymer films in iCVD process. In Figure 5.18, FTIR spectrum of the copolymer films for two different peak regions has been magnified. The upper one was created by enlarging the area containing the Si-CH_3 symmetric bending (1260 cm^{-1}), which is the specific peak of pV4D4. The spectra clearly indicated the direct proportion effect of cross-linker density on copolymer deposition (gradually decreasing of F_{V4D4}/F_{GMA} ratio from 1.0 to 0.25 causes decreasing in the peak intensity of pV4D4 at 1260 cm^{-1}). This verified that the copolymerization carried out correctly in iCVD system. The area based on the C=O stretching peak at 1730 cm^{-1} belonging to pGMA was also enlarged. The peak intensities increased as the F_{V4D4}/F_{GMA} ratio decreased gradually from 4.0 to 1.0, that is, as the cross-linker density decreased. As a result, the flow rate ratio changes (F_{V4D4}/F_{GMA}) directly affected the content of copolymer films.

In this study, the main aim is to develop robust polymer based QD-4AT sensor nanoprobe for detection of target heavy metal ion. For this reason, chemical and mechanical durability test procedures published in literature study (Karabıyık, Cihanoğlu, and Ebil 2023) were followed to decide the most durable copolymer film. It was shown that fabricated iCVD films. Durability in organic solvent (toluene, dichloromethane (DCM), ethanol, isopropyl alcohol (IPA), acetone, dimethylformamide (DMF) and tetrahydrofuran (THF)), salt resistance, water solubility and adhesion tests were performed. The criterion for success in all tests was set to less than 5% reduction in film thickness. The following table illustrates the durability test results for all copolymer films.

Table 5.2. Chemical and Mechanical Durability Test Results.

iCVD sample	Resistance to Organic Solvent							Salt Resistance	Water Solubility	Adhesion
	Toluene	DCM	Ethanol	IPA	Acetone	DMF	THF			
pGMA								•	•	•
cop-1	•	•	•	•	•	•	•	•	•	•
cop-2			•	•	•	•		•	•	•
cop-3				•				•	•	•
cop-4	•		•	•		•		•	•	•
cop-5			•	•		•		•	•	•
cop-6			•	•		•		•	•	•
cop-7			•	•		•		•	•	•
pV4D4				•		•		•	•	•

• passed the test (result with less than 5% change in film thickness)

Durability of homopolymer pGMA was not sufficient as the films were completely dissolved in organic solvents although it successfully passed salt resistance, water solubility and adhesion tests. Homopolymer pV4D4 fared better compared to pGMA as it also survived DMF and IPA immersion tests. Cross-linked copolymer film synthesized using a flow rate ratio of 0.1/0.4 (V4D4/GMA) achieved the best durability by passing all tests while all other copolymer films were partially successful.

The reactive sites per monomer determines whether the final structure of polymer will be linear or crosslinked. According to the functionality, reactants (monomers) are divided into 3 as monofunctional, bifunctional and multifunctional in polymerization. Especially, multifunctional reactants lead to formation of cross-linked structures and to achieve 3D cross-linked structures, at least one of them must be multifunctional (Shokuhfar and Arab 2013). V4D4 is a multifunctional cross-linker having four reactive sites, so GMA and V4D4 are able to produce 3D cross-linked epoxy polymers. Each V4D4 molecule can react at most with four GMA molecules as GMA is a monofunctional monomer and each of which is capable of being connected to another molecule through its C-H site. Although V4D4 is theoretically thought to be able to pair all its functional bonds during the synthesis of poly(GMA-co-V4D4) copolymer, not all vinyl bonds in the V4D4 monomer participate in crosslinking, as discussed earlier (steric hindrance effect). However, even if this is the case, cross-linking efficiency with GMA was quite high with 0.1/0.4 (V4D4/GMA) monomer ratio compared to other copolymers.

5.3.2.2. Epoxy Ring Opening Reactions for poly(GMA-co-V4D4) Films

EDX analysis was performed to investigate the chemical composition of iCVD fabricated films before and after epoxy ring opening reactions and to examine which amine group gives the best result in terms of functionalization of the polymeric films. Although trace elements are not suitable for this analysis, most elements up to a concentration (1-10wt %) can be detected with EDX analysis. Therefore, elemental analysis of polymeric films with this technique can be useful before and after the ring opening reaction. Table 5.3 shows elemental composition of as deposited p(GMA-co-

EGDMA) films and after the ring opening reactions with propylamine and ethylenediamine.

Table 5.3. EDX analysis before and after epoxy ring opening reaction of p(GMA-co V4D4) copolymer film.

Element	p(GMA-co-V4D4)		Propylamine (1M)		Ethylenediamine (1M)		Ethylenediamine (10M)	
	Wt%	Atomic %	Wt%	Atomic %	Wt%	Atomic %	Wt%	Atomic %
C	52.40	59.46	52.10	59.02	51.72	58.53	37.17	42.79
O	47.60	40.54	45.88	39.02	44.52	37.82	39.20	33.88
N			2.02	1.96	3.76	3.65	23.63	23.33
Total	100.00	100.00	100.00	100.00	100.00	100.00	100.00	100.00

The highest nitrogen content was found in ethylenediamine functionalized copolymers (in especially 10M solution) when compared with propylamine. Due to its bifunctional structure in terms of the amine group, its bonding performance to the polymer backbone is higher than that of propylamine. The increase in the concentration of the solution also increased the functionalization of the polymer surface. These prove that ethylenediamine reactivity in the epoxy ring opening reaction is higher than propylamine.

Fluorescence spectroscopy analysis was also performed to confirm EDX results and to determine which amine group functionalized polymer surface (propylamine or ethylenediamine) exhibited better bonding with QD-based nanoprobe (Cd^{2+} ion detection). The results are shown below in Figure 5.19.

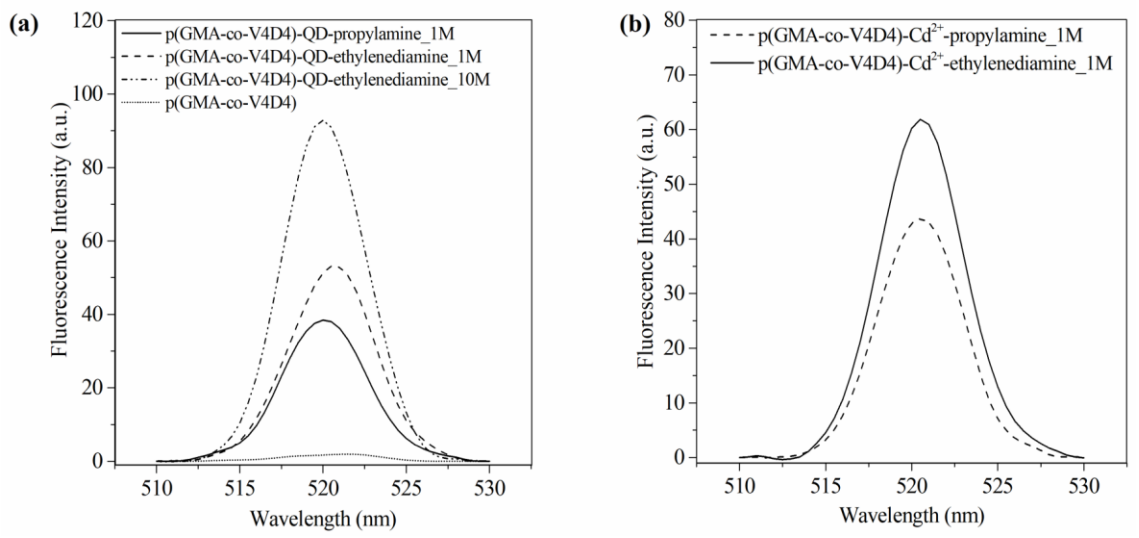

Figure 5.19. Examination of amine group effect on (a) PL response of QDs at 520 nm and (b) Cd^{2+} ion detection.

The rate of QD binding on ethylenediamine functionalized polymer surface was found to be higher than that of propylamine-functionalized surface. A high PL response was obtained at 520 nm, especially on the 10M ethylenediamine-functionalized polymer film. When Figure 5.19b is examined, it appears that Cd^{2+} ions can be detected more effectively with ethylenediamine-functionalized polymer film. The results support EDX analysis results. In summary, functionalized cross-linked copolymer film by 10M ethylenediamine was chosen to successfully bind the QD-4AT nanoprobe to the polymer film surface.

5.3.2.3. Cd^{2+} ion Detection with Polymer Bonded QD-4AT Nanoprobe

Cd^{2+} ion detection study was carried out with cross-linked copolymer-based QD-4AT sensor nanoprobe. QD fluorescence recovery was evaluated by both fluorescence spectroscopy and microscopy analyses. The results were shown below in Figure 5.20.

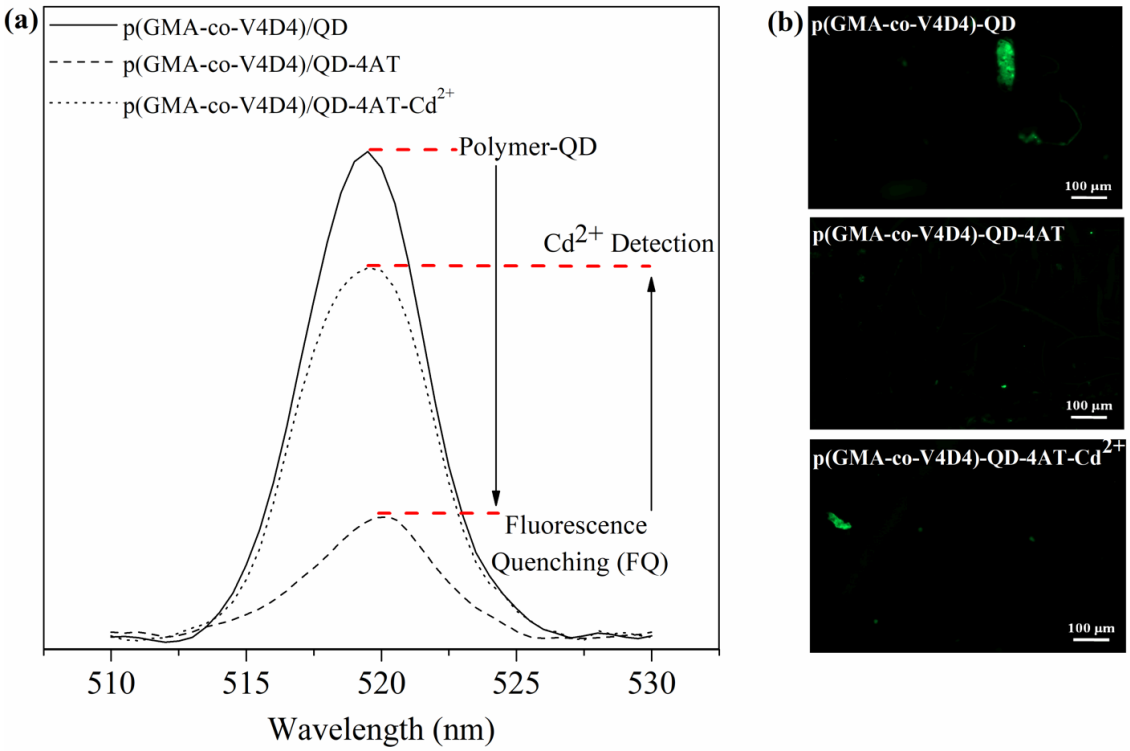

Figure 5.20. The results of Cd^{2+} ion detection with p(GMA-co-V4D4)-QD-4AT nanoprobe by using (a) fluorescence spectroscopy and (b) fluorescence microscopy analyses.

Fluorescence spectroscopy and microscopy results show that QD and QD-4AT nanoprobe successfully bonded to iCVD deposited cross-linked copolymer p(GMA-co-V4D4) films in separate experiments. A strong fluorescence emission was obtained when only QDs are attached to the film surface. A clear fluorescence quenching was observed after QDs are interacted with 4AT. It should be also noted that fluorescence microscopy revealed strong indication of isolated pockets of high QD concentration on polymer film surface that may be a result of non-uniform bonding over the film surface area. After the polymer based nanoprobe was immersed into the solution containing Cd^{2+} ion, fluorescence recovery was observed due to interaction with Cd^{2+} ions. The results of both analyzes proved that the main goal of this study was achieved with the developed polymer bonded QD-4AT fluorescence sensor nanoprobe.

5.3.2.4. Detection Limit of Proposed Sensor Nanoprobe for Cd^{2+} Ion

Detection limit of Cd^{2+} ions plays an important role for determining sensitivity of the fluorescence sensor. There are several sensor probe structures in the literature for the detection of Cd^{2+} ions in liquid media, while some of these studies did not calculate the detection limit of Cd^{2+} ions (Banerjee, Kar, and Santra 2008), the others reported the LOD values as 2.72 mM (Knopp, Scherbaum, and Kim 1996), 1 μM (Bronson et al. 2005), 0.5 μM (Xu, Miao, et al. 2011) and 0.8 nM (Preeyanka and Sarkar 2021). In this study, in order to find the detection limit for Cd^{2+} ion, experiments were performed to evaluate the fluorescence intensity changes with the change of Cd^{2+} ion concentration in the medium where the polymer based QD-4AT nanoprobe was immersed. After the experiment, F/F_0 versus metal ion concentration (Cd^{2+}) plot was plotted where F and F_0 are the fluorescence intensities observed after and before addition of Cd^{2+} ion into the medium, respectively. From the created calibration plot, the limit of detection (LOD) calculation was performed using the following equation (Walekar et al. 2013; Du et al. 2017).

$$LOD = 3\sigma k \tag{5.2}$$

where σ is the standard deviation of the y-intercepts of the regression lines and k is the slope of the calibration graph. The calibration plot described above was generated by using the fluorescence intensities of polymer-based QD-4AT nanoprobe obtained by increasing the Cd^{2+} ion concentration from 0.0784 to 40 μM in fluorescence spectroscopy.

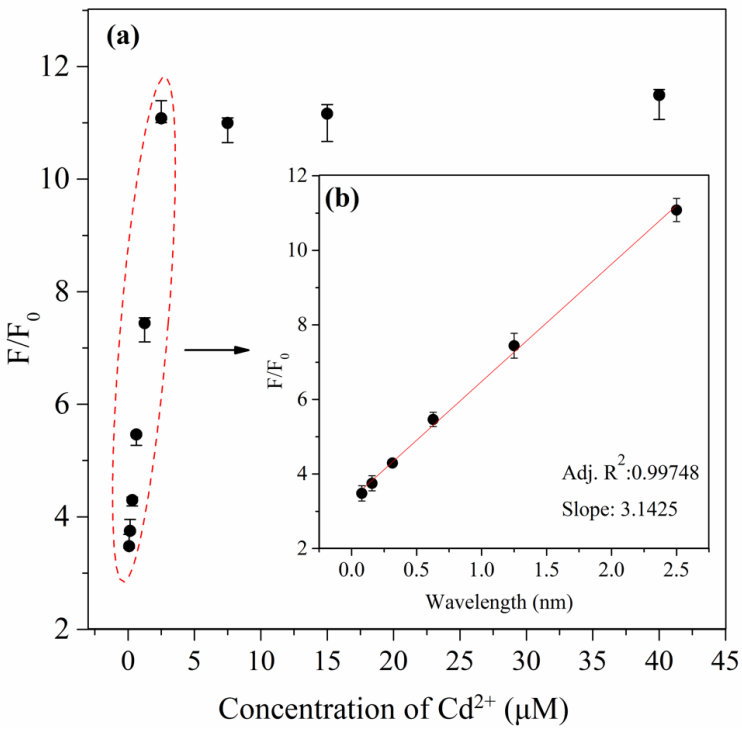

Figure 5.21. Relative PL response (F/F0) of polymer-based QD-4AT nanoprobe in the presence of different amount of Cd^{2+} ion (concentration range 0.0784-40 μM) (b) the linear relationship between fluorescence intensity variation and Cd^{2+} concentration in the range 0. 0784–2.5 μM.

Figure 5.21a shows the effect of Cd^{2+} ion concentration on the PL enhancement of polymer-based QD-4AT nanoprobe. The fluorescence intensity of nanoprobe gradually enhanced with sequential addition of Cd^{2+} ion demonstrating that the nanoprobe can be used as an on-off-on fluorescent probe for Cd^{2+} ion detection. As the concentration of Cd^{2+} ion increased from 0.0784 to 40 μM, fluorescence intensity of nanoprobe enhanced and reached the maximum value and kept almost constant upon the addition of 2.5 μM of Cd^{2+} ion. F/F_0 versus metal ion concentration (Cd^{2+}) plot was plotted in Figure 5.21b which shows a linear behavior. This linearity in the concentration range of the 0.0784–2.5 μM region without any spectral shift allows one to use the linear regression equation to calculate the detection limit of Cd^{2+} ion. From Figure 5.21b, the slope and the R^2 values were obtained as 3.1425 and 0.99748, respectively and limit of detection (LOD) of Cd^{2+} ion was found as 0.195 μM. When compared with previously reported studies in literature related to Cd^{2+} ion sensitivity, the sensitivity of new polymer-based nanoprobe developed

in this study is very promising (Knopp, Scherbaum, and Kim 1996; Bronson et al. 2005; Banerjee, Kar, and Santra 2008; Xu, Miao, et al. 2011).

5.3.3. Part III. Cd^{2+} Ion Detection in Real Water Sources and Multi-Use Study

To investigate applicability and reliability of developed polymer-based QD-4AT nanoprobe, real water samples (tap, commercial bottled and sea water) were used as solvent for detection of Cd^{2+} ion and analysis was performed by the standard addition method. The same samples were also analyzed using ICP-MS and results are given in Table 5.4 for comparison.

Table 5.4. Determination of Cd^{2+} in real water sources.

Nanoprobe Type	Sample	Original Concentration of Cd^{2+} (μM)	Cd^{2+} Added (μM)	Cd^{2+} Found[b] (μM)	Recovery (%)	Cd^{2+} found by ICP-MS (μM)
QD-4AT	Tap Water	< LOD[a]	500	447.8	89.6	579.7
	Commercial bottled water			472.8	94.6	965.3
	Sea water			492.9	98.6	661.9
Polymer-QD-4AT	Tap Water			450.8	90.2	579.7
	Commercial bottled water			451.2	90.2	965.3
	Sea water			454.2	90.8	661.9

a: LOD of Cd^{2+} is 0.195 μM.

b: Values determined by QD-4AT and Polymer-QD-4AT as fluorescence probes; for 3 and 4 replicate measurements, respectively.

During the part of the study, Cd^{2+} ion detection in real water sources was performed by using both QD-4AT as liquid nanoprobe and polymer-QD-4AT as polymer based nanoprobe. The recovery of Cd^{2+} ion in three different real water samples was obtained in a range of 89.6–98.6%. Results indicate that the response of developed sensor nanoprobes was not affected by the type of water samples. The original concentrations

values of Cd^{2+} ions obtained by ICP-MS analysis were $2.9x10^{-3}$, $4.36x10^{-4}$ and $1.04x10^{-2}$ μM for tap, commercial bottled and sea water, respectively. This proved that the Cd^{2+} ion in real water sources was below the detection limit of the developed nanoprobe structure as obtained in Table 5.4. Also, high recovery percentages show that developed nanoprobe structure, especially the polymer based nanoprobe, has great potential for the specific identification and quantification of Cd^{2+} ion in different real water samples with high accuracy. When compared with the ICP-MS analysis results, the sensor probe developed in this study gave values much closer to the original concentration value (500 μM). This is a very strong indication that the sensor developed in this study is a promising alternative for the detection of Cd^{2+} ions in different real water sources.

The results reported in literature and the experiments carried out during this study reveals that high pH values (pH > 8) are not suitable for Cd^{2+} ion detection. At high pH values, Cd^{2+} ion will react with OH^- to form metal hydroxides in the environment (high pH values lead to high OH^- concentration in the solution). Considering this situation, to investigate whether the developed polymer-based nanoprobe can be used for Cd^{2+} ion detection multiple times, a separate study was conducted based on the change in solution pH. The main purpose here is to provide suitable conditions (like pH) in which Cd^{2+} ion can interact more easily with another structure in the medium to detach from the nanoprobe. During the detection of Cd^{2+} ions, an electrostatic interaction occurs between Cd^{2+} ion and 4AT, so it is possible to detach Cd^{2+} ion from this structure by optimizing the ambient conditions. Figure 5.22 shows the multiuse study results.

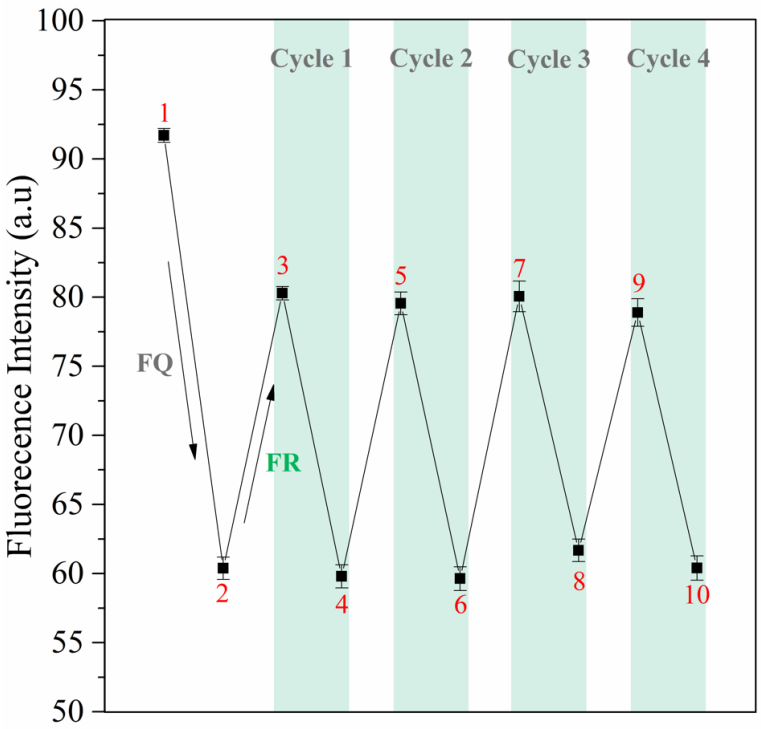

Figure 5.22. Multi-use study for detection of Cd^{2+} ion with polymer based QD-4AT nanoprobe (1: polymer-QD, 2: polymer-QD-4AT, 3-5-7-9: Cd^{2+} ion detection at pH=8, 4-6-8-10: Cd^{2+} ion removal at pH=12).

As seen in Figure 5.22, Cd^{2+} ion detection was performed with the polymer-based QD-4AT nanoprobe. A PL response at 520 nm was obtained by binding the QDs to the cross-linked copolymer film (1). The formation of the polymer-QD-4AT nanoprobe caused the fluorescence quenching (FQ) (2). Cd^{2+} ions were successfully detected by immersing this nanoprobe into a medium containing Cd^{2+} ions at pH=8, resulting in fluorescence recovery (FR) (3). To detach Cd^{2+} ions from the nanoprobe structure, polymer-QD-4AT nanoprobe was immersed into the pH=12 medium. As a result of fluorescence analysis, Cd^{2+} ion moved away from the nanoprobe to form a complex with hydroxide ion (OH^-) leading to fluorescence quenching (4). In this way, the first cycle was completed by detecting Cd^{2+} ions (at pH=8) and detaching them it from the nanoprobe (at pH=12).

Additional cycles were performed to examine whether the polymer based QD-4AT nanoprobe could be used for detection and removal process again multiple times.

In the following 3 additional cycles (cycle 2, 3, and 4), Cd^{2+} ions were successfully detected. After 4 cycles, deviations in fluorescence intensity were observed

leading to inaccurate results. In summary, the multi-use study proved that the polymer based QD-4AT nanoprobe can be used at least 4 times in Cd^{2+} ion detection.

Considering all these results, it can be concluded that an inspiring solid state nanoprobe has been developed for sensor application, when compared to sensor nanoprobes previously developed in liquid media. The newly developed polymer based QD-4AT nanoprobe, in addition to its ability to be used repeatedly for heavy metal ion detection, exhibits a very robust structure that can be used in harsh environments.

5.4. Conclusion

As a first in literature, a multi-use, robust cross-linked copolymer bonded CdTe QD-4AT fluorescent sensor nanoprobe was developed to selectively detect Cd^{2+} ion in real water sources. The optimal conditions were determined to effectively detect Cd^{2+} ion through optimizing the solution pH, solvent type, concentrations of QD-4AT and PBS and reaction time. A strong PL response was obtained after the attachment of QDs on polymer thin film surfaces and fluorescence quenching (FQ) was realized with electron transfer between QD and 4AT. Interaction with QD and 4AT was blocked by the presence of Cd^{2+} ions in the environment, 4AT turned into diamagnetic counterpart due to electron transfer with Cd^{2+} ion and fluorescence recovery (FR) was achieved. It has been also demonstrated that the polymer-based nanoprobe can work effectively even in the presence of different ions in the environment and can successfully detect Cd^{2+} ions.

In literature, detection limit for Cd^{2+} ion sensor probes (all of them are single use only) were rarely reported. In a few studies where the detection limits were reported, the values were much lower than the value obtained with the polymer-based sensor nanoprobe (LOD is 0.195µM).

Moreover, it has been shown that developed sensor nanoprobe achieved high recovery performance (>90 %) in tap water, commercial bottled water and sea water indicating Cd^{2+} ion selectivity is not affected in the presence of other ions in the sample. Finally, the multi-use study has proven that the polymer-based fluorescence nanoprobe can be repeatedly used at least 4 times (and in different water samples) for Cd^{2+} ion detection without any performance loss.

CHAPTER 6

CONCLUSION

The main purpose of this thesis study is to investigate the feasibility of selective detection of Cd^{2+} ion in real water sources by developing a multi-use, highly durable cross-linked copolymer based CdTe QD-4AT fluorescent sensor nanoprobe. The study is divided into 3 main sections and the results obtained in each section are summarized as follows.

Chapter 3 is the first part of this thesis study and includes a novel functional polymer based QDs-nitroxide radical complex development as nanoprobe for fluorescent sensors. Epoxy polymer based thin films were fabricated in iCVD system to achieve functional surfaces through epoxy ring opening reactions. This is significant for QDs' attachment to the polymer films. Aliphatic primary amine (propylamine) was found as the most effective amine functional group for surface modification of iCVD deposited thin films and CdTe QD attachment to functionalized polymer surface. The fluorescence quenching efficiency of the nitroxide radical was investigated for QD-nitroxide radical on-off complex structure. The longer reaction times showed that the interaction between QD and 4AT increased. EPR, fluorescence spectroscopy and microscopy analysis confirmed that the covalent bonding of the QD-4AT nanoprobe to the epoxy polymer surface was successfully achieved. The results proved the possibility of multiple and easy use of polymer bonded QD-nitroxide radical complex as sensor structures in various applications.

In Chapter 4, cross-linked epoxy copolymer films were fabricated via iCVD to obtain chemically and mechanically durable thin-films on a variety of surfaces, especially optical systems. These copolymer films were found to be very suitable for integration into sensor development as described in Chapter 5. Poly(GMA-co-V4D4) copolymers produced using V4D4 monomer, which is one of the two selected cross-linkers in this study, showed high resistant to water (<1% thickness loss), salt solution (<1.5% thickness loss), organic solvents (<5% thickness loss) and high optical transparency (~90% in the

visible spectrum). This proved that p(GMA-co-V4D4) cross-linked copolymer film is a good alternative as ideal coating materials for protection purposes in different applications.

Chapter 5 covers the development of robust polymer bonded QD-4AT fluorescence sensor nanoprobe for detection of Cd^{2+} ions in various water sources, using the cross-linked p(GMA-co-V4D4) copolymer film and CdTe QD-4AT nanoprobe. Optimum conditions for Cd^{2+} ion detection were investigated by evaluating the effects of different parameters such as solution pH, reaction time, solvent type, and a low LOD (0.195 μM) and high recovery rate (> 90%) were obtained. It was confirmed that the same sensor nanoprobe could be used several times for the detection of Cd^{2+} ion without any loss of performance.

In summary, the thesis study successfully demonstrated, as a first in literature, the development of a chemically and mechanically stable, sensitive, muti-use polymer-bonded fluorescent sensor nanoprobe.

REFERENCES

Abessolo Ondo, Dominique, François Loyer, Florian Werner, Renaud Leturcq, Phillip J. Dale, and Nicolas D. Boscher. 2019. "Atmospheric-Pressure Synthesis of Atomically Smooth, Conformal, and Ultrathin Low-k Polymer Insulating Layers by Plasma-Initiated Chemical Vapor Deposition." ACS Applied Polymer Materials 1 (12):3304-3312. https://doi.org/10.1021/acsapm.9b00759.

Achadu, O. J., J. Britton, and T. Nyokong. 2016. "Graphene Quantum Dots Functionalized with 4-Amino-2, 2, 6, 6-Tetramethylpiperidine-N-Oxide as Fluorescence "Turn-ON" Nanosensors." J Fluoresc 26 (6):2199-2212. https://doi.org/10.1007/s10895-016-1916-y.

Adegoke, O., S. Khene, and T. Nyokong. 2013. "Fluorescence "switch on" of conjugates of CdTe@ZnS quantum dots with Al, Ni and Zn tetraamino-phthalocyanines by hydrogen peroxide: characterization and applications as luminescent nanosensors." J Fluoresc 23 (5):963-74. https://doi.org/10.1007/s10895-013-1222-x.

Adegoke, Oluwasesan, Eric Hosten, Cedric McCleland, and Tebello Nyokong. 2012. "CdTe quantum dots functionalized with 4-amino-2,2,6,6-tetramethylpiperidine-N-oxide as luminescent nanoprobe for the sensitive recognition of bromide ion." Analytica Chimica Acta 721:154-161. https://doi.org/10.1016/j.aca.2012.01.040.

Afkhami, Abbas, Ali Shirzadmehr, Tayyebeh Madrakian, and Hasan Bagheri. 2015. "New nano-composite potentiometric sensor composed of graphene nanosheets/thionine/molecular wire for nanomolar detection of silver ion in various real samples." Talanta 131:548-555. https://doi.org/10.1016/j.talanta.2014.08.004.

Alf, Mahriah E., Ayse Asatekin, Miles C. Barr, Salmaan H. Baxamusa, Hitesh Chelawat, Gozde Ozaydin-Ince, Christy D. Petruczok, Ramaswamy Sreenivasan, Wyatt E. Tenhaeff, Nathan J. Trujillo, Sreeram Vaddiraju, Jingjing Xu, and Karen K. Gleason. 2010. "Chemical Vapor Deposition of Conformal, Functional, and Responsive Polymer Films." Advanced Materials 22 (18):1993-2027. https://doi.org/10.1002/adma.200902765.

Alf, Mahriah E., T. Alan Hatton, and Karen K. Gleason. 2011. "Initiated chemical vapor deposition of responsive polymeric surfaces." Thin Solid Films 519 (14):4412-4414. http://dx.doi.org/10.1016/j.tsf.2011.01.286.

Alice Lee, N., and Ivan R. Kennedy. 2007. "Chapter 5 - Immunoassays." In Food Toxicants Analysis, edited by Yolanda Picó, 91-145. Amsterdam: Elsevier. https://doi.org/10.1016/b978-044452843-8/50006-7.

Allcock, H.R., F.W. Lampe, and J.E. Mark. 2003. Contemporary Polymer Chemistry: Prentice Hall. https://doi.org/10.1002/PI.1494.

Allmér, K., A. Hult, and B. Rånby. 1989. "Surface modification of polymers. II. Grafting with glycidyl acrylates and the reactions of the grafted surfaces with amines." Journal of Polymer Science Part A: Polymer Chemistry 27 (5):1641-1652. https://doi.org/10.1002/pola.1989.080270516.

Althues, H., P. Simon, and S. Kaskel. 2007. "Transparent and luminescent YVO4 : Eu/polymer nanocomposites prepared by in situ polymerization." Journal of Materials Chemistry 17 (8):758-765. https://doi.org/10.1039/B611917D.

Amjadi, Mohammad, Roghayeh Shokri, and Tooba Hallaj. 2016. "A new turn-off fluorescence probe based on graphene quantum dots for detection of Au(III) ion." Spectrochimica Acta Part A: Molecular and Biomolecular Spectroscopy 153:619-624. https://doi.org/10.1016/j.saa.2015.09.037.

Aresta, G., J. Palmans, M. C. M. van de Sanden, and M. Creatore. 2012. "Initiated-chemical vapor deposition of organosilicon layers: Monomer adsorption, bulk growth, and process window definition." Vacuum Science & Technology 30. https://doi.org/10.1116/1.4711762.

Arivarasan, Ayyaswamy, Ganapathy Sasikala, and Ramasamy Jayavel. 2014. "In situ synthesis of CdTe:CdS quantum dot nanocomposites for photovoltaic applications." Materials Science in Semiconductor Processing 25:238-243. https://doi.org/10.1016/j.mssp.2013.12.018.

Arndt, K.-F., A. Richter, S. Ludwig, J. Zimmermann, J. Kressler, D. Kuckling, and H.-J. Adler. 1999. "Poly(vinyl alcohol)/poly(acrylic acid) hydrogels: FT-IR spectroscopic characterization of crosslinking reaction and work at transition point." Acta Polymerica 50 (11-12):383-390. https://doi.org/10.1002/(SICI)1521-4044(19991201)50:11/12<383::AID-APOL383>3.0.CO;2-Z.

Asatekin, A., and K. K. Gleason. 2010. "Functional nanotube membranes for hydrophobicity-based separations by initiated chemical vapor deposition (iCVD)."

Abstracts of Papers of the American Chemical Society 240. https://doi.org/10.1021/bk-2011-1078.ch004.

Asatekin, Ayse, Miles C. Barr, Salmaan H. Baxamusa, Kenneth K. S. Lau, Wyatt Tenhaeff, Jingjing Xu, and Karen K. Gleason. 2010. "Designing polymer surfaces via vapor deposition." Materials Today 13 (5):26-33. https://doi.org/10.1016/S1369-7021(10)70081-X.

Atkins, P., and J. de Paula. 2006. ATKINS' PHYSICAL CHEMISTRY. 8th ed. New York, NY: Great Britain by Oxford University Press.

Bakker, R., V. Verlaan, C. H. M. van der Werf, J. K. Rath, K. K. Gleason, and R. E. I. Schropp. 2007. "Initiated chemical vapour deposition (iCVD) of thermally stable poly-glycidyl methacrylate." Surface and Coatings Technology 201 (22–23):9422-9425. http://dx.doi.org/10.1016/j.surfcoat.2007.03.058.

Balali-Mood, Mahdi, Kobra Naseri, Zoya Tahergorabi, Mohammad Reza Khazdair, and Mahmood Sadeghi. 2021. "Toxic Mechanisms of Five Heavy Metals: Mercury, Lead, Chromium, Cadmium, and Arsenic." Frontiers in Pharmacology 12. https://doi.org/10.3389/fphar.2021.643972.

Banerjee, Subhash, Soumitra Kar, and Swadeshmukul Santra. 2008. "A simple strategy for quantum dot assisted selective detection of cadmium ions." Chemical Communications (26):3037-3039. https://doi.org/10.1039/B803166E.

Barbey, Raphael, and Harm-Anton Klok. 2010. "Room Temperature, Aqueous Post-Polymerization Modification of Glycidyl Methacrylate-Containing Polymer Brushes Prepared via Surface-Initiated Atom Transfer Radical Polymerization." Langmuir 26 (23):18219-18230. https://doi.org/10.1021/la102400z.

Bassam, Rajaa, Achraf El hallaoui, Marouane El Alouani, Maissara Jabrane, El Hassan El Khattabi, Malika Tridane, and Said Belaaouad. 2021. "Studies on the Removal of Cadmium Toxic Metal Ions by Natural Clays from Aqueous Solution by Adsorption Process." Journal of Chemistry 2021:7873488. https://doi.org/10.1155/2021/7873488.

Baxamusa, Salmaan H., Sung Gap Im, and Karen K. Gleason. 2009. "Initiated and oxidative chemical vapor deposition: a scalable method for conformal and functional polymer films on real substrates." Physical Chemistry Chemical Physics 11 (26):5227-5240. https://doi.org/10.1039/B900455F.

Bayramoglu, Gulay, Verda Bitirim, Yagmur Tunali, Mehmet Yakup Arica, and Kamil Can Akcali. 2013. "Poly (hydroxyethyl methacrylate-glycidyl methacrylate) films

modified with different functional groups: In vitro interactions with platelets and rat stem cells." Materials Science and Engineering: C 33 (2):801-810. https://doi.org/10.1016/j.msec.2012.11.004.

Bhattacharjee, Brinta, Sudip Mukherjee, Riya Mukherjee, and Jayanta Haldar. 2022. "Easy Fabrication of a Polymeric Transparent Sheet to Combat Microbial Infection." ACS Applied Bio Materials 5 (8):3951-3959. https://doi.org/10.1021/acsabm.2c00476.

Bian, Zhao-Yang, Xiang-Qun Guo, Yi-Bing Zhao, and Jun-Ou Du. 2005. "Probing the Hydroxyl Radical-Mediated Reactivity of Peroxynitrite by a Spin-Labeling Fluorophore." Analytical Sciences 21 (5):553-559. https://doi.org/10.2116/analsci.21.553.

Birck, C., S. Degoutin, M. Maton, C. Neut, M. Bria, M. Moreau, F. Fricoteaux, V. Miri, and M. Bacquet. 2016. "Antimicrobial citric acid/poly(vinyl alcohol) crosslinked films: Effect of cyclodextrin and sodium benzoate on the antimicrobial activity." LWT - Food Science and Technology 68:27-35. https://doi.org/10.1016/j.lwt.2015.12.009.

Blaskó, Ágnes, Zoltán Gazdag, Pál Gróf, Gábor Máté, Szilvia Sárosi, Judit Krisch, Csaba Vágvölgyi, Lilla Makszin, and Miklós Pesti. 2017. "Effects of clary sage oil and its main components, linalool and linalyl acetate, on the plasma membrane of Candida albicans: an in vivo EPR study." Apoptosis 22 (2):175-187. https://doi.org/10.1007/s10495-016-1321-7.

Boentoro, T. W., and B. Szyszka. 2013. "14 - Protective coatings for optical surfaces." In Optical Thin Films and Coatings, edited by Angela Piegari and François Flory, 540-563. Woodhead Publishing. https://doi.org/10.1533/9780857097316.4.540.

Bose, Ranjita K., Alex M. Heming, and Kenneth K. S. Lau. 2012. "Microencapsulation of a Crop Protection Compound by Initiated Chemical Vapor Deposition." Macromolecular Rapid Communications 33 (16):1375-1380. https://doi.org/10.1002/marc.201200214.

Bose, Ranjita K., Kenneth Lau, University Drexel, and Engineering College of. 2011. "Initiated chemical vapor deposition of polymer thin films and coatings for biological applications." Drexel University, http://worldcat.org.

Briffa, Jessica, Emmanuel Sinagra, and Renald Blundell. 2020. "Heavy metal pollution in the environment and their toxicological effects on humans." Heliyon 6 (9):e04691. https://doi.org/10.1016/j.heliyon.2020.e04691.

Bronson, R. Todd, David J. Michaelis, Randy D. Lamb, Ghaleb A. Husseini, Paul B. Farnsworth, Matthew R. Linford, Reed M. Izatt, Jerald S. Bradshaw, and Paul B. Savage. 2005. "Efficient Immobilization of a Cadmium Chemosensor in a Thin Film: Generation of a Cadmium Sensor Prototype." Organic Letters 7 (6):1105-1108. https://doi.org/10.1021/ol050027t.

Cai, Cheng, Heyong Cheng, Yuanchao Wang, and Haifeng Bao. 2014. "Mercaptosuccinic acid modified CdTe quantum dots as a selective fluorescence sensor for Ag+ determination in aqueous solutions." RSC Advances 4 (103):59157-59163. https://doi.org/10.1039/C4RA07891H.

Çaykara, Tuncer, Ferhat Çakar, and Serkan Demirci. 2008. "A new type of poly(glycidyl methacrylate) microbeads with surface grafted iminodiacetic acid: Synthesisand characterization." Polymer Bulletin 61 (3):311-318. https://doi.org/10.1007/s00289-008-0958-y.

Chambers, L. D., K. R. Stokes, F. C. Walsh, and R. J. K. Wood. 2006. "Modern approaches to marine antifouling coatings." Surface and Coatings Technology 201 (6):3642-3652. https://doi.org/10.1016/j.surfcoat.2006.08.129.

Chan, Kelvin, and Karen K. Gleason. 2006. "A Mechanistic Study of Initiated Chemical Vapor Deposition of Polymers: Analyses of Deposition Rate and Molecular Weight." Macromolecules 39 (11):3890-3894. https://doi.org/10.1021/ma051776t.

Chan, Kelvin, Lara E. Kostun, Wyatt E. Tenhaeff, and Karen K. Gleason. 2006. "Initiated chemical vapor deposition of polyvinylpyrrolidone-based thin films." Polymer 47 (20):6941-6947. http://dx.doi.org/10.1016/j.polymer.2006.07.068.

Chen, Bin, Junjie Liu, Tong Yang, Lin Chen, Jia Hou, Changhao Feng, and Cheng Zhi Huang. 2019. "Development of a portable device for Ag+ sensing using CdTe QDs as fluorescence probe via an electron transfer process." Talanta 191:357-363. https://doi.org/10.1016/j.talanta.2018.08.088.

Chen, Bin, Jun Ma, Tong Yang, Lin Chen, Peng Fei Gao, and Cheng Zhi Huang. 2017. "A portable RGB sensing gadget for sensitive detection of Hg2+ using cysteamine-capped QDs as fluorescence probe." Biosensors and Bioelectronics 98:36-40. https://doi.org/10.1016/j.bios.2017.05.032.

Chen, Chun-Yen, Chiu-Ting Cheng, Chih-Wei Lai, Pei-Wen Wu, Kun-Chan Wu, Pi-Tai Chou, Yi-Hsuan Chou, and Hsin-Tien Chiu. 2006. "Potassium ion recognition by

15-crown-5 functionalized CdSe/ZnS quantum dots in H2O." Chemical Communications (3):263-265. https://doi.org/10.1039/B512677K.

Chen, Hengye, Shuo Wang, Haiyan Fu, Hongliang Xie, Wei Lan, Lu Xu, Lei Zhang, and Yuanbin She. 2020. "Dual-QDs ratios fluorescent probe for sensitive and selective detection of silver ions contamination in real sample." Spectrochimica Acta Part A: Molecular and Biomolecular Spectroscopy 234:118248. https://doi.org/10.1016/j.saa.2020.118248.

Chen, Nan, Do Han Kim, Peter Kovacik, Hossein Sojoudi, Minghui Wang, and Karen K. Gleason. 2016. "Polymer Thin Films and Surface Modification by Chemical Vapor Deposition: Recent Progress." Annual Review of Chemical and Biomolecular Engineering 7 (1):373-393. https://doi.org/10.1146/annurev-chembioeng-080615-033524.

Chen, Wenbin, Xin Wang, Xijuan Tu, Dejun Pei, Yue Zhao, and Xiangqun Guo. 2008. "Water-Soluble Off–On Spin-Labeled Quantum-Dots Conjugate." Small 4 (6):759-764. https://doi.org/10.1002/smll.200700788.

Cheng, Ningyan, Ping Jiang, Qian Liu, Jingqi Tian, Abdullah M. Asiri, and Xuping Sun. 2014. "Graphitic carbon nitride nanosheets: one-step, high-yield synthesis and application for Cu2+ detection." Analyst 139 (20):5065-5068. https://doi.org/10.1039/C4AN00914B.

Chern, M., J. C. Kays, S. Bhuckory, and A. M. Dennis. 2019. "Sensing with photoluminescent semiconductor quantum dots." Methods Appl Fluoresc 7 (1):012005. https://doi.org/10.1088/2050-6120/aaf6f8.

Chithiraikumar, Somasundaram, Chithiraivel Balakrishnan, and M. A. Neelakantan. 2017. "Tuning ligand vicinity towards development of “turn-on” fluorescence for cadmium(II) ions under physiological pH and bio-imaging." Sensors and Actuators B: Chemical 249:235-245. https://doi.org/10.1016/j.snb.2017.04.106.

Christian, P., A. M. Coclite, and Beilstein J. 2017. "Vapor-phase-synthesized fluoroacrylate polymer thin films: thermal stability and structural properties." Nanotechnology 8:933-942. https://doi.org/10.3762/bjnano.8.95.

Cihanoğlu, Gizem, and Özgenç Ebil. 2021. "Robust fluorinated siloxane copolymers via initiated chemical vapor deposition for corrosion protection." Journal of Materials Science 56 (20):11970-11987. https://doi.org/10.1007/s10853-021-06060-4.

Coclite, Anna Maria, Gozde Ozaydin-Ince, Riccardo d’Agostino, and Karen K. Gleason. 2009. "Flexible Cross-Linked Organosilicon Thin Films by Initiated Chemical

Vapor Deposition." Macromolecules 42 (21):8138-8145. https://doi.org/10.1021/ma901431m.

Coclite, Anna Maria, Yujun Shi, and Karen K. Gleason. 2013. "Super-Hydrophobic and Oloephobic Crystalline Coatings by Initiated Chemical Vapor Deposition." Physics Procedia 46:56-61. http://dx.doi.org/10.1016/j.phpro.2013.07.045.

D'Ischia, Marco, and Daniel Ruiz-Molina. 2017. "Bioinspired Catechol-Based Systems: Chemistry and Applications." Biomimetics 2 (4):25. https://doi.org/10.3390/biomimetics2040025.

Dakin, J. P., and R. G. W. Brown. 2006. Handbook of Optoelectronics. Vol. 1. https://doi.org/10.1201/9781315157009.

Dang, Ya-Min, and Xiang-Qun Guo. 2006. "New Approach for the Detection of Peptide- and Protein-Based Radicals Using A Pre-fluorescent Probe." Applied Spectroscopy 60 (2):203-207. https://doi.org/10.1366/000370206776023269.

De Acha, Nerea, César Elosúa, Jesús M. Corres, and Francisco J. Arregui. 2019. "Fluorescent Sensors for the Detection of Heavy Metal Ions in Aqueous Media." Sensors 19 (3):599. https://doi.org/10.3390/s19030599.

Diaz, David, Juvencio Robles, Tong Ni, Silvia-Elena Castillo-Blum, Datattri Nagesha, Octavio-Jaime Alvarez-Fregoso, and Nicholas A. Kotov. 1999. "Surface Modification of CdS Nanoparticles with MoS42-: A Case Study of Nanoparticle−Modifier Electronic Interaction." The Journal of Physical Chemistry B 103 (45):9859-9866. https://doi.org/10.1021/jp992122n.

Dijksman, Arné, Isabel W. C. E. Arends, and Roger A. Sheldon. 2003. "Cu(ii)-nitroxyl radicals as catalytic galactose oxidase mimics." Organic & Biomolecular Chemistry 1 (18):3232-3237. https://doi.org/10.1039/B305941C.

Ding, Yongling, Shirley Z. Shen, Huadong Sun, Kangning Sun, and Futian Liu. 2014. "Synthesis of l-glutathione-capped-ZnSe quantum dots for the sensitive and selective determination of copper ion in aqueous solutions." Sensors and Actuators B: Chemical 203:35-43. https://doi.org/10.1016/j.snb.2014.06.054.

Drouet, Christophe, Pierre Alphonse, and Abel Rousset. 2001. "IR spectroscopic study of NO and CO adsorptions on nonstoichiometric nickel–copper manganites." Physical Chemistry Chemical Physics 3 (17):3826-3830. https://doi.org/10.1039/B101523K.

Du, Wenqi, Yu Cheng, Weixin Shu, and Zhengjian Qi. 2017. "A Novel Rhodamine-Based Fluorescence Chemosensor Containing Polyether For Mercury (II) Ions in

Aqueous Solution." Química Nova 40. https://doi.org/10.21577/0100-4042.20170060

Ellairaja, Sundaram, Ramar Manikandan, Muthunan Thevar Vijayan, Seenivasan Rajagopal, and Vairathevar Sivasamy Vasantha. 2015. "A simple highly sensitive and selective TURN-ON fluorescent chemosensor for the detection of cadmium ions in physiological conditions." RSC Advances 5 (78):63287-63295. https://doi.org/10.1039/C5RA10612E.

Elmizadeh, Hamideh, Majid Soleimani, Farnoush Faridbod, and GhasemRezanejade Bardajee. 2019. "Fabrication of a nanomaterial-based fluorescence sensor constructed from ligand capped CdTe quantum dots for ultrasensitive and rapid detection of silver ions in aqueous samples." Spectrochimica Acta Part A: Molecular and Biomolecular Spectroscopy 211:291-298. https://doi.org/10.1016/j.saa.2018.12.016.

Enikolopiyan, N. S. 1976. "New Aspects of the Nucleophilic Opening of Epoxide Rings." Pure and Applied Chemistry 48:317 - 328. https://doi.org/10.1351/pac197648030317

Es-said, Amine, Hicham Nafai, Ghita Lamzougui, Ahmed Bouhaouss, and Rahma Bchitou. 2021. "Comparative adsorption studies of cadmium ions on phosphogypsum and natural clay." Scientific African 13:e00960. https://doi.org/10.1016/j.sciaf.2021.e00960.

Faria, Marisa, Carla Vilela, Faranak Mohammadkazemi, Armando J. D. Silvestre, Carmen S. R. Freire, and Nereida Cordeiro. 2019. "Poly(glycidyl methacrylate)/bacterial cellulose nanocomposites: Preparation, characterization and post-modification." International Journal of Biological Macromolecules 127:618-627. https://doi.org/10.1016/j.ijbiomac.2019.01.133.

Faten, Divsar. 2020. "Introductory Chapter: Quantum Dots." In Quantum Dots, edited by Divsar Faten, Ch. 1. Rijeka: IntechOpen. https://doi.org/10.5772/intechopen.92151

Gan, Ting-Ting, Yu-Jun Zhang, Nan-Jing Zhao, Xue Xiao, Gao-Fang Yin, Shao-Hui Yu, Huan-Bo Wang, Jing-Bo Duan, Chao-Yi Shi, and Wen-Qing Liu. 2012. "Hydrothermal synthetic mercaptopropionic acid stabled CdTe quantum dots as fluorescent probes for detection of Ag+." Spectrochimica Acta Part A: Molecular and Biomolecular Spectroscopy 99:62-68. https://doi.org/10.1016/j.saa.2012.09.005.

García-Garrido, C., P. E. Sánchez-Jiménez, L. A. Pérez-Maqueda, A. Perejón, and José M. Criado. 2016. "Combined TGA-MS kinetic analysis of multistep processes. Thermal decomposition and ceramification of polysilazane and polysiloxane preceramic polymers." Physical Chemistry Chemical Physics 18 (42):29348-29360. https://doi.org/10.1039/C6CP03677E.

García-Miranda Ferrari, Alejandro, Paul Carrington, Samuel J. Rowley-Neale, and Craig E. Banks. 2020. "Recent advances in portable heavy metal electrochemical sensing platforms." Environmental Science: Water Research & Technology 6 (10):2676-2690. https://doi.org/10.1039/D0EW00407C.

Geißlmeir, David, Walther G. Jary, and Heinz Falk. 2005. "The TEMPO/Copper Catalyzed Oxidation of Primary Alcohols to Aldehydes Using Oxygen as Stoichiometric Oxidant." Monatshefte für Chemie / Chemical Monthly 136 (9):1591-1599. https://doi.org/10.1007/s00706-005-0349-0.

Gleason, K.K. 2015. CVD Polymers: Fabrication of Organic Surfaces and Devices: Wiley. https://doi.org/10.1002/9783527690275.

Gokan, H., S. Esho, and Y. Ohnishi. 1983. "Dry Etch Resistance of Organic Materials." Journal of The Electrochemical Society 130 (1):143-146. https://doi.org/10.1149/1.2119642.

Göksel, Yaman, and Yasar Akdogan. 2019. "Increasing spontaneous wet adhesion of DOPA with gelation characterized by EPR spectroscopy." Materials Chemistry and Physics 228:124-130. https://doi.org/10.1016/j.matchemphys.2019.02.054.

Gong, Tingting, Junfeng Liu, Xinxin Liu, Jie Liu, Jinkun Xiang, and Yiwei Wu. 2016. "A sensitive and selective sensing platform based on CdTe QDs in the presence of l-cysteine for detection of silver, mercury and copper ions in water and various drinks." Food Chemistry 213:306-312. https://doi.org/10.1016/j.foodchem.2016.06.091.

Green, S. A., D. J. Simpson, G. Zhou, P. S. Ho, and Neil V. Blough. 1990. "Intramolecular quenching of excited singlet states by stable nitroxyl radicals." Journal of the American Chemical Society 112 (20):7337-7346. https://doi.org/10.1021/ja00176a038.

Guo, Qiuquan, Maxim Paliy, Brad Kobe, Tomas Trebicky, Natalie Suhan, Gilles Arsenault, Lorenzo Ferrari, and Jun Yang. 2015. "Characterization of cross-linking depth for thin polymeric films using atomic force microscopy." Journal of Applied Polymer Science 132 (8). https://doi.org/10.1002/app.41493.

Gupta, Malancha, and Karen K. Gleason. 2006a. "Initiated Chemical Vapor Deposition of Poly(1H,1H,2H,2H-perfluorodecyl Acrylate) Thin Films." Langmuir 22 (24):10047-10052. https://doi.org/10.1021/la061904m.

Gupta, Malancha, and Karen K. Gleason. 2006b. "Large-scale initiated chemical vapor deposition of poly(glycidyl methacrylate) thin films." Thin Solid Films 515 (4):1579-1584. http://dx.doi.org/10.1016/j.tsf.2006.05.021.

Gupta, Malancha, V. Kapur, Nathalie M. Pinkerton, and Karen K. Gleason. 2008a. "Initiated Chemical Vapor Deposition (iCVD) of Conformal Polymeric Nanocoatings for the Surface Modification of High-Aspect-Ratio Pores." Chemistry of Materials 20 (4):1646–1651. https://doi.org/10.1021/cm702810j.

H. Gunzler, and H. U. Gremlich. 2002. IR Spectroscopy: Wiley-VCH.

Haloi, Dhruba J., Prithwiraj Mandal, and Nikhil K. Singha. 2013. "Atom Transfer Radical Polymerization of Glycidyl Methacrylate (GMA) in Emulsion." Journal of Macromolecular Science, Part A 50 (1):121-127. https://doi.org/10.1080/10601325.2013.736270.

Hao, Lifen, Wei Xu, and Qiufeng An. 2014. "Synthesis, film morphology and performance of novel crosslinked polysiloxane with end-capped epoxy groups on cotton substrates." Fibers and Polymers 15 (8):1567-1574. https://doi.org/10.1007/s12221-014-1567-z.

Haoue, Sara, Hodhaifa Derdar, Mohammed Belbachir, and Amine Harrane. 2020. "Polymerization of Ethylene Glycol Dimethacrylate (EGDM), Using An Algerian Clay as Eco-catalyst (Maghnite-H+ and Maghnite-Na+)." 2020:10. https://doi.org/10.9767/bcrec.15.1.6297.221-230.

Haugland, Marius M., Janet E. Lovett, and Edward A. Anderson. 2018. "Advances in the synthesis of nitroxide radicals for use in biomolecule spin labelling." Chemical Society Reviews 47 (3):668-680. https://doi.org/10.1039/C6CS00550K.

Hemmati, Maryam, Maryam Rajabi, and Alireza Asghari. 2018. "Magnetic nanoparticle based solid-phase extraction of heavy metal ions: A review on recent advances." Microchimica Acta 185 (3):160. https://doi.org/10.1007/s00604-018-2670-4.

Hilt, J. Zachary, Amit K. Gupta, Rashid Bashir, and Nicholas A. Peppas. 2003. "Ultrasensitive Biomems Sensors Based on Microcantilevers Patterned with Environmentally Responsive Hydrogels." Biomedical Microdevices 5 (3):177-184. https://doi.org/10.1023/A:1025786023595.

Hoffman, Allan S. 1996. "Surface modification of polymers: Physical, chemical, mechanical and biological methods." Macromolecular Symposia 101 (1):443-454. https://doi.org/10.1002/masy.19961010150.

Hu, Juan, Zi-yue Wang, Chen-chen Li, and Chun-yang Zhang. 2017. "Advances in single quantum dot-based nanosensors." Chemical Communications 53 (100):13284-13295. https://doi.org/10.1039/C7CC07752A.

Huang, Heqin, Rui Chen, Jiale Ma, Li Yan, Yingqi Zhao, Yu Wang, Wenjun Zhang, Jun Fan, and Xianfeng Chen. 2014. "Graphitic carbon nitride solid nanofilms for selective and recyclable sensing of Cu2+ and Ag+ in water and serum." Chemical Communications 50 (97):15415-15418. https://doi.org/10.1039/C4CC06659F.

Iqbal, M. S., Yasmeen Jamil, T. Kausar, and M. Akhtar. 2009. "Thermal degradation study of glycidyl methacrylate acrylonitrile copolymers." Journal of Thermal Analysis and Calorimetry 96 (1):225-233. https://doi.org/10.1007/s10973-008-9009-z.

Irzhak, Vadim I., Igor E. Uflyand, and Gulzhian I. Dzhardimalieva. 2022. "Self-Healing of Polymers and Polymer Composites." Polymers 14 (24):5404. https://doi.org/10.3390/polym14245404.

J. Brandrup , E. H. Immergut, E. A. Grulke. 1999. Polymer Handbook. 4th ed. ed. https://doi.org/10.1002/1097-0126(200007)49:73.0.CO;2-1.

Jaganathan, Saravana Kumar, Arunpandian Balaji, Muthu Vignesh Vellayappan, Aruna Priyadarshni Subramanian, Agnes Aruna John, Manjeesh Kumar Asokan, and Eko Supriyanto. 2015. "Review: Radiation-induced surface modification of polymers for biomaterial application." Journal of Materials Science 50 (5):2007-2018. https://doi.org/10.1007/s10853-014-8718-x.

Jeevendrakumar, Vijay Jain Bharamaiah, Daniel N. Pascual, and Magnus Bergkvist. 2015. "Wafer Scale Solventless Adhesive Bonding with iCVD Polyglycidylmethacrylate: Effects of Bonding Parameters on Adhesion Energies." Advanced Materials Interfaces 2 (9):1500076. https://doi.org/10.1002/admi.201500076.

Jin, Wei Jun, José M. Costa-Fernández, Rosario Pereiro, and Alfredo Sanz-Medel. 2004. "Surface-modified CdSe quantum dots as luminescent probes for cyanide determination." Analytica Chimica Acta 522 (1):1-8. https://doi.org/10.1016/j.aca.2004.06.057.

Kane, C. F., and R. R. Krchnavek. 1995. "Benzocyclobutene optical waveguides." IEEE Photonics Technology Letters 7 (5):535-537. https://doi.org/10.1109/68.384535.

Karabıyık, Merve, Gizem Cihanoğlu, and Özgenç Ebil. 2023. "CVD Deposited Epoxy Copolymers as Protective Coatings for Optical Surfaces." Polymers 15 (3):652. https://doi.org/10.3390/polym15030652.

Karabiyik, Merve, and Özgenç Ebil. 2022. "Polymer-bonded CdTe quantum dot-nitroxide radical nanoprobes for fluorescent sensors." Journal of Materials Science 57 (34):16258-16279. https://doi.org/10.1007/s10853-022-07640-8.

Karaman, Mustafa, and Nihat Çabuk. 2012. "Initiated chemical vapor deposition of pH responsive poly(2-diisopropylamino)ethyl methacrylate thin films." Thin Solid Films 520 (21):6484-6488. https://doi.org/10.1016/j.tsf.2012.06.083.

Karoui, Hakim, François Le Moigne, Olivier Ouari, and Paul Tordo. 2010. "Nitroxide Radicals: Properties, Synthesis and Applications." In Stable Radicals, 173-229. https://doi.org/10.1002/9780470666975.ch5.

Kennedy, C D. 1990. "Ionic strength and the dissociation of acids." Biochemical Education 18 (1):35-40. https://doi.org/10.1016/0307-4412(90)90017-I.

Khan, Md Motiar R., Tapas Mitra, and Dibakar Sahoo. 2020. "Metal oxide QD based ultrasensitive microsphere fluorescent sensor for copper, chromium and iron ions in water." RSC Advances 10 (16):9512-9524. https://doi.org/10.1039/C9RA09985A.

Khanmohammadi, Akbar, Arash Jalili Ghazizadeh, Pegah Hashemi, Abbas Afkhami, Fabiana Arduini, and Hasan Bagheri. 2020. "An overview to electrochemical biosensors and sensors for the detection of environmental contaminants." Journal of the Iranian Chemical Society 17 (10):2429-2447. https://doi.org/10.1007/s13738-020-01940-z.

Kim, Ha Na, Wen Xiu Ren, Jong Seung Kim, and Juyoung Yoon. 2012. "Fluorescent and colorimetric sensors for detection of lead, cadmium, and mercury ions." Chemical Society Reviews 41 (8):3210-3244. https://doi.org/10.1039/C1CS15245A.

Kim, Jae-Pil, Won-Young Lee, Jae-Wook Kang, Soon-Ki Kwon, Jang-Joo Kim, and Jae-Suk Lee. 2001. "Fluorinated Poly(arylene ether sulfide) for Polymeric Optical Waveguide Devices." Macromolecules 34 (22):7817-7821. https://doi.org/10.1021/ma010439r.

Kim, Min, Satoshi Kiyohara, Satoshi Konishi, Satoshi Tsuneda, Kyoichi Saito, and Takanobu Sugo. 1996. "Ring-opening reaction of poly-GMA chain grafted onto a

porous membrane." Journal of Membrane Science 117 (1):33-38. https://doi.org/10.1016/0376-7388(96)00026-9.

Kim, T. H., J. H. Kim, M. D. Le Kim, W. D. Suh, J. E. Kim, H. J. Yeon, Y. S. Park, S. H. Kim, Y. H. Oh, and G. H. Jo. 2020. "Exposure assessment and safe intake guidelines for heavy metals in consumed fishery products in the Republic of Korea." Environ Sci Pollut Res Int 27 (26):33042-33051. https://doi.org/10.1007/s11356-020-09624-0.

Kimmins, Scott D., Paul Wyman, and Neil R. Cameron. 2014. "Amine-functionalization of glycidyl methacrylate-containing emulsion-templated porous polymers and immobilization of proteinase K for biocatalysis." Polymer 55 (1):416-425. https://doi.org/10.1016/j.polymer.2013.09.019.

Knopp, R., F. J. Scherbaum, and J. I. Kim. 1996. "Laser induced breakdown spectroscopy (LIBS) as an analytical tool for the detection of metal ions in aqueous solutions." Fresenius' Journal of Analytical Chemistry 355 (1):16-20. https://doi.org/10.1007/s0021663550016.

Koneswaran, Masilamany, and Ramaier Narayanaswamy. 2009. "RETRACTED: Mercaptoacetic acid capped CdS quantum dots as fluorescence single shot probe for mercury(II)." Sensors and Actuators B: Chemical 139 (1):91-96. https://doi.org/10.1016/j.snb.2008.09.011.

Kumar, Pawan, Ki-Hyun Kim, Vasudha Bansal, Theodore Lazarides, and Naresh Kumar. 2017. "Progress in the sensing techniques for heavy metal ions using nanomaterials." Journal of Industrial and Engineering Chemistry 54:30-43. https://doi.org/10.1016/j.jiec.2017.06.010.

Labbé, Amélie, Anne-Laure Brocas, Emmanuel Ibarboure, Takashi Ishizone, Akira Hirao, Alain Deffieux, and Stéphane Carlotti. 2011. "Selective Ring-Opening Polymerization of Glycidyl Methacrylate: Toward the Synthesis of Cross-Linked (Co)polyethers with Thermoresponsive Properties." Macromolecules 44 (16):6356-6364. https://doi.org/10.1021/ma201075n.

Laferrière, Marie, Raquel E. Galian, Vincent Maurel, and J. C. Scaiano. 2006. "Non-linear effects in the quenching of fluorescent quantum dots by nitroxyl free radicals." Chemical Communications (3):257-259. https://doi.org/10.1039/B511515A.

Lau, K. K. S., and K. K. Gleason. 2006a. "Initiated chemical vapor deposition (iCVD) of poly(alkyl acrylates): An experimental study." Macromolecules 39 (10):3688-3694. https://doi.org/10.1021/ma0601619.

Lau, K. K. S., and K. K. Gleason. 2006b. "Initiated chemical vapor deposition (iCVD) of poly(alkyl acrylates): A kinetic model." Macromolecules 39 (10):3695-3703. https://doi.org/10.1021/ma0601621.

Lau, K. K. S., and K. K. Gleason. 2007a. "Particle functionalization and encapsulation by initiated chemical vapor deposition (iCVD)." Surface & Coatings Technology 201 (22-23):9189-9194. https://doi.org/10.1016/j.surfcoat.2007.04.045.

Lau, K. K. S., and K. K. Gleason. 2008. "Initiated chemical vapor deposition (iCVD) of copolymer thin films." Thin Solid Films 516 (5):678-680. https://doi.org/10.1016/j.tsf.2007.06.046.

Lau, K. K. S., and K. K. Gleason. 2006c. "Particle Surface Design using an All-Dry Encapsulation Method." Advanced Materials 18 (15):1972-1977. https://doi.org/10.1002/adma.200600896.

Lau, Kenneth K. S., José Bico, Kenneth B. K. Teo, Manish Chhowalla, Gehan A. J. Amaratunga, William I. Milne, Gareth H. McKinley, and Karen K. Gleason. 2003. "Superhydrophobic Carbon Nanotube Forests." Nano Letters 3 (12):1701-1705. https://doi.org/10.1021/nl034704t.

Lau, Kenneth K. S., and Karen K. Gleason. 2007b. "All-Dry Synthesis and Coating of Methacrylic Acid Copolymers for Controlled Release." Macromolecular Bioscience 7 (4):429-434. https://doi.org/10.1002/mabi.200700017.

Lau, Kenneth K. S., and Karen K. Gleason. 2007c. "Particle functionalization and encapsulation by initiated chemical vapor deposition (iCVD)." Surface and Coatings Technology 201 (22–23):9189-9194. http://dx.doi.org/10.1016/j.surfcoat.2007.04.045.

Lee, Hyo Seong, Hayeong Kim, Jeong Heon Lee, and Jae B. Kwak. 2019. "Fabrication of a Conjugated Fluoropolymer Film Using One-Step iCVD Process and its Mechanical Durability." Coatings 9 (7):430. https://doi.org/10.3390/coatings9070430.

Lee, Nanju, and Ivan Kennedy. 2007. "Chapter 5. Immunoassays." In, 91-145. https://doi.org/10.1016/b978-044452843-8/50006-7.

Lee, William, Tatsuya Oshikiri, Kyoichi Saito, Kazuyuki Sugita, and Takanobu Sugo. 1996. "Comparison of Formation Site of Graft Chain between Nonporous and Porous Films Prepared by RIGP." Chemistry of Materials 8 (11):2618-2621. https://doi.org/10.1021/cm950405w.

Lemon, Christopher M., Elizabeth Karnas, Xiaoxing Han, Oliver T. Bruns, Thomas J. Kempa, Dai Fukumura, Moungi G. Bawendi, Rakesh K. Jain, Dan G. Duda, and Daniel G. Nocera. 2015. "Micelle-Encapsulated Quantum Dot-Porphyrin Assemblies as in Vivo Two-Photon Oxygen Sensors." Journal of the American Chemical Society 137 (31):9832-9842. https://doi.org/10.1021/jacs.5b04765.

Li, Gang, Xiulin Zhu, Jian Zhu, Zhenping Cheng, and Wei Zhang. 2005. "Homogeneous reverse atom transfer radical polymerization of glycidyl methacrylate and ring-opening reaction of the pendant oxirane ring." Polymer 46 (26):12716-12721. https://doi.org/10.1016/j.polymer.2005.10.061.

Li, Haibing, and Xiaoqiong Wang. 2008. "Single quantum dot-micelles coated with gemini surfactant for selective recognition of a cation and an anion in aqueous solutions." Sensors and Actuators B: Chemical 134 (1):238-244. https://doi.org/10.1016/j.snb.2008.04.041.

Li, Pingjing, Yayu Hong, Huatao Feng, and Sam F. Y. Li. 2017. "An efficient “off–on” carbon nanoparticle-based fluorescent sensor for recognition of chromium(vi) and ascorbic acid based on the inner filter effect." Journal of Materials Chemistry B 5 (16):2979-2988. https://doi.org/10.1039/C7TB00017K.

Li, Pingjing, and Sam F. Y. Li. 2021. "Recent advances in fluorescence probes based on carbon dots for sensing and speciation of heavy metals." Nanophotonics 10 (2):877-908. https://doi.org/10.1515/nanoph-2020-0507.

Li, Shuang, Te Wei, Guojuan Ren, Fang Chai, Hongbo Wu, and Fengyu Qu. 2017. "Gold nanoparticles based colorimetric probe for Cr(III) and Cr(VI) detection." Colloids and Surfaces A: Physicochemical and Engineering Aspects 535:215-224. https://doi.org/10.1016/j.colsurfa.2017.09.028.

Lin, Feng, Dejun Pei, Weina He, Zhaoxia Huang, Yanjie Huang, and Xiangqun Guo. 2012. "Electron transfer quenching by nitroxide radicals of the fluorescence of carbon dots." Journal of Materials Chemistry 22 (23):11801-11807. https://doi.org/10.1039/C2JM31191G.

Lin, Liping, Yuhan Wang, Yanling Xiao, and Wei Liu. 2019. "Hydrothermal synthesis of carbon dots codoped with nitrogen and phosphorus as a turn-on fluorescent probe for cadmium(II)." Microchimica Acta 186 (3):147. https://doi.org/10.1007/s00604-019-3264-5.

Liu, Jia, Xinyu Zhao, Hanyu Xu, Zhaoyin Wang, and Zhihui Dai. 2019. "Amino Acid-Capped Water-Soluble Near-Infrared Region CuInS2/ZnS Quantum Dots for

Selective Cadmium Ion Determination and Multicolor Cell Imaging." Analytical Chemistry 91 (14):8987-8993. https://doi.org/10.1021/acs.analchem.9b01183.

Liu, Wenhao, Mark Howarth, Andrew B. Greytak, Yi Zheng, Daniel G. Nocera, Alice Y. Ting, and Moungi G. Bawendi. 2008. "Compact Biocompatible Quantum Dots Functionalized for Cellular Imaging." Journal of the American Chemical Society 130 (4):1274-1284. https://doi.org/10.1021/ja076069p.

Liu, Yongchao, Lili Teng, Hong-Wen Liu, Chengyan Xu, Haowei Guo, Lin Yuan, Xiao-Bing Zhang, and Weihong Tan. 2019. "Recent advances in organic-dye-based photoacoustic probes for biosensing and bioimaging." Science China Chemistry 62 (10):1275-1285. https://doi.org/10.1007/s11426-019-9506-2.

Lu, Wenbo, Xiaoyun Qin, Sen Liu, Guohui Chang, Yingwei Zhang, Yonglan Luo, Abdullah M. Asiri, Abdulrahman O. Al-Youbi, and Xuping Sun. 2012. "Economical, Green Synthesis of Fluorescent Carbon Nanoparticles and Their Use as Probes for Sensitive and Selective Detection of Mercury(II) Ions." Analytical Chemistry 84 (12):5351-5357. https://doi.org/10.1021/ac3007939.

Ma, H., A.K.-Y. Jen, and L.R. Dalton. 2002. "Polymer-Based Optical Waveguides: Materials, Processing, and Devices." Advanced Materials 14 (19):1339-1365. https://doi.org/10.1002/1521-4095(20021002)14:19<1339::AID-ADMA1339>3.0.CO;2-O.

Maiti, Siddhartha, Ziya Aydin, Yi Zhang, and Maolin Guo. 2015. "Reaction-based turn-on fluorescent probes with magnetic responses for Fe2+ detection in live cells." Dalton Transactions 44 (19):8942-8949. https://doi.org/10.1039/C4DT03792H.

Mandal, Abhijit, Anirban Dandapat, and Goutam De. 2012. "Magic sized ZnS quantum dots as a highly sensitive and selective fluorescence sensor probe for Ag+ ions." Analyst 137 (3):765-772. https://doi.org/10.1039/C1AN15653E.

Manjumeena, Rajarathinam, Dhanapal Duraibabu, Thangavelu Rajamuthuramalingam, Ramasamy Venkatesan, and Puthupalayam Thangavelu Kalaichelvan. 2015. "Highly responsive glutathione functionalized green AuNP probe for precise colorimetric detection of Cd^{2+} contamination in the environment." RSC Advances 5 (85):69124-69133. https://doi.org/10.1039/C5RA12427A.

Mao, Yu, and Karen K. Gleason. 2004. "Hot Filament Chemical Vapor Deposition of Poly(glycidyl methacrylate) Thin Films Using tert-Butyl Peroxide as an Initiator." Langmuir 20 (6):2484-2488. https://doi.org/10.1021/la0359427.

Mao, Yu, and Karen K. Gleason. 2006. "Vapor-Deposited Fluorinated Glycidyl Copolymer Thin Films with Low Surface Energy and Improved Mechanical Properties." Macromolecules 39 (11):3895-3900. https://doi.org/10.1021/ma052591p.

Marinović, S., Z. Vuković, A. Nastasović, A. Milutinović-Nikolić, and D. Jovanović. 2011. "Poly(glycidyl methacrylate-co-ethylene glycol dimethacrylate)/clay composites." Materials Chemistry and Physics 128 (1):291-297. https://doi.org/10.1016/j.matchemphys.2011.03.018.

Martin, Tyler P., Kenneth K. S. Lau, Kelvin Chan, Yu Mao, Malancha Gupta, W. Shannan O'Shaughnessy, and Karen K. Gleason. 2007. "Initiated chemical vapor deposition (iCVD) of polymeric nanocoatings." Surface and Coatings Technology 201 (22–23):9400-9405. http://dx.doi.org/10.1016/j.surfcoat.2007.05.003.

Maurel, Vincent, Marie Laferrière, Paul Billone, Robert Godin, and J. C. Scaiano. 2006. "Free Radical Sensor Based on CdSe Quantum Dots with Added 4-Amino-2,2,6,6-Tetramethylpiperidine Oxide Functionality." The Journal of Physical Chemistry B 110 (33):16353-16358. https://doi.org/10.1021/jp061115d.

McElroy, N., R. C. Page, D. Espinbarro-Valazquez, E. Lewis, S. Haigh, P. O'Brien, and D. J. Binks. 2014. "Comparison of solar cells sensitised by CdTe/CdSe and CdSe/CdTe core/shell colloidal quantum dots with and without a CdS outer layer." Thin Solid Films 560:65-70. https://doi.org/10.1016/j.tsf.2013.10.085.

Medintz, Igor L., H. Tetsuo Uyeda, Ellen R. Goldman, and Hedi Mattoussi. 2005. "Quantum dot bioconjugates for imaging, labelling and sensing." Nature Materials 4 (6):435-446. https://doi.org/10.1038/nmat1390.

Michaeli, Walter, Sebastian Hessner, and Fritz Klaiber. 2009. "Analysis of different compression-molding techniques regarding the quality of optical lenses." Journal of Vacuum Science & Technology B: Microelectronics and Nanometer Structures Processing, Measurement, and Phenomena 27 (3):1442-1444. https://doi.org/10.1116/1.3079765.

Mohammed Safiullah, S., K. Abdul Wasi, and K. Anver Basha. 2014. "Preparation of poly(Glycidyl methacrylate)–copper nanocomposite by in-situ suspension polymerization – A novel synthetic method." Materials Letters 133:60-63. http://dx.doi.org/10.1016/j.matlet.2014.06.127.

Mori, Masaru, Yoshikimi Uyama, and Yoshito Ikada. 1994. "Surface modification of polyethylene fiber by graft polymerization." Journal of Polymer Science Part A:

Polymer Chemistry 32 (9):1683-1690. https://doi.org/10.1002/pola.1994.080320910.

Muñoz, Eduardo, Julia Pérez-Prieto, Javier Román, Víctor Rojas, Rodrigo Henríquez, Paula Grez, Ricardo Schrebler, Ricardo Córdova, and Emilio Navarrete. 2019. "Interaction between nitroxyl radicals and CdTe quantum dots: Determination of fluorescence-quenching mechanisms in aqueous solution." Journal of Photochemistry and Photobiology A: Chemistry 383:112024. https://doi.org/10.1016/j.jphotochem.2019.112024.

Muzammil, Ezzah M, Anzar Khan, and Mihaiela C. Stuparu. 2017. "Post-polymerization modification reactions of poly(glycidyl methacrylate)s." RSC Advances 7 (88):55874-55884. https://doi.org/10.1039/C7RA11093F.

Nemani, Srinivasa Kartik, Rama Kishore Annavarapu, Behrouz Mohammadian, Asif Raiyan, Jamie Heil, Md. Ashraful Haque, Ahmed Abdelaal, and Hossein Sojoudi. 2018. "Surface Modification of Polymers: Methods and Applications." Advanced Materials Interfaces 5 (24):1801247. https://doi.org/10.1002/admi.201801247.

Niu, Wen-Jun, Dan Shan, Rong-Hui Zhu, Sheng-Yuan Deng, Serge Cosnier, and Xue-Ji Zhang. 2016. "Dumbbell-shaped carbon quantum dots/AuNCs nanohybrid as an efficient ratiometric fluorescent probe for sensing cadmium (II) ions and l-ascorbic acid." Carbon 96:1034-1042. https://doi.org/10.1016/j.carbon.2015.10.051.

Nutting, Jordan E., Mohammad Rafiee, and Shannon S. Stahl. 2018. "Tetramethylpiperidine N-Oxyl (TEMPO), Phthalimide N-Oxyl (PINO), and Related N-Oxyl Species: Electrochemical Properties and Their Use in Electrocatalytic Reactions." Chemical Reviews 118 (9):4834-4885. https://doi.org/10.1021/acs.chemrev.7b00763.

Nyquist, R.A. 2001. Interpreting Infrared, Raman, and Nuclear Magnetic Resonance Spectra: Factors affecting molecular vibrations and chemical shifts of infrared, Raman, and nuclear magnetic resonance spectra: Academic Press. https://doi.org/10.5860/choice.39-0947.

Ohring, M. , and L. Kasprzak. 2015. Reliability and Failure of ELECTRONIC MATERIALS AND DEVICES. Second ed.

Oliveira, Elisabete, Cristina Núñez, Hugo Miguel Santos, Javier Fernández-Lodeiro, Adrián Fernández-Lodeiro, José Luis Capelo, and Carlos Lodeiro. 2015. "Revisiting the use of gold and silver functionalised nanoparticles as colorimetric

and fluorometric chemosensors for metal ions." Sensors and Actuators B: Chemical 212:297-328. https://doi.org/10.1016/j.snb.2015.02.026.

Ozaydin-Ince, Gozde, and Karen K. Gleason. 2010. "Thermal Stability of Acrylic/Methacrylic Sacrificial Copolymers Fabricated by Initiated Chemical Vapor Deposition." Journal of The Electrochemical Society 157 (1):D41. https://doi.org/10.1149/1.3251308.

Özpirin, Merve, and Özgenç Ebil. 2018. "Transparent block copolymer thin films for protection of optical elements via chemical vapor deposition." Thin Solid Films 660:391-398. https://doi.org/10.1016/j.tsf.2018.06.044.

Pan, Kaibo, Chongming Liu, Zhicheng Zhu, Tanglue Feng, Songyuan Tao, and Bai Yang. 2022. "Soft–Hard Segment Combined Carbonized Polymer Dots for Flexible Optical Film with Superhigh Surface Hardness." ACS Applied Materials & Interfaces 14 (12):14504-14512. https://doi.org/10.1021/acsami.2c00702.

Parker, Thomas C., Daniel Baechle, and John Derek Demaree. 2011. "Polymeric barrier coatings via initiated chemical vapor deposition." Surface and Coatings Technology 206 (7):1680-1683. http://dx.doi.org/10.1016/j.surfcoat.2011.09.021.

Pazos, Miguel, Juan Baselga, and Julio Bravo. 2003. "Limiting thickness estimation in polycarbonate lenses injection using CAE tools." Journal of Materials Processing Technology 143-144:438-441. https://doi.org/10.1016/S0924-0136(03)00425-4.

Pei, Jiying, Hui Zhu, Xiaolei Wang, Hanchang Zhang, and Xiurong Yang. 2012. "Synthesis of cysteamine-coated CdTe quantum dots and its application in mercury (II) detection." Analytica Chimica Acta 757:63-68. https://doi.org/10.1016/j.aca.2012.10.037.

Petruczok, Christy D., Rong Yang, and Karen K. Gleason. 2013. "Controllable Cross-Linking of Vapor-Deposited Polymer Thin Films and Impact on Material Properties." Macromolecules 46 (5):1832-1840. https://doi.org/10.1021/ma302566r.

Piegari, A., and F. Flory. 2013. Optical Thin Films and Coatings: From Materials to Applications: Elsevier Science. https://doi.org/10.1016/C2016-0-02583-4.

Pinson, J., and D. Thiry. 2020. Surface Modification of Polymers: Methods and Applications: Wiley. https://doi.org/10.1002/9783527819249.

Pitois, C., D. Wiesmann, M. Lindgren, and A. Hult. 2001. "Functionalized Fluorinated Hyperbranched Polymers for Optical Waveguide Applications." Advanced

Materials 13 (19):1483-1487. https://doi.org/10.1002/1521-4095(200110)13:19<1483::AID-ADMA1483>3.0.CO;2-D.

Pooja, and Papia Chowdhury. 2020. "Optical and electronic properties of CdTe quantum dots in their freezed solid matrix phase and solution phase." Materials Today: Proceedings 28:201-204. https://doi.org/10.1016/j.matpr.2020.01.561.

Pooja, and Papia Chowdhury. 2021. "Functionalized CdTe fluorescence nanosensor for the sensitive detection of water borne environmentally hazardous metal ions." Optical Materials 111:110584. https://doi.org/10.1016/j.optmat.2020.110584.

Pooja, Meenakshi Rana, and Papia Chowdhury. 2019. "Influence of size and shape on optical and electronic properties of CdTe quantum dots in aqueous environment." AIP Conference Proceedings 2136 (1). https://doi.org/10.1063/1.5120920.

Poznyak, Sergey K., Nikolai P. Osipovich, Alexey Shavel, Dmitri V. Talapin, Mingyuan Gao, Alexander Eychmüller, and Nikolai Gaponik. 2005. "Size-Dependent Electrochemical Behavior of Thiol-Capped CdTe Nanocrystals in Aqueous Solution." The Journal of Physical Chemistry B 109 (3):1094-1100. https://doi.org/10.1021/jp0460801.

Prabhakaran, Prem, Won Jin Kim, Kwang-Sup Lee, and Paras N. Prasad. 2012. "Quantum dots (QDs) for photonic applications." Optical Materials Express 2 (5):578-593. https://doi.org/10.1364/OME.2.000578.

Preeyanka, Naupada, and Moloy Sarkar. 2021. "Probing How Various Metal Ions Interact with the Surface of QDs: Implication of the Interaction Event on the Photophysics of QDs." Langmuir 37 (23):6995-7007. https://doi.org/10.1021/acs.langmuir.1c00548.

Radhakrishnan, K., S. Sivanesan, and P. Panneerselvam. 2020. "Turn-On fluorescence sensor based detection of heavy metal ion using carbon dots@graphitic-carbon nitride nanocomposite probe." Journal of Photochemistry and Photobiology A: Chemistry 389:112204. https://doi.org/10.1016/j.jphotochem.2019.112204.

Ramírez-Herrera, Doris E., Ana Patricia Reyes-Cruzaley, Giselle Dominguez, Francisco Paraguay-Delgado, Antonio Tirado-Guízar, and Georgina Pina-Luis. 2019. "CdTe Quantum Dots Modified with Cysteamine: A New Efficient Nanosensor for the Determination of Folic Acid." Sensors 19 (20):4548. https://doi.org/10.3390/s19204548.

Rasheed, Tahir, Muhammad Bilal, Faran Nabeel, Hafiz M. N. Iqbal, Chuanlong Li, and Yongfeng Zhou. 2018. "Fluorescent sensor based models for the detection of

environmentally-related toxic heavy metals." Science of The Total Environment 615:476-485. https://doi.org/10.1016/j.scitotenv.2017.09.126.

Ravindran, Aswathy, M. Elavarasi, T. C. Prathna, Ashok M. Raichur, N. Chandrasekaran, and Amitava Mukherjee. 2012. "Selective colorimetric detection of nanomolar Cr (VI) in aqueous solutions using unmodified silver nanoparticles." Sensors and Actuators B: Chemical 166-167:365-371. https://doi.org/10.1016/j.snb.2012.02.073.

Remelli, Maurizio, Valeria M. Nurchi, Joanna I. Lachowicz, Serenella Medici, M. Antonietta Zoroddu, and Massimiliano Peana. 2016. "Competition between Cd(II) and other divalent transition metal ions during complex formation with amino acids, peptides, and chelating agents." Coordination Chemistry Reviews 327-328:55-69. https://doi.org/10.1016/j.ccr.2016.07.004.

Resnick, R., and W. H. Buck. 1997. Modern Fluoropolymers. Chichester, UK: John Wiley & Sons.

Ribeiro, David S. M., Gustavo C. S. de Souza, Armindo Melo, José X. Soares, S. Sofia M. Rodrigues, Alberto N. Araújo, Maria Conceição B. S. M. Montenegro, and João L. M. Santos. 2017. "Synthesis of distinctly thiol-capped CdTe quantum dots under microwave heating: multivariate optimization and characterization." Journal of Materials Science 52 (6):3208-3224. https://doi.org/10.1007/s10853-016-0610-4.

Riche, Carson T., Brandon C. Marin, Noah Malmstadt, and Malancha Gupta. 2011. "Vapor deposition of cross-linked fluoropolymer barrier coatings onto pre-assembled microfluidic devices." Lab on a Chip 11 (18):3049-3052. https://doi.org/10.1039/C1LC20396G.

Rizvi S, Rouhi S, Taniguchi S, Yang SY, Green M, Keshtgar M, Seifalian A. 2014. "Near-infrared quantum dots for HER2 localization and imaging of cancer cells." Int J Nanomedicine 9(1):1323-1337. https://doi.org/10.2147/IJN.S51535.

Rodríguez-Valencia, Cosme, Miriam López-Álvarez, Stefan Stefanov, Stefano Chiussi, Julia Serra, and Pío González. 2014. "Biomineralization of marine-patterned C-scaffolds." Bioinspired, Biomimetic and Nanobiomaterials 3 (2):106-114. https://doi.org/10.1680/bbn.13.00029.

Rong, Mingcong, Liping Lin, Xinhong Song, Yiru Wang, Yunxin Zhong, Jiawei Yan, Yufeng Feng, Xiuya Zeng, and Xi Chen. 2015. "Fluorescence sensing of chromium (VI) and ascorbic acid using graphitic carbon nitride nanosheets as a fluorescent

“switch”." Biosensors and Bioelectronics 68:210-217. https://doi.org/10.1016/j.bios.2014.12.024.

Samanta, Partha, Sumanta Let, Writakshi Mandal, Subhajit Dutta, and Sujit K. Ghosh. 2020. "Luminescent metal–organic frameworks (LMOFs) as potential probes for the recognition of cationic water pollutants." Inorganic Chemistry Frontiers 7 (9):1801-1821. https://doi.org/10.1039/D0QI00167H.

Sarıipek, Fatma, and Mustafa Karaman. 2014. "Initiated CVD of Tertiary Amine-Containing Glycidyl Methacrylate Copolymer Thin Films for Low Temperature Aqueous Chemical Functionalization." Chemical Vapor Deposition 20 (10-11-12):373-379. https://doi.org/10.1002/cvde.201407129.

Scaiano, J. C., Marie Laferrière, Raquel E. Galian, Vincent Maurel, and Paul Billone. 2006. "Non-linear effects in the quenching of fluorescent semiconductor nanoparticles by paramagnetic species." physica status solidi (a) 203 (6):1337-1343. https://doi.org/10.1002/pssa.200566186.

Scheirs, John. 1997. Modern fluoropolymers : high performance polymers for diverse applications, Wiley series in polymer science: Wiley.

Schreier, Shirley, Jose Roberto Ernandes, Iolanda Cuccovia, and Hernan Chaimovich. 1978. "Spin label studies of structural and dynamical properties of detergent aggregates." Journal of Magnetic Resonance (1969) 30 (2):283-298. https://doi.org/10.1016/0022-2364(78)90102-6.

Selvan, S. T., P. K. Patra, C. Y. Ang, and J. Y. Ying. 2007. "Synthesis of silica-coated semiconductor and magnetic quantum dots and their use in the imaging of live cells." Angew Chem Int Ed Engl 46 (14):2448-52. https://doi.org/10.1002/anie.200604245.

Seok, Ji-Hoo, Sung Hee Kim, Sung Min Cho, Gi-Ra Yi, and Jun Young Lee. 2018. "Crosslinked Organosilicon-Acrylate Copolymer Moisture Barrier Thin Film Fabricated by Initiated Chemical Vapor Deposition (iCVD)." Macromolecular Research 26 (13):1257-1264. https://doi.org/10.1007/s13233-019-6149-2.

Serra, P.A. 2011. New Perspectives in Biosensors Technology and Applications. IntechOpen.

Sevim Ünlütürk, Seçil, Yaşar Akdoğan, and Serdar Özçelik. 2021. "Mn2+ ions incorporated into ZnS x Se1−x colloidal quantum dots: controlling size and composition of nanoalloys and regulating magnetic dipolar interactions." Nanotechnology 32 (16):165701. https://doi.org/10.1088/1361-6528/abdb65.

Shanmugharaj, A. M., J. H. Yoon, W. J. Yang, and Sung Hun Ryu. 2013. "Synthesis, characterization, and surface wettability properties of amine functionalized graphene oxide films with varying amine chain lengths." Journal of Colloid and Interface Science 401:148-154. https://doi.org/10.1016/j.jcis.2013.02.054.

Shen, Jiulin, Pengfei Jiang, Yao Wang, Feng Zhang, Fu Li, and Guoli Tu. 2022. "Soluble sulfoxide biphenyl polyimide film with transmittance exceeding 90%." Polymer 254:125050. https://doi.org/10.1016/j.polymer.2022.125050.

Shen, Lei. 2011. "Biocompatible Polymer/Quantum Dots Hybrid Materials: Current Status and Future Developments." Journal of Functional Biomaterials 2 (4):355-372. https://doi.org/10.3390/jfb2040355.

Shi, Bingfang, Liangliang Zhang, Chuanqing Lan, Jingjin Zhao, Yubin Su, and Shulin Zhao. 2015. "One-pot green synthesis of oxygen-rich nitrogen-doped graphene quantum dots and their potential application in pH-sensitive photoluminescence and detection of mercury(II) ions." Talanta 142:131-139. https://doi.org/10.1016/j.talanta.2015.04.059.

Shokuhfar, Ali, and Behrouz Arab. 2013. "The effect of cross linking density on the mechanical properties and structure of the epoxy polymers: molecular dynamics simulation." Journal of Molecular Modeling 19 (9):3719-3731. https://doi.org/10.1007/s00894-013-1906-9.

Singh, Sanjeev, Avinashi Kapoor, S. C. K. Misra, and K. N. Tripathi. 1996. "Optimization of waveguide parameters of bisphenol A polycarbonate." Solid State Communications 100 (7):503-506. https://doi.org/10.1016/0038-1098(96)00431-0.

Snee, Preston T., Rebecca C. Somers, Gautham Nair, John P. Zimmer, Moungi G. Bawendi, and Daniel G. Nocera. 2006. "A Ratiometric CdSe/ZnS Nanocrystal pH Sensor." Journal of the American Chemical Society 128 (41):13320-13321. https://doi.org/10.1021/ja0618999.

Song, Ting, Xuefeng Zhu, Shenghai Zhou, Guang Yang, Wei Gan, and Qunhui Yuan. 2015. "DNA derived fluorescent bio-dots for sensitive detection of mercury and silver ions in aqueous solution." Applied Surface Science 347:505-513. https://doi.org/10.1016/j.apsusc.2015.04.143.

Stefanović, Ivan S., Bojana M. Ekmeščić, Danijela D. Maksin, Aleksandra B. Nastasović, Zoran P. Miladinović, Zorica M. Vuković, Darko M. Micić, and Marija V. Pergal. 2015. "Structure, Thermal, and Morphological Properties of Novel Macroporous

Amino-Functionalized Glycidyl Methacrylate Based Copolymers." Industrial & Engineering Chemistry Research 54 (27):6902-6911. https://doi.org/10.1021/acs.iecr.5b01285.

Sun, Ye, Rajdeep Singh Rawat, and Zhong Chen. 2022. "A Mechanically Reliable Transparent Antifogging Coating on Polymeric Lenses." Advanced Materials Interfaces 9 (4):2101864. https://doi.org/10.1002/admi.202101864.

Suvarapu, Lakshmi Narayana, and Sung-Ok Baek. 2015. "Recent Developments in the Speciation and Determination of Mercury Using Various Analytical Techniques." Journal of Analytical Methods in Chemistry 2015:372459. https://doi.org/10.1155/2015/372459.

T.Drzal, Lawrence. 1986. Advances in Polymer Science-Epoxy Resins and Composites II.

Tansakul, Chittreeya, Erin Lilie, Eric D. Walter, Frank Rivera, Abraham Wolcott, Jin Z. Zhang, Glenn L. Millhauser, and Rebecca Braslau. 2010. "Distance-Dependent Fluorescence Quenching and Binding of CdSe Quantum Dots by Functionalized Nitroxide Radicals." The Journal of Physical Chemistry C 114 (17):7793-7805. https://doi.org/10.1021/jp1005023.

Tao, Ran, and Mitchell Anthamatten. 2016. "Quenching Phase Separation by Vapor Deposition Polymerization." Macromolecular Materials and Engineering 301 (1):99-109. https://doi.org/10.1002/mame.201500280.

Tarducci, C., E. J. Kinmond, J. P. S. Badyal, S. A. Brewer, and C. Willis. 2000. "Epoxide-Functionalized Solid Surfaces." Chemistry of Materials 12 (7):1884-1889. https://doi.org/10.1021/cm0000954.

Tenhaeff, W. E., and K. K. Gleason. 2008. "Initiated and oxidative chemical vapor deposition of polymeric thin films: iCVD and oCVD." Advanced Functional Materials 18 (7):979-992. https://doi.org/10.1002/adfm.200701479.

Tian, J., Q. Liu, A. M. Asiri, A. O. Al-Youbi, and X. Sun. 2013. "Ultrathin graphitic carbon nitride nanosheet: a highly efficient fluorosensor for rapid, ultrasensitive detection of Cu(2+)." Anal Chem 85 (11):5595-9. https://doi.org/10.1021/ac400924j.

Träger, F. 2012. Springer Handbook of Lasers and Optics: Springer. https://doi.org/10.1007/978-3-642-19409-2.

Trivedi, M., A. Branton, D. Trivedi, G. Nayak, R. Kumar Mishra, and S. Jana. 2015. "Comparative Physicochemical Evaluation of Biofield Treated Phosphate Buffer

Saline and Hanks Balanced Salt Medium." American Journal of BioScience 6 (3):267-277. https://doi.org/10.11648/j.ajbio.20150306.20.

Trujillo, N. J., Q. G. Wu, and K. K. Gleason. 2010. "Ultralow Dielectric Constant Tetravinyltetramethylcyclotetrasiloxane Films Deposited by Initiated Chemical Vapor Deposition (iCVD)." Advanced Functional Materials 20 (4):607-616. https://doi.org/10.1002/adfm.200900999.

Varghese, Anish M., and Vikas Mittal. 2018. "5 - Surface modification of natural fibers." In Biodegradable and Biocompatible Polymer Composites, edited by Navinchandra Gopal Shimpi, 115-155. Woodhead Publishing.

Velásquez-Hernández, Miriam de J., Raffaele Ricco, Francesco Carraro, F. Ted Limpoco, Mercedes Linares-Moreau, Erich Leitner, Helmar Wiltsche, Johannes Rattenberger, Hartmuth Schröttner, Philipp Frühwirt, Eduard M. Stadler, Georg Gescheidt, Heinz Amenitsch, Christian J. Doonan, and Paolo Falcaro. 2019. "Degradation of ZIF-8 in phosphate buffered saline media." CrystEngComm 21 (31):4538-4544. https://doi.org/10.1039/C9CE00757A.

Venkatram, Shruti, Chiho Kim, Anand Chandrasekaran, and Rampi Ramprasad. 2019. "Critical Assessment of the Hildebrand and Hansen Solubility Parameters for Polymers." Journal of Chemical Information and Modeling 59 (10):4188-4194. https://doi.org/10.1021/acs.jcim.9b00656.

Walekar, Laxman S., Anil H. Gore, Prashant V. Anbhule, V. Sudarsan, Shivajirao R. Patil, and Govind B. Kolekar. 2013. "A novel colorimetric probe for highly selective recognition of Hg2+ ions in aqueous media based on inducing the aggregation of CPB-capped AgNPs: accelerating direct detection for environmental analysis." Analytical Methods 5 (20):5501-5507. https://doi.org/10.1039/C3AY40827B.

Wang, Dengpeng, Feng Gao, Xianran Wang, Xiaomei Ning, Kaituo Wang, Xinpeng Wang, Yuezhou Wei, and Toyohisa Fujita. 2022. "Detection of Cd2+ in Aqueous Solution by the Fluorescent Probe of CdSe/CdS QDs Based on OFF–ON Mode." Toxics 10 (7):367. https://doi.org/10.3390/toxics10070367.

Wang, Jing, Jiangong Liang, Zonghai Sheng, and Heyou Han. 2009. "A novel strategy for selective detection of Ag+ based on the red-shift of emission wavelength of quantum dots." Microchimica Acta 167 (3):281. https://doi.org/10.1007/s00604-009-0244-1.

Wang, Yong, Jie Hu, Qianfen Zhuang, and Yongnian Ni. 2016. "Label-Free Fluorescence Sensing of Lead(II) Ions and Sulfide Ions Based on Luminescent Molybdenum Disulfide Nanosheets." ACS Sustainable Chemistry & Engineering 4 (5):2535-2541. https://doi.org/10.1021/acssuschemeng.5b01639.

Wang, Zhong-Xia, and Shou-Nian Ding. 2014. "One-Pot Green Synthesis of High Quantum Yield Oxygen-Doped, Nitrogen-Rich, Photoluminescent Polymer Carbon Nanoribbons as an Effective Fluorescent Sensing Platform for Sensitive and Selective Detection of Silver(I) and Mercury(II) Ions." Analytical Chemistry 86 (15):7436-7445. https://doi.org/10.1021/ac501085d.

Wątły, J., A. Hecel, R. Wieczorek, J. Świątek-Kozłowska, H. Kozłowski, and M. Rowińska-Żyrek. 2019. "Uncapping the N-terminus of a ubiquitous His-tag peptide enhances its Cu2+ binding affinity." Dalton Transactions 48 (36):13567-13579. https://doi.org/10.1039/C9DT01635J.

Weinberger, Robert. 2000. "CHAPTER 6 - Size Separations in Capillary Gels and Polymer Networks." In Practical Capillary Electrophoresis (Second Edition), edited by Robert Weinberger, 245-292. San Diego: Academic Press.

Wen, Yanqin, Cheng Peng, Di Li, Lin Zhuo, Shijiang He, Lihua Wang, Qing Huang, Qing-Hua Xu, and Chunhai Fan. 2011. "Metal ion-modulated graphene-DNAzyme interactions: design of a nanoprobe for fluorescent detection of lead(ii) ions with high sensitivity, selectivity and tunable dynamic range." Chemical Communications 47 (22):6278-6280. https://doi.org/10.1039/C1CC11486G.

WHO, Organization. 2011. Guidelines for drinking-water quality. Edited by W. Press. 4 ed.

Wilson, J., and J. Hawkes. 1998. Optoelectronics: An introduction. Third ed.

Wing Fen, Yap, and W. Mahmood Mat Yunus. 2013. "Surface plasmon resonance spectroscopy as an alternative for sensing heavy metal ions: a review." Sensor Review 33 (4):305-314. https://doi.org/10.1108/SR-01-2012-604.

Wu, G., X. Tang, Z. Lin, M. Meyyappan, and K. W. C. Lai. 2017. "The effect of ionic strength on the sensing performance of liquid-gated biosensors." 2017 IEEE 17th International Conference on Nanotechnology (IEEE-NANO), 25-28 July 2017. https://doi.org/10.1109/NANO.2017.8117313.

Wu, Jie, and Hong-Guang Xia. 2005. "Tertiary amines as highly efficient catalysts in the ring-opening reactions of epoxides with amines or thiols in H2O: expeditious

approach to β-amino alcohols and β-aminothioethers." Green Chemistry 7 (10):708-710. https://doi.org/10.1039/B509288D.

Wu, Peng, Ting Zhao, Shanling Wang, and Xiandeng Hou. 2014. "Semicondutor quantum dots-based metal ion probes." Nanoscale 6 (1):43-64. https://doi.org/10.1039/C3NR04628A.

Xie, Yuan, Kai Zhang, Yusuke Yamauchi, Kenichi Oyaizu, and Zhongfan Jia. 2021. "Nitroxide radical polymers for emerging plastic energy storage and organic electronics: fundamentals, materials, and applications." Materials Horizons 8 (3):803-829. https://doi.org/10.1039/D0MH01391A.

Xu, Hu, Ran Miao, Zheng Fang, and Xinhua Zhong. 2011. "Quantum dot-based “turn-on” fluorescent probe for detection of zinc and cadmium ions in aqueous media." Analytica Chimica Acta 687 (1):82-88. https://doi.org/10.1016/j.aca.2010.12.002.

Xu, Jingjing, and Karen K. Gleason. 2010b. "Conformal, Amine-Functionalized Thin Films by Initiated Chemical Vapor Deposition (iCVD) for Hydrolytically Stable Microfluidic Devices." Chemistry of Materials 22 (5):1732-1738. https://doi.org/10.1021/cm903156a.

Xu, Kehua, Huachao Chen, Huixia Wang, Jiangwei Tian, Jing Li, Qingling Li, Na Li, and Bo Tang. 2011. "A nanoprobe for nonprotein thiols based on assembling of QDs and 4-amino-2,2,6,6-tetramethylpiperidine oxide." Biosensors and Bioelectronics 26 (11):4632-4636. https://doi.org/10.1016/j.bios.2011.05.020.

Yager, T. D., G. R. Eaton, and S. S. Eaton. 1979. "Metal-nitroxyl interactions. 12. Nitroxyl spin probes in the presence of tris(oxalato)chromate(III)." Inorganic Chemistry 18 (3):725-727. https://doi.org/10.1021/ic50193a039.

Yan, Ze, Yi Cai, Jing Zhang, and Yong Zhao. 2022. "Fluorescent sensor arrays for metal ions detection: A review." Measurement 187:110355. https://doi.org/10.1016/j.measurement.2021.110355.

Yang, G. H., E. T. Kang, and K. G. Neoh. 2000. "Surface modification of poly(tetrafluoroethylene) films by plasma polymerization of glycidyl methacrylate and its relevance to the electroless deposition of copper." Journal of Polymer Science Part A: Polymer Chemistry 38 (19):3498-3509. https://doi.org/10.1002/1099-0518(20001001)38:19<3498::AID-POLA60>3.0.CO;2-U.

Yang, Rong, and Karen K. Gleason. 2012. "Ultrathin Antifouling Coatings with Stable Surface Zwitterionic Functionality by Initiated Chemical Vapor Deposition (iCVD)." Langmuir 28 (33):12266-12274. https://doi.org/10.1021/la302059s.

Yang, Rong, Jingjing Xu, Gozde Ozaydin-Ince, Sze Yinn Wong, and Karen K. Gleason. 2011. "Surface-Tethered Zwitterionic Ultrathin Antifouling Coatings on Reverse Osmosis Membranes by Initiated Chemical Vapor Deposition." Chemistry of Materials 23 (5):1263-1272. https://doi.org/10.1021/cm1031392.

Yang Shen, Jiwen Hu, Tingting Liu, Hongwen Gao, Zhangjun Hu. 2019. "Colorimetric and Fluorogenic Chemosensors for Mercury Ion Based on Nanomaterials." Progress in Chemistry 31 (4):536-549. https://doi.org/10.7536/PC180933.

Yeo, Hyunki, Siddhartha Akkiraju, Ying Tan, Hamas Tahir, Neil R. Dilley, Brett M. Savoie, and Bryan W. Boudouris. 2022. "Electronic and Magnetic Properties of a Three-Arm Nonconjugated Open-Shell Macromolecule." ACS Polymers Au 2 (1):59-68. https://doi.org/10.1021/acspolymersau.1c00026.

Yildiz, Remziye, Sercan Ozen, Hasan Sahin, and Yasar Akdogan. 2020. "The effect of DOPA hydroxyl groups on wet adhesion to polystyrene surface: An experimental and theoretical study." Materials Chemistry and Physics 243:122606. https://doi.org/10.1016/j.matchemphys.2019.122606.

Yin, Jiajia, Haohao Hui, Bin Fan, Jiang Bian, Junfeng Du, and Hu Yang. 2022. "Preparation and Properties of Polyimide Composite Membrane with High Transmittance and Surface Hydrophobicity for Lightweight Optical System." Membranes 12 (6):592. https://doi.org/10.3390/membranes12060592.

Yin, Yuan, Qingliang Yang, and Gang Liu. 2020. "Ammonium Pyrrolidine Dithiocarbamate-Modified CdTe/CdS Quantum Dots as a Turn-on Fluorescent Sensor for Detection of Trace Cadmium Ions." Sensors 20 (1):312. https://doi.org/10.3390/s20010312.

Yoo, Youngmin, Jae Bem You, Wonjae Choi, and Sung Gap Im. 2013. "A stacked polymer film for robust superhydrophobic fabrics." Polymer Chemistry 4 (5):1664-1671. https://doi.org/10.1039/C2PY20963B.

Yu, Bing, and Andrew B. Lowe. 2009. "Synthesis of di- and tri-tertiary amine containing methacrylic monomers and their (co)polymerization via RAFT." Journal of Polymer Science Part A: Polymer Chemistry 47 (7):1877-1890. https://doi.org/10.1002/pola.23281.

Yuan, Xiao-Lin, Xiao-Yi Wu, Miao He, Jia-Ping Lai, and Hui Sun. 2022. "A Ratiometric Fiber Optic Sensor Based on CdTe QDs Functionalized with Glutathione and Mercaptopropionic Acid for On-Site Monitoring of Antibiotic Ciprofloxacin in Aquaculture Water." Nanomaterials 12 (5):829. https://doi.org/10.3390/nano12050829.

Zang, Yang, Jianping Lei, Qing Hao, and Huangxian Ju. 2014. "“Signal-On” Photoelectrochemical Sensing Strategy Based on Target-Dependent Aptamer Conformational Conversion for Selective Detection of Lead(II) Ion." ACS Applied Materials & Interfaces 6 (18):15991-15997. https://doi.org/10.1021/am503804g.

Zhang, Bao-Hua, Li Qi, and Fang-Ying Wu. 2010. "Functionalized manganese-doped zinc sulfide core/shell quantum dots as selective fluorescent chemodosimeters for silver ion." Microchimica Acta 170 (1):147-153. https://doi.org/10.1007/s00604-010-0381-6.

Zhang, Jian, Xuan Sun, and Jayne Wu. 2019. "Heavy Metal Ion Detection Platforms Based on a Glutathione Probe: A Mini Review." Applied Sciences 9 (3):489. https://doi.org/10.3390/app9030489.

Zhang, Junfeng, Koichi Kato, Yoshikimi Uyama, and Yoshito Ikada. 1995. "Surface graft polymerization of glycidyl methacrylate onto polyethylene and the adhesion with epoxy resin." Journal of Polymer Science Part A: Polymer Chemistry 33 (15):2629-2638. https://doi.org/10.1002/pola.1995.080331509.

Zhang, Ruizhong, and Wei Chen. 2014. "Nitrogen-doped carbon quantum dots: Facile synthesis and application as a “turn-off” fluorescent probe for detection of Hg2+ ions." Biosensors and Bioelectronics 55:83-90. https://doi.org/10.1016/j.bios.2013.11.074.

Zhao, Huaixia, Lizbeth Ofelia Prieto-López, Xiaozhuang Zhou, Xu Deng, and Jiaxi Cui. 2019. "Multistimuli Responsive Liquid-Release in Dynamic Polymer Coatings for Controlling Surface Slipperiness and Optical Performance." Advanced Materials Interfaces 6 (20):1901028. https://doi.org/10.1002/admi.201901028.

Zhao, Jiangna, Jianhui Deng, Yinhui Yi, Haitai Li, Youyu Zhang, and Shouzhuo Yao. 2014. "Label-free silicon quantum dots as fluorescent probe for selective and sensitive detection of copper ions." Talanta 125:372-377. https://doi.org/10.1016/j.talanta.2014.03.031.

Zhao, Jiling, Shixing Wang, Libo Zhang, Chen Wang, and Bing Zhang. 2018. "Kinetic, Isotherm, and Thermodynamic Studies for Ag(I) Adsorption Using Carboxymethyl Functionalized Poly(glycidyl methacrylate)." Polymers 10 (10):1090. https://doi.org/10.3390/polym10101090.

Zhao, X., R. P. Bagwe, and W. Tan. 2004. "Development of Organic-Dye-Doped Silica Nanoparticles in a Reverse Microemulsion." Advanced Materials 16 (2):173-176. https://doi.org/10.1002/adma.200305622.

Zhao, Y.-G., W.-K. Lu, Y. Ma, S.-S. Kim, S. T. Ho, and T. J. Marks. 2000. "Polymer waveguides useful over a very wide wavelength range from the ultraviolet to infrared." Applied Physics Letters 77 (19):2961-2963. https://doi.org/10.1063/1.1323547.

Zhao, Yineng, Ni Huo, Sheng Ye, Arman Boromand, Andrew J. Ouderkirk, and Wyatt E. Tenhaeff. 2021. "Stretchable, Transparent, Permeation Barrier Layer for Flexible Optics." Advanced Optical Materials 9 (12):2100334. https://doi.org/10.1002/adom.202100334.

Zhou, Juan, Yong Yang, and Chun-yang Zhang. 2015. "Toward Biocompatible Semiconductor Quantum Dots: From Biosynthesis and Bioconjugation to Biomedical Application." Chemical Reviews 115 (21):11669-11717. https://doi.org/10.1021/acs.chemrev.5b00049.

Zhou, Tian, Yizhou Zhu, Xia Li, Xiangmei Liu, Kelvin W. K. Yeung, Shuilin Wu, Xianbao Wang, Zhenduo Cui, Xianjin Yang, and Paul K. Chu. 2016. "Surface functionalization of biomaterials by radical polymerization." Progress in Materials Science 83:191-235. https://doi.org/10.1016/j.pmatsci.2016.04.005.

Zhou, Wenbo, Wenjie Liu, Meng Qin, Zhidong Chen, Juan Xu, Jianyu Cao, and Jun Li. 2020. "Fundamental properties of TEMPO-based catholytes for aqueous redox flow batteries: effects of substituent groups and electrolytes on electrochemical properties, solubilities and battery performance." RSC Advances 10 (37):21839-21844. https://doi.org/10.1039/D0RA03424J.

Zong, Jie, Xiaoling Yang, Adrian Trinchi, Simon Hardin, Ivan Cole, Yihua Zhu, Chunzhong Li, Tim Muster, and Gang Wei. 2014. "Carbon dots as fluorescent probes for “off–on” detection of Cu2+ and l-cysteine in aqueous solution." Biosensors and Bioelectronics 51:330-335. https://doi.org/10.1016/j.bios.2013.07.042.

APPENDIX A

PERMISSIONS TO REPRODUCE FIGURES AND TEXTS

Permissions have been taken to reproduce the full text given in Chapter 3 and 4 through the Copyright Clearance Center and MDPI. Documentations of the approvals are given on the following pages.

CHAPTER 3

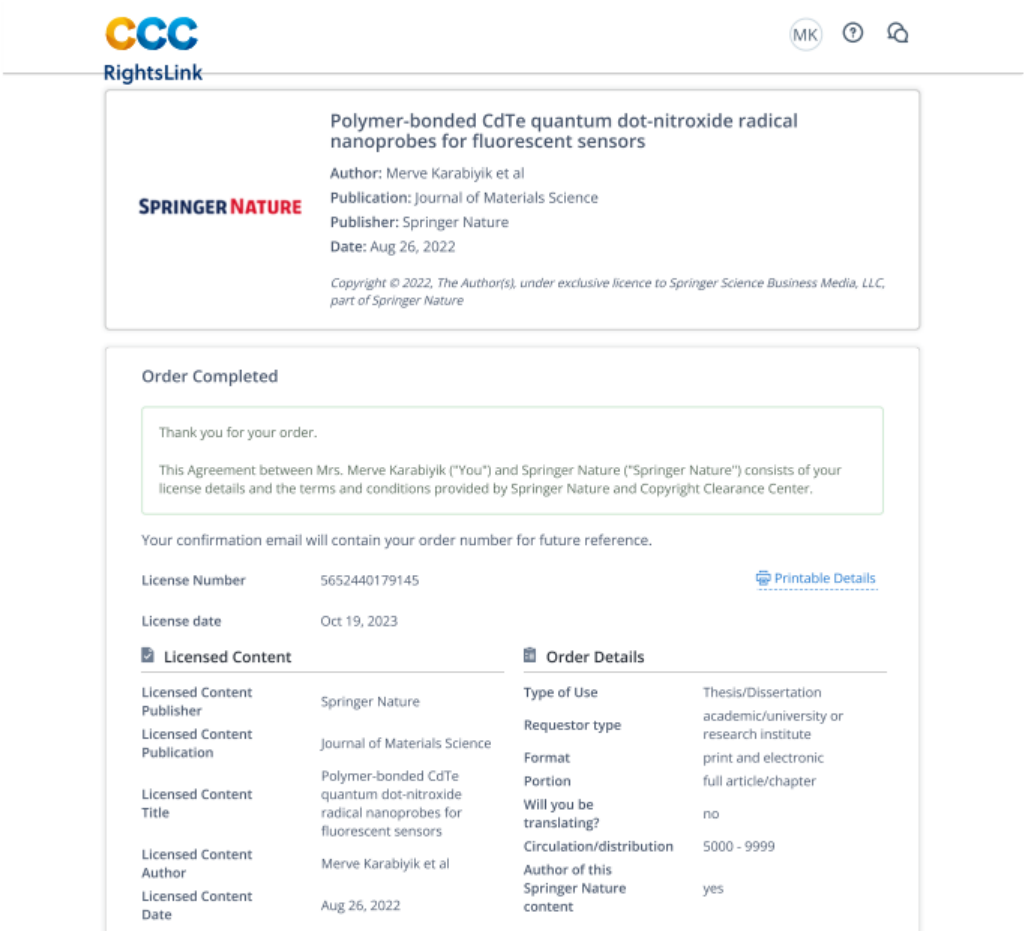

CCC RightsLink

MK

SPRINGER NATURE

Polymer-bonded CdTe quantum dot-nitroxide radical nanoprobes for fluorescent sensors

Author: Merve Karabiyik et al
Publication: Journal of Materials Science
Publisher: Springer Nature
Date: Aug 26, 2022

Copyright © 2022, The Author(s), under exclusive licence to Springer Science Business Media, LLC, part of Springer Nature

Order Completed

Thank you for your order.

This Agreement between Mrs. Merve Karabiyik ("You") and Springer Nature ("Springer Nature") consists of your license details and the terms and conditions provided by Springer Nature and Copyright Clearance Center.

Your confirmation email will contain your order number for future reference.

Printable Details

License Number	5652440179145
License date	Oct 19, 2023

Licensed Content

Licensed Content Publisher	Springer Nature
Licensed Content Publication	Journal of Materials Science
Licensed Content Title	Polymer-bonded CdTe quantum dot-nitroxide radical nanoprobes for fluorescent sensors
Licensed Content Author	Merve Karabiyik et al
Licensed Content Date	Aug 26, 2022

Order Details

Type of Use	Thesis/Dissertation
Requestor type	academic/university or research institute
Format	print and electronic
Portion	full article/chapter
Will you be translating?	no
Circulation/distribution	5000 - 9999
Author of this Springer Nature content	yes

About Your Work

Title of new work	Chemical Vapor Deposited Reusable Fluorescent Thin Film Sensor Nanoprobes for the Detection of Heavy Metal Ions
Institution name	İzmir Institute of Technology
Expected presentation date	Dec 2023

Additional Data

Requestor Location

Requestor Location	Mrs. Merve Karabiyik Izmir Institute of Technology, Chemical Engineering Department, room:z04, Gulbahce St. Urla/Izmir Izmir, 35430 Turkey Attn: Mrs. Merve Karabiyik

Tax Details

Total: 0.00 USD

CLOSE WINDOW ORDER MORE

SPRINGER NATURE LICENSE
TERMS AND CONDITIONS

Oct 19, 2023

This Agreement between Mrs. Merve Karabiyik ("You") and Springer Nature ("Springer Nature") consists of your license details and the terms and conditions provided by Springer Nature and Copyright Clearance Center.

License Number	5652440179145
License date	Oct 19, 2023
Licensed Content Publisher	Springer Nature
Licensed Content Publication	Journal of Materials Science
Licensed Content Title	Polymer-bonded CdTe quantum dot-nitroxide radical nanoprobes for fluorescent sensors
Licensed Content Author	Merve Karabiyik et al
Licensed Content Date	Aug 26, 2022
Type of Use	Thesis/Dissertation
Requestor type	academic/university or research institute

Format	print and electronic
Portion	full article/chapter
Will you be translating?	no
Circulation/distribution	5000 - 9999
Author of this Springer Nature content	yes
Title of new work	Chemical Vapor Deposited Reusable Fluorescent Thin Film Sensor Nanoprobes for the Detection of Heavy Metal Ions
Institution name	İzmir Institute of Technology
Expected presentation date	Dec 2023
Requestor Location	Mrs. Merve Karabiyik Izmir Institute of Technology, Chemical Engineering Department, room:z04, Gulbahce St. Urla/Izmir Izmir, 35430 Turkey Attn: Mrs. Merve Karabiyik
Total	0.00 USD

CHAPTER 4

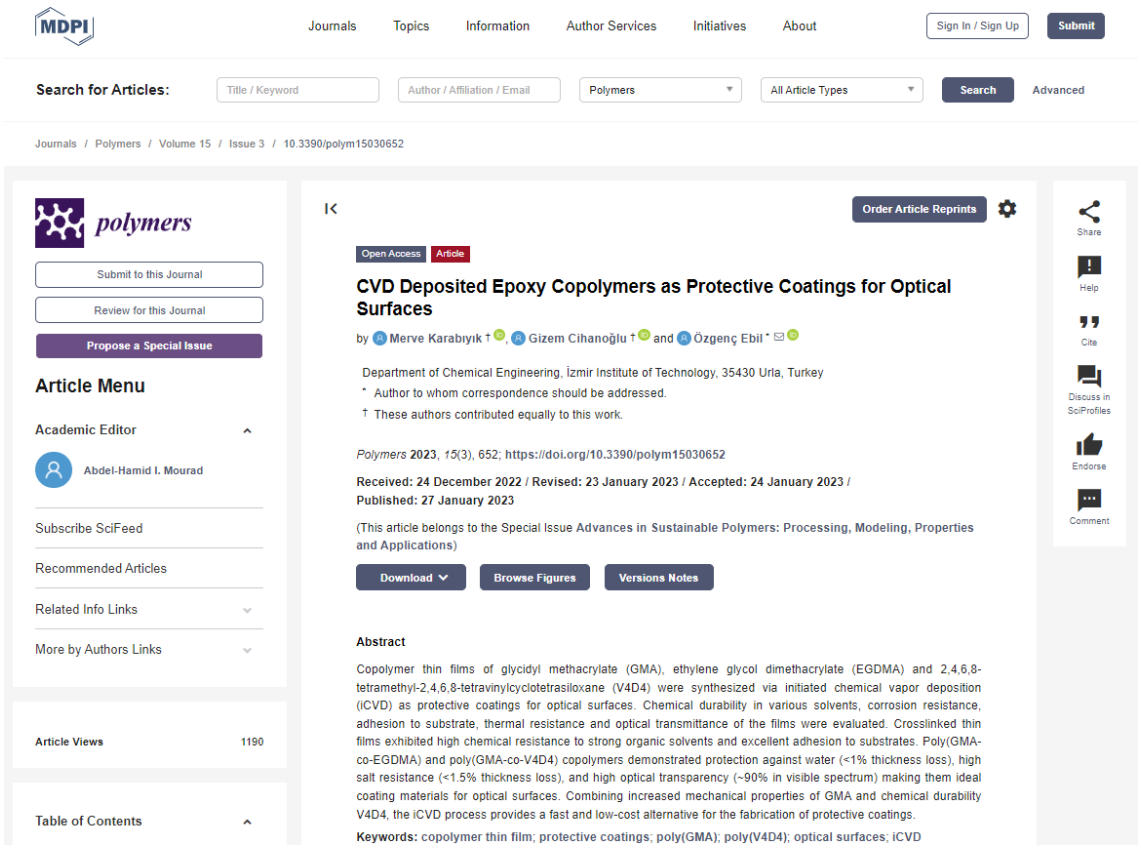
MDPI
Journals
Topics
Information
Author Services
Initiatives
About
Sign In / Sign Up
Submit
Search for Articles:
Title / Keyword
Author / Affiliation / Email
Polymers
All Article Types
Search
Advanced
Journals / Polymers / Volume 15 / Issue 3 / 10.3390/polym15030652
polymers
Submit to this Journal
Review for this Journal
Propose a Special Issue
Article Menu
Academic Editor
Abdel-Hamid I. Mourad
Subscribe SciFeed
Recommended Articles
Related Info Links
More by Authors Links
Article Views 1190
Table of Contents
Order Article Reprints
Open Access
Article
CVD Deposited Epoxy Copolymers as Protective Coatings for Optical Surfaces
by Merve Karabıyık †, Gizem Cihanoğlu † and Özgenç Ebil *
Department of Chemical Engineering, İzmir Institute of Technology, 35430 Urla, Turkey
* Author to whom correspondence should be addressed.
† These authors contributed equally to this work.
Polymers 2023, 15(3), 652; https://doi.org/10.3390/polym15030652
Received: 24 December 2022 / Revised: 23 January 2023 / Accepted: 24 January 2023 / Published: 27 January 2023
(This article belongs to the Special Issue Advances in Sustainable Polymers: Processing, Modeling, Properties and Applications)
Download
Browse Figures
Versions Notes
Abstract
Copolymer thin films of glycidyl methacrylate (GMA), ethylene glycol dimethacrylate (EGDMA) and 2,4,6,8-tetramethyl-2,4,6,8-tetravinylcyclotetrasiloxane (V4D4) were synthesized via initiated chemical vapor deposition (iCVD) as protective coatings for optical surfaces. Chemical durability in various solvents, corrosion resistance, adhesion to substrate, thermal resistance and optical transmittance of the films were evaluated. Crosslinked thin films exhibited high chemical resistance to strong organic solvents and excellent adhesion to substrates. Poly(GMA-co-EGDMA) and poly(GMA-co-V4D4) copolymers demonstrated protection against water (<1% thickness loss), high salt resistance (<1.5% thickness loss), and high optical transparency (~90% in visible spectrum) making them ideal coating materials for optical surfaces. Combining increased mechanical properties of GMA and chemical durability V4D4, the iCVD process provides a fast and low-cost alternative for the fabrication of protective coatings.
Keywords: copolymer thin film; protective coatings; poly(GMA); poly(V4D4); optical surfaces; iCVD
Share
Help
Cite
Discuss in SciProfiles
Endorse
Comment

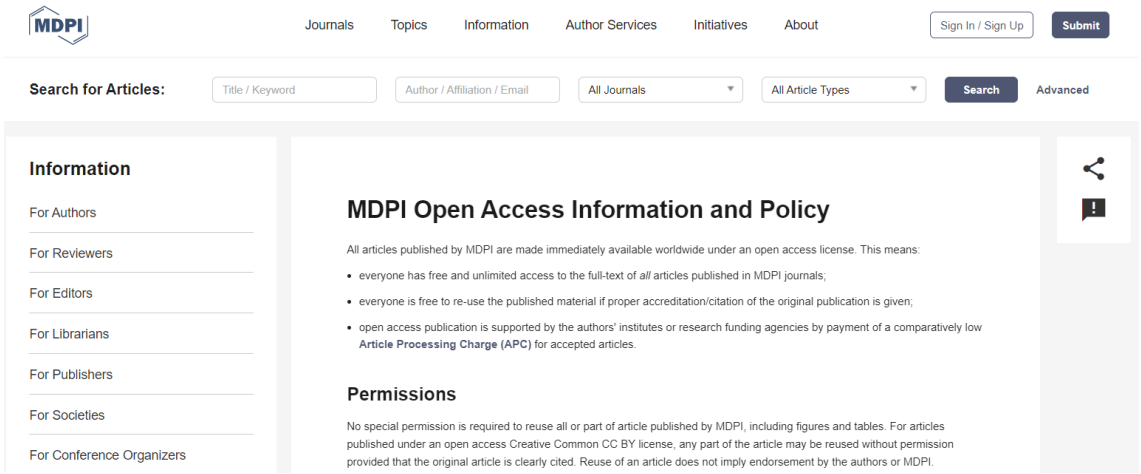
MDPI
Journals
Topics
Information
Author Services
Initiatives
About
Sign In / Sign Up
Submit
Search for Articles:
Title / Keyword
Author / Affiliation / Email
All Journals
All Article Types
Search
Advanced
Information
For Authors
For Reviewers
For Editors
For Librarians
For Publishers
For Societies
For Conference Organizers
MDPI Open Access Information and Policy
All articles published by MDPI are made immediately available worldwide under an open access license. This means:
everyone has free and unlimited access to the full-text of all articles published in MDPI journals;
everyone is free to re-use the published material if proper accreditation/citation of the original publication is given;
open access publication is supported by the authors' institutes or research funding agencies by payment of a comparatively low Article Processing Charge (APC) for accepted articles.
Permissions
No special permission is required to reuse all or part of article published by MDPI, including figures and tables. For articles published under an open access Creative Common CC BY license, any part of the article may be reused without permission provided that the original article is clearly cited. Reuse of an article does not imply endorsement by the authors or MDPI.

VITA

Education

Ph.D. Chemical Engineering, *Izmir Institute of Technology*, Izmir, Turkey 2023
Thesis: "Chemical Vapor Deposited Reusable Fluorescent Thin Film Sensor Nanoprobes for the Detection of Heavy Metal Ions"
Advisor: Prof. Özgenç EBİL

M.Sc. Chemical Engineering, *Izmir Institute of Technology*, Izmir, Turkey 2016
Thesis: "Development of Protective Nano-Coatings for Electro-Optical Systems" (TUBITAK 1001 Project)
Advisor: Assoc. Prof. Özgenç EBİL

B.S. Chemical Engineering, *Izmir Institute of Technology*, Izmir, Turkey 2014
Senior Thesis: "Protein Stabilized Oil/Water Emulsions"
Advisor: Prof. Dr. Mehmet POLAT

Academic Experience

Research Assistant Chemical Engineering, *Izmir Institute of Technology*, Izmir, Turkey 2016-present

Project Assistant Chemical Engineering, *Izmir Institute of Technology*, Izmir, Turkey 2015-2016
TUBITAK 1001- "Development of Protective Nano-Coatings for Electro-Optical Systems"

Honors and Awards

- TUBITAK 2224-International Scientific Meetings Fellowship Programme 2019/4
- Certificate of Honour from Chemical Engineering Department, *Izmir Institute of Technology*, Izmir, Turkey. 2010-2013

Publications

- Karabıyık, Merve, Gizem Cihanoğlu, and Özgenç Ebil. 2023. "CVD Deposited Epoxy Copolymers as Protective Coatings for Optical Surfaces." *Polymers* 15 (3):652.

- Karabiyik, Merve, and Özgenç Ebil. 2022. "Polymer-bonded CdTe quantum dot-nitroxide radical nanoprobes for fluorescent sensors." *Journal of Materials Science* 57 (34):16258-16279.

- Özpirin, Merve, and Özgenç Ebil. 2018. "Transparent block copolymer thin films for protection of optical elements via chemical vapor deposition." *Thin Solid Films* 660:391-398.

Conferences

- Karabiyik, Merve, and Özgenç Ebil "Selective On-Off-On Polymer Bonded Quantum Dot-Nitroxide Radical Fluorescent Sensor to Detect Cd^{2+} Ion in Aqueous Media", Materials Research Society (MRS), December 5-7, 2023, in Boston, Massachusetts (Virtual).

- Cihanoglu Gizem, Karabiyik, Merve and Özgenç Ebil "Effects of Protective Epoxy Copolymer Obtained by Chemical Vapor Deposition Method on the Transmittance Behavior of Optical Surfaces", 15th National Chemical Engineering Meeting, September 4-7, 2023, Çanakkale, Turkey.

- Karabiyik, Merve, Cihanoglu Gizem and Özgenç Ebil "Protective Epoxy Copolymers via Chemical Vapor Deposition for Optical Surfaces" Nanoscience & Nanotechnology Conference, August 27-29 2023, Izmir Institute of Technology, Izmir, Turkey.

- Karabiyik, Merve, and Özgenç Ebil "Functionalization of CVD Compatible Polymer Films for Sensing Applications", European Materials Research Society (E-MRS), September 16-19 2019, Warsaw, Poland.

- Özpirin, Merve, and Özgenç Ebil. “Protective Nano-Coatings for Electro-Optical Systems”, Nanoscience & Nanotechnology Conference (NanoTr-13), October 22-25 2017, Antalya, Turkey.

- Özpirin, Merve, and Özgenç Ebil. “Development of Protective Nano-Coatings for Electro-Optical Systems” Science and Applications of Thin Films, Conference & Exhibition (SATF), September 19-23 2016, Çeşme, İzmir, Turkey.

- Olcay, Aybike Nil, Ozpirin Merve, Kirkose Sema and Mehmet Polat “Stabilization of Oil-Water Emulsion System with BSA Protein” 11th National Chemical Engineering Meeting, September 2-5 2014, Eskişehir, Turkey.